Marshall University
Marshall Digital Scholar

Theses, Dissertations and Capstones

1-1-2009

Efficacy of Deferasirox in Preventing Complications of Iron Overload in the Iron Overloaded Gerbil

Rabaa M. Al-Rousan
rabaaal-rousan@ucwv.edu

Follow this and additional works at: http://mds.marshall.edu/etd

Part of the Biological Phenomena, Cell Phenomena, and Immunity Commons, and the Chemicals and Drugs Commons

Recommended Citation
Al-Rousan, Rabaa M., "Efficacy of Deferasirox in Preventing Complications of Iron Overload in the Iron Overloaded Gerbil" (2009). *Theses, Dissertations and Capstones.* Paper 77.

This Dissertation is brought to you for free and open access by Marshall Digital Scholar. It has been accepted for inclusion in Theses, Dissertations and Capstones by an authorized administrator of Marshall Digital Scholar. For more information, please contact zhangj@marshall.edu.

EFFICACY OF DEFERASIROX IN PREVENTING COMPLICATIONS OF IRON OVERLOAD IN THE IRON OVERLOADED GERBIL

Dissertation submitted to the

Graduate college of

Marshall University

In partial fulfillment of the

Requirements for

the degree of

Doctor of Philosophy

in Biomedical Sciences

by

Rabaa M. Al-Rousan

Approved by

Eric Blough, Ph.D., Committee Chairperson

Monica Valentovic, Ph.D.

Elsa Mangiarua, Ph.D.

Nalini Santanam, Ph.D.

Todd Green, Ph.D.

.

Department of Pharmacology, Physiology, and Toxicology

Marshall University

Huntington, West Virginia

December 2009

ABSTRACT

EFFICACY OF DEFERASIROX IN PREVENTING COMPLICATIONS OF IRON OVERLOAD IN THE IRON OVERLOADED GERBIL

By Rabaa M. Al-Rousan

Iron overload is a significant, world-wide problem that results in several chronic diseases including cardiovascular, hepatic and pancreatic complications. The newly developed, orally effective, iron chelating agent deferasirox is thought to offer tremendous promise as an alternative to deferoxamine. However, the efficacy and safety profile of deferasirox is not yet clear. In the present study, the efficacy of deferasirox in removing iron from target tissues has been examined using the gerbil model of iron overload.

Deferasirox administration resulted in a significant reduction of iron from cardiac and hepatic tissue. In addition deferasirox reduced iron induced increase in cardiac and hepatic oxidative stress indices including ferritin expression, superoxide production, protein oxidation, and ERK1/2, P38, and JNK phosphorylation. These results indicate that deferasirox is capable of attenuating iron- induced oxidative stress. Continuing our investigation we observed that iron overload was also associated with an increase in hepatic cell death and upregulation of Bax/Bcl-22, Bad expression, and caspase-3 cleavage. These levels were significantly lower with deferasirox treatment suggesting a protective role against cell death.

The primary overall goal of managing iron overload is to reduce/prevent cardiac or other organ complications. In the present study we examined the effect of iron overload on cardiac remodeling and functional parameters, and the

effectiveness of chronic deferasirox administration to prevent or reduce these changes using electro- and echocardiographic procedures. Compared to control, iron overload was associated with left ventricular remodeling, arrhythmia, valve regurgitation, and a decline in cardiac function. These changes were highly preserved with deferasirox treatment.

Following the preceding studies, we demonstrated a reduction in tissue iron with deferasirox treatment in the iron overloaded gerbil model. The findings of the present report established for the first time that deferasirox treatment is capable of attenuating iron-induced increase in oxidative stress indices, tissue ferritin protein expression, cell death, and more importantly, iron related cardiovascular alterations. These findings suggest that deferasirox may be useful in protection against iron-induced organ damage. The present report also provides data elaborating on the possible mechanism by which iron overload contributes to cellular injury, thereby allowing the development of better therapeutic regimens to control this disorder.

ACKNOWLEDGEMENTS

This work would not have been possible without the support of my advisor, Dr. Eric Blough. Eric has been a wonderful source of innovative research ideas, and his encouragement and support helped to instill in me a sense of confidence in my own work. He continually challenged me to see the bigger picture and has helped me to achieve more than I could have ever imagined was possible. Most of my knowledge related to cardiovascular physiology and cell signaling is the direct result of his open-door policy, patience, and dedication to teaching. I will always remember his warm personality and positive outlook which made my graduate experience all the more enjoyable. I'm also grateful to Dr. Ernest Walker from the Department of Pathology. Dr. Walker's knowledge of pathology has been invaluable during my research project. He spent many hours with me reviewing my tissue sections and helped to interpret the research findings. I will always remember his sense of humor and devotion to research. Dr. Blough and Dr. Walker are both wonderful role models and I am honored to have worked with such intelligent and generous individuals.

I'm also grateful to Dr. Monica Valentovic for including me in the Toxicology and Environmental Health Sciences Cluster. Dr. Valentovic is an incredible teacher and researcher and has taught me a great deal about toxicology. I'm also grateful to Dr. Nalini Santanam, Dr. Todd Green, and Dr. Elsa Mangiarua who provided valuable comments throughout the course of my project.

Many thanks to the Laboratory of Molecular Physiology team. I consider myself fortunate to have been a part of such a warm and collegial group of people who set high standards for research, and continually motivate and inspire me. Kevin Rice, Satyanarayana Paturi, Sunil Kakarla, Ravi Arvapalli, Miaozong Wu, Kamran Manzoor, Lucy Darnon, Raja Nawaz, Brent Kidd, and Anjaiah Katta have all been a huge help to me throughout this dissertation. I can't thank them enough for all of their advice and moral support during my research.

I am so grateful to my colleagues in the Byrd Biotechnology Science Center; Jackie Fannin, Lauren Waugh, Mike Brown, and Aileen Marcelo. I am lucky to have such wonderful friends who have made my time at Marshall University a lot more enjoyable experience.

Last but not least, thanks to my incredible family for their never-ending love and support. They have always encouraged me to follow my dreams and have made this experience a reality.

Thank you!

DEDICATION

To my parents Majed & Asia Al-Rousan who believed I could be anything I want to be

To my brothers and sisters Rabab, Sahel, Ruba, Razan, Batool, & Hisham

To my husband, Fadi Alkhateeb, who stood by my side and supported me from A to Z in this Journey

To my little superman, Haroon

&

To all of those who suffer iron overload

TABLE OF CONTENTS

ABSTRACT ii

ACKNOWLEDGEMENTS iv

DEDICATION vi

LIST OF TABLES xiii

LIST OF FIGURES xiv

CHAPTER I - INTRODUCTION 1

PURPOSE 6

SPECIFIC AIMS 7

CHAPTER II – REVIEW OF THE LITERATURE 9

2.1 BODY IRON HOMEOSTASIS 9

2.1.1 Normal distribution of body iron stores 9

2.1.2 Regulation of iron absorption 10

2.1.3 Regulation of systemic iron homeostasis 12

2.1.4 The IRP-IRE regulation of cellular iron homeostasis 13

2.2 DISORDERS OF IRON OVERLOAD 14

2.2.1 Primary iron overload (Hereditary hemochromatosis) 15

2.2.2 Secondary iron overload 16

2.3 CLINICAL MANIFESTATION OF IRON OVERLOAD 18

2.4 MECHANISMS OF IRON MEDIATED TOXICITY 20

2.4.1 Formation of non-transferrin bound iron 20

2.4.2 Chemistry of iron and ROSs 21

2.4.3 Targets of iron-driven cellular damage 23

2.4.4 ROS and iron-mediated intracellular signaling 26

2.5 METHODS OF DETECTING BODY IRON 28

2.5.1 Indirect Assessment 28

2.5.2 Direct assessment 30

2.6 MANAGEMENT OF IRON OVERLOAD 30

2.6.1 Phlebotomy 31

2.6.2 Chelation therapy 32

2.7 ANIMAL MODELS OF IRON OVERLOAD 39

CHAPTER III – MATERIALS AND METHODS 41

3.1 Animal selection and care 41

3.2 Iron loading and chelation 42

3.3 Electrocardiographic procedures 43

3.4 Transthoracic echocardiography 44

3.5 Tissue collection 45

3.6 Tissue iron assessment 46

3.7 Histological analysis 47

3.8 SDS-PAGE and immunoblotting **48**

3.9 Oxidative fluorescent microscopy **49**

3.10 Oxidized Protein Analysis **50**

3.11 In situ cell death detection (TUNEL) **50**

3.12 Statistical analysis **51**

3.13 Materials **51**

CHAPTER IV - RESULTS **53**

DEFERASIROX REMOVES CARDIAC IRON AND ATTENUATES OXIDATIVE STRESS IN THE IRON-OVERLOADED GERBIL **54**

Abstract **55**

Introduction **56**

Results **57**

Characterization of animals 57

Cardiac iron levels 57

Ferritin protein expression 59

Superoxide abundance 60

Protein oxidation 61

Determination of ERK1/2-, p38-, and JNK-MAPK phosphorylation 63

Discussion **64**

Deferasirox decreases cardiac iron and ferritin levels in the iron overloaded gerbil 65

Reduced cardiac iron levels are associated with decreases in tissue ROS 66

Reduced cardiac iron levels are associated with decreases in iron-associated MAPK phosphorylation 67

DEFERASIROX PROTECTS AGAINST IRON-INDUCED HEPATIC INJURY IN MONGOLIAN GERBIL 71

Abstract 72

Introduction 73

Results 74

Characterization of animals 74

Hepatic iron levels 75

Ferritin protein expression 78

Superoxide abundance 79

Cell death 82

Bcl-2 apoptotic signaling 84

Caspase-3 activation 86

Discussion 88

Deferasirox decreases hepatic iron and ferritin levels in the iron-overloaded gerbil 89

Reduced hepatic iron levels are associated with decreases in iron-associated cell death 93

LONG TERM EFFICACY OF DEFERASIROX IN PREVENTING CARDIOVASCULAR COMPLICATIONS IN THE IRON OVERLOADED GERBIL 97

Abstract 98

Introduction 99

Results 101

Characterization of animals 101

Cardiac, aortic, and hepatic iron levels 101

Electrocardiographic evaluation 103

Echocardiographic evaluation (cardiac structure) 105

Echocardiographic evaluation (cardiac function) 108

Discussion 112

Deferasirox removes cardiac, aortic, and hepatic iron 112

Deferasirox treatment preserves cardiac structure and prevents ventricular remodeling 113

Deferasirox treatment preserves cardiac function and reduces incidence of arrhythmia 114

IRON LEVELS IN OTHER TISSUES 116

Pancreatic iron level 116

Kidney iron level 118

CHAPTER V – GENERAL DISCUSSION 119

Effect of iron overload and deferasirox treatment on tissue iron concentration.....120

Effect of iron overload and deferasirox treatment on tissue iron distribution.....121

Effect of iron overload and deferasirox treatment on ferritin protein expression.....121

Effect of iron overload and deferasirox treatment on oxidative stress indices and apoptosis 123

Effect of iron overload and deferasirox treatment on cardiac structure and function.....126

CONCLUSIONS.....129

FUTURE DIRECTIONS 131

REFERENCES.....133

CURRICULUM VITAE 149

LIST OF TABLES

Table 1. Hereditary hemochromatosis; Classification and associated gene products.....15

Table 2. Comparison of the main available iron chelators to an ideal chelating drug 38

Table 3. Deposition of gerbils in the experimental groups.....43

Table 4. Deposition of gerbils in the experimental groups and heart/body weights.....57

Table 5. Deposition of gerbils in the experimental groups and liver/body weights.....75

Table 6. Regression analysis of the relationship between expression levels of specific proteins and TUNEL, HE staining intensity, liver weight, and hepatic iron levels obtained from experimental groups.....88

Table 7. Average heart, liver, and Kidney weights of gerbils in the experimental groups followed for 9 months.....101

LIST OF FIGURES

Figure 1. Schematic representation of iron transport across duodenal epithelial cells 11

Figure 2. Role of cellular iron level in the regulation of ferritin and transferrin receptor expression via the IRE/IRP system 14

Figure 3. Catalysis and autocatalysis in the Haber-Weiss and Fenton reactions leading to the production of the hydroxyl radical, including the liberation by superoxide of free iron from ferritin. 23

Figure 4. Chemical structure of the iron chelating agents in clinical use and their corresponding iron binding ratio. 39

Figure 5. Average iron levels in mg/g tissue weight in cardiac tissue of gerbils in the experimental groups 58

Figure 6. Histological examination of left ventricular myocardium of Ctrl (A), IO (B), and IO+DFR (C) gerbils 59

Figure 7. Effect of iron overload and iron chelation on ferritin heavy chain (FerH) protein expression in cardiac tissue of gerbils in the experimental groups.....60

Figure 8. Detection of cardiac superoxide by dihydroethidium in Ctrl, IO, and IO+DFR groups. 61

Figure 9. Effect of iron overload or deferasirox treatment on cardiac protein carbonylation. 62

Figure 10. Effect of iron overload or deferasirox treatment on the expression of total and phosphorylated ERK1/2-, P38-, and JNK-MAPKs.....64

Figure 11. Average iron levels in mg/g tissue weight in hepatic tissue of gerbils in the experimental groups 76

Figure 12. Iron deposition in hepatic tissue of Ctrl (A), IO (B,C), and IO+DFR (D) gerbils. 77

Figure 13. Western blot analysis of ferritin heavy chain (ferH) protein expression in hepatic tissue of gerbils in the experimental groups. 78

Figure 14. Detection of cardiac superoxide by hydroethidine in Ctrl, IO, and IO+DFR. 80

Figure 15. Representative oxy-blots of hepatic protein isolates from Ctrl, IO, and IO+DFR 81

Figure 16. Representative cross sections showing the changes in nuclei exhibiting DNA strand breakage as determined by TUNEL staining in Ctrl, IO, and IO +DFR. 83

Figure 17. Effects of iron overload and deferasirox treatment on Bax/Bcl-2 protein level in hepatic tissue of gerbils in the experimental groups 85

Figure 18. Effects of iron overload and deferasirox treatment on Bad protein level in hepatic tissue of gerbils in the experimental groups. 86

Figure 19. Effects of iron overload and deferasirox treatment on full length and cleaved caspase-3 in hepatic tissue of gerbils in the experimental groups 87

Figure 20. Average iron levels in mg/g tissue weight in cardiac (A), aortic (B), and hepatic (C) tissue of gerbils in the experimental groups followed for 9 months 102

Figure 21. Histological analysis of cardiac and aortic tissue of Ctrl (A), IO (B), and IO+DFR (C) gerbils. 103

Figure 22. Representative ECGs (standard leads I, II, III) from control, iron overload, a deferasirox (DFR) treated groups followed for 9 months 104

Figure 23. Frequency of electrocardiographic abnormalities observed in Ctrl, IO, and IO+DFR followed for 9 months 105

Figure 24. Effect of iron overload and deferasirox treatment on left ventricular dimension. 107

Figure 25. Representative M-mode echocardiograms from control (A), iron overload (B), and deferasirox treated (C) groups followed for 9 months 108

Figure 26. Effect of iron overload and deferasirox treatment on left ventricular ejection fraction (EF), and fractional shortening (FS) in gerbils from experimental groups. 109

Figure 27. Frequency of cardiac valvular regurgitations observed in control, iron overload, and deferasirox treated groups followed for 9 months.....110

Figure 28. Correlation between cardiac iron concentration and heart/body wt, or echocardiographic parameters 111

Figure 29. Average iron levels in mg/g tissue weight in pancreatic tissue of gerbils in the experimental groups. 117

Figure 30. Histological analysis of pancreatic tissue of control, iron overload, and deferasirox treated groups followed for 3 months 117

Figure 31. Average iron levels in mg/g tissue weight in kidney tissue of gerbils in the experimental groups 118

ABBREVIATIONS

AALAC	Association for accreditation of laboratory animal care
ALB	Albumin
ANOVA	Analysis of variance
BBB	Bundle branch block
BSA	Bovine serum albumin
DH_2O	Distilled water
Dcytb	Duodenal cytochrome b
DMT-1	Divalent metal transporter-1
DFO	Deferoxamine
ECL	Enhanced chemiluminiscence
EDTA	Ethylene diamine tetra acetic Acid
EF	Ejection fraction
ERK	Extracellular signal regulated kinase
FDA	Food and drug administration
FS	Fractional shortening

GDF 15	Growth-differentiation factor 15
HAMP	Hepcidin antimicrobial peptide
HE	Hydroethidine
HJV	Haemojuvelin
HMGCoAR	3-hydroxy-3-methylglutaryl coenzyme A reductase
ICP-AES	Inductively coupled plasma-atomic emission spectrometry
IOD	Integrated optical density
i.p.	Intraperitoneal
IRE	Iron responsive element
IRP	Iron responsive element-binding protein
JNK	c- jun-N-terminal kinase
KRB	Krebs-ringers buffer
LIC	Liver iron concentration
LIP	Labile iron pool
LTCC	L type calcium channels
LVSd	Left ventricular septum dimension during diastole
LVIDd	Left ventricular internal dimension during diastole

LVPWd	Left ventricular posterior wall dimension during diastole
MAPK	Mitogen activated protein kinase
MRI	Magnetic resonance imaging
NTBI	Non-transferrin bound iron
PBS	Phosphate buffered saline
PBST	Phosphate buffered saline with 0.5% tween-20
PLAX	Parasternal long axis view
p.o.	Oral
PSAX	Parasternal short axis view
PUFA	Polyunsaturated fatty acid
PVC	Premature ventricular contraction
ROS	Reactive oxygen species
SAPK	Stress activated protein kinase
SEM	Standard error of mean
SDS-PAGE	Sodium dodecyl sulfate-polyacrylamide gel electrophoresis
SOD	Superoxide dismutase
SQUID	Superconducting quantum interference device

SVT	Supraventricular tachycardia
TBS	Tris buffered saline
TBST	Tris buffered saline with 0.5% tween-20
TGF-β	Transforming growth factor-β
TIBC	Total iron binding capacity
Tf	Transferrin
TfR-1	Transferrin receptor-1
TfR-2	Transferrin receptor-2
t.i.d	Three times daily
T-PER	Tissue protein extraction reagent
TUNEL	Terminal deoxynucleotidyl transferase dUTP nick end labeling
UTR	Untranslated region
VT	Ventricular tachycardia

CHAPTER I

INTRODUCTION

Iron represents a paradox for living systems as it is essential for a wide variety of metabolic processes, but also toxic if in excess. Iron is an indispensable constituent of living cells and organisms due to its involvement in fundamental functions, which, among others, include oxygen transport, transfer of electrons in the respiratory chain and DNA synthesis (Ponka 1999). The chemical basis underlying the versatility of iron for use in such crucial functions is provided by its unique ability to serve as both an electron donor and acceptor, thus representing a potential partner in redox reactions. However, this fundamental chemical property also is the basis of its toxicity, which poses a threat when iron is present in excess or in non-protected forms (Eaton and Qian 2002). Thus, organisms were compelled to solve one of the many paradoxes of life, that is, to keep "free iron" at the lowest possible level through the evolution of specialized molecules for the acquisition, transport, and storage of iron in a soluble, nontoxic form to meet cellular and organismal iron requirements. Moreover, organisms are equipped with highly sophisticated mechanisms that coordinately regulate cellular iron uptake and storage and maintain iron in the intracellular labile pool at appropriate levels (MacKenzie, Iwasaki et al. 2008).

Under conditions of iron overload this tight regulatory mechanism is disrupted resulting in the accumulation of iron in toxic levels (Hershko, Link et al. 1998). Iron overload can result from both primary and secondary causes. Primary iron overload (hereditary hemochromatosis) results from genetic disorders of iron metabolism that

cause excessive absorption of iron from the diet or deficient iron transport within the body. Secondary iron overload results from factors that bypass normal iron metabolic pathways, such as multiple blood transfusions (transfusional iron overload), or acute or chronic iron poisoning (Kushner, Porter et al. 2001). As transfusion therapy for chronic anemias and medical care has become more widely used, iron overload has become increasingly more common (Wood, Skoien et al. 2009). Indeed, it is estimated that in excess of two million individuals in the United States and up to one hundred million humans worldwide acquire some degree of iron overload and tissue accumulation of the metal (Hahalis, Alexopoulos et al. 2005).

Iron toxicity occurs when the amount of circulating iron exceeds the amount of transferrin available to bind it forming non-transferrin bound iron (NTBI) (Andrews 2005). NTBI enters the cell at a high rate through a transferrin receptor-independent pathway leading to iron accumulation in metabolically active tissues such as the liver, heart, and pancreas (Hershko 2007). If left undiagnosed or untreated, excess iron in the body is likely to cause cumulative toxicity which can lead to heart failure, hepatic cirrhosis, and diabetes mellitus (Kohgo, Ikuta et al. 2008).

The mechanism(s) for iron mediated cellular injury are not clear, However, the formation of the highly toxic hydroxyl radical via the Fenton reaction has been suggested to be involved. Hydroxyl radical and other iron-mediated reactive oxygen species (ROS) induce protein oxidation, lipid peroxidation, and DNA damage resulting in loss of normal cellular functions (Galaris and Pantopoulos 2008). Iron is also inhibitory to the proper functioning of ion channels including L-type calcium channels, ryanodine sensitive calcium channels, fast-sodium channels, as well as the rectifier

potassium channels, which can lead to the development of arrhythmias and poor cardiac function in iron overload conditions (Wood, Enriquez et al. 2005).

As the human body has no inherent mechanism to remove excess iron, iron chelating agents are used to treat iron overload. The goal of iron chelation therapy is to remove the amount of iron accumulated and, as required, to reduce the existing iron burden (Hershko, Link et al. 2005; Cianciulli 2008). To date, only deferoxamine is globally available for the first-line treatment of transfusion-related iron overload. While deferoxamine is effective, its administration is burdensome as it requires overnight subcutaneous infusions for 5-7 nights/week. As such, many patients do not undergo iron chelation therapy, exposing themselves to the dangers of iron overload (Chaston and Richardson 2003). Deferiprone has been used for approximately 20 years and is approved in Canada and Europe as a second-line therapy for patients unable to receive deferoxamine or for those in which deferoxamine is less effective (Victor Hoffbrand 2005). Although administered orally, the short half live of deferiprone necessitates multiple daily oral doses for effectiveness. Like deferoxamine, deferiprone therapy is also problematic as it is associated with serious toxic side effects including transaminase increase, joint problems, severe neutropenia, and rare but life threatening agranulocytosis (Kontoghiorghes, Neocleous et al. 2003). Further, because three molecules of deferiprone are required to bind one molecule of iron, the ability of deferiprone to adequately control body iron burden for long periods of time (4-6 years) is questionable. Studies have demonstrated that liver iron levels are not as well controlled with deferiprone as with deferoxamine, with liver iron levels remaining at levels above the threshold associated with systemic complications (Kontoghiorghes, Neocleous et al. 2003).

Despite dramatic gains in life expectancy with deferoxamine chelation therapy, the leading cause of death for iron overload patients remains cardiac disease from cardiac iron deposition (Neufeld 2006). Strategies to reduce cardiac disease by improving chelation regimens have been of the highest priority. These strategies have included development of novel oral iron chelators to improve compliance, improved assessment of cardiac iron status, and careful epidemiologic assessment of outcomes with the current chelation regimens (Hider and Zhou 2005; Taher, Hershko et al. 2009). As a result of these efforts, the novel oral chelator deferasirox was recently approved by the Food and Drug Administration (FDA) for treatment of chronic iron overload in transfusion dependent patients and is the first oral medication approved in the United States for this purpose (Lindsey and Olin 2007; Stumpf 2007).

Unlike deferoxamine, deferasirox is a long acting, orally effective iron chelating agent with favorable patient satisfaction (Neufeld 2006; Cappellini and Pattoneri 2009). Deferasirox is a novel rationally designed iron chelator that has been selected from more than 700 compounds (Cappellini and Piga 2008). It represents a new class of tridentate iron chelators with a high specificity for iron (Cario, Janka-Schaub et al. 2007). Deferasirox possesses oral activity with around 70% bioavailability and long plasma half life (8 to 16 hours) allowing once daily dosing. Deferasirox is well tolerated as it is associated with relatively few side effects and a favorable pharmacokinetic profile (Stumpf 2007). As such, deferasirox is expected to greatly enhance the acceptance of iron chelation therapy, especially for children, and offers a new alternative to the burdensome continuous infusion therapy. However, due to the limited information regarding its effectiveness in removing tissue iron, deferasirox is less frequently prescribed and is only available through specialty pharmacies where patients

have limited access to the medication. Deferoxamine has been the mainstay of iron chelation therapy and still remains the most commonly used for the control of iron overload conditions (Vichinsky, Pakbaz et al. 2008). It is clear that there is a critical lack of information regarding several aspects of deferasirox therapy including whether or not deferasirox is protective against iron-induced cardiac complications. This latter point is important as this information is crucial to establishing the efficacy and safety profile of deferasirox for fully justified use in human iron-overload therapy.

PURPOSE

To date, only one investigation has examined the efficacy of deferasirox in removing tissue iron in the gerbil model (Wood, Otto-Duessel et al. 2006). The effect of deferasirox treatment on cellular indices of oxidative stress and iron-related cardiac complications is not known. To address these gaps in our understanding, the purpose of this research project was to examine: i) whether deferasirox is effective in removing iron from target tissues and whether iron removal, if present, is associated with the reduction of iron overload-related cell injury, and ii) whether deferasirox treatment can reduce or prevent cardiovascular complications associated with iron overload. It is anticipated that the outcomes derived from this study will be invaluable for understanding the efficacy profile of deferasirox and will contribute important insight into the nature of the protective mechanism(s) involved.

SPECIFIC AIMS

Iron overload is an increasing worldwide problem associated with serious complications. The present standard of care for iron overload is iron chelation by deferoxamine; however, the use of this treatment is burdensome, invasive and thus associated with low patient adherence (Brittenham 2003). The new iron chelating agent deferasirox is thought to offer tremendous promise as an alternative to deferoxamine (Olivieri and Brittenham 1997; Franchini 2005; Cappellini and Taher 2008). A review of the scientific literature, however, demonstrates that the efficacy and safety profile of deferasirox is not yet clear (Porter, Taher et al. 2008; Vichinsky 2008). Specifically, information regarding the ability of deferasirox to protect against iron induced cardiovascular alterations is lacking. This is important as it limits the utilization of a potentially useful medication. The long-term goals are to improve our understanding of deferasirox efficacy and safety in an endeavor to help improve the quality of life of patients with iron overload. This study aims to firstly, determine whether deferasirox is capable of removing iron from target tissues and reduce oxidative stress associated with iron overload and secondly, to determine whether deferasirox is protective against iron overload-induced cardiovascular alterations. These goals will be accomplished by the following specific aims.

SPECIFIC AIM I: To determine if deferasirox is able to reduce cardiac iron content, iron-induced ferritin upregulation, and iron-related increases in indices of oxidative stress such as superoxide overproduction, protein oxidation, and the phosphorylation of the mitogen activated protein kinase (MAPK) proteins

extracellular signal regulated kinase 1/2 (ERK1/2)-, p38-, and c-Jun N-terminal kinase (JNK).

SPECIFIC AIM II: To determine if deferasirox is able to reduce hepatic iron content, iron-induced ferritin upregulation, and iron related increases in indices of oxidative stress and the effect of these changes, if present, on the incidence of iron-related changes in cell death and apoptotic signaling.

SPECIFIC AIM III: To determine the long term cardiovascular complications associated with iron overload and to determine if chronic deferasirox administration is able to prevent/reduce these complications including those related to cardiac remodeling and functional abnormalities.

CHAPTER II

REVIEW OF THE LITERATURE

The following chapter presents a review of the pertinent literature concerning the present study. Specifically, the following areas will be addressed: Body iron homeostasis, disorders of iron overload, mechanisms of iron mediated toxicity, methods of detecting body iron, management of iron overload, and animal models of iron overload.

2.1 BODY IRON HOMEOSTASIS

2.1.1 Normal distribution of body iron stores

The total amount of iron in the human body is approximately 3-4 g (Andrews 2005). The vast majority of body iron (about 2.5 g) is contained in hemoglobin. A significant portion of iron (~ 400 mg) is devoted to cellular proteins that use iron for important cellular processes like storing oxygen (myoglobin), or performing energy-producing redox reactions (cytochromes). Approximately 3-4 mg circulates in the plasma as an exchangeable pool bound to transferrin. This chelation serves three purposes: it renders iron soluble under physiologic conditions, it prevents iron-mediated free radical toxicity, and it facilitates transport into cells (MacKenzie, Iwasaki et al. 2008). The sum of all iron binding sites on transferrin constitutes the total iron binding capacity (TIBC) of plasma. Under normal circumstances, about one-third of transferrin iron-binding pockets are filled and non-transferrin-bound iron in the circulation is virtually nonexistent.

Physiologically, most stored iron (~1g) is bound by ferritin molecules; the largest amount of ferritin-bound iron is found in hepatocytes, bone marrow, and spleen (Lash and Saleem 1995). Of these, the liver is considered the primary physiologic source of reserve iron in the body. Reticuloendothelial cells store iron as part of the process of phagocytosis and breakdown of aging red cells. These cells extract iron from heme and return it to the circulation bound to transferrin (Andrews and Schmidt 2007). There is no specific physiological mechanism for iron excretion from the body and thus the amount of body iron is controlled by the rate of its absorption by duodenal enterocytes. On a daily basis, adult humans absorb 1–2 mg of iron from the diet to compensate for non-specific iron losses such as that which occurs following desquamation or blood loss (Donovan, Roy et al. 2006).

2.1.2 Regulation of iron absorption

It is thought that the first step of iron absorption involves the reduction of Ferric iron Fe(III) in the intestinal lumen by ferroreductase Dcytb (duodenal cytochrome b), to the more soluble form Fe(II) (Pantopoulos 2004). Ferrous iron Fe(II) is then transported across the basolateral membranes of the enterocytes by divalent metal transporter 1 (DMT1) (Figure 1, Panel A). The export of Fe(II) across the basolateral membranes of enterocytes to circulation is mediated by ferroportin. This step is coupled with reoxidation of ferrous to ferric iron by membrane-bound hephastin (or its plasma-soluble homologue ceruloplasmin) (Donovan and Andrews 2004; Pantopoulos 2004). Plasma iron is immediately scavenged by the plasma iron carrier transferrin (Tf) in 2:1 ratio. Plasma Tf binds to its cell surface receptor (TfR) and the complex is internalized by endocytosis. Acidification of the endosomes results in the release of ferric iron from Tf

and reduction and subsequent transport of ferrous iron across the endosomal membranes by DMT1. The pathway is completed by recycling of the apo Tf-TfR complex to the cell surface and release of apoTf which is transported back to the circulation to carry new iron ions (Figure 1, Panel B).

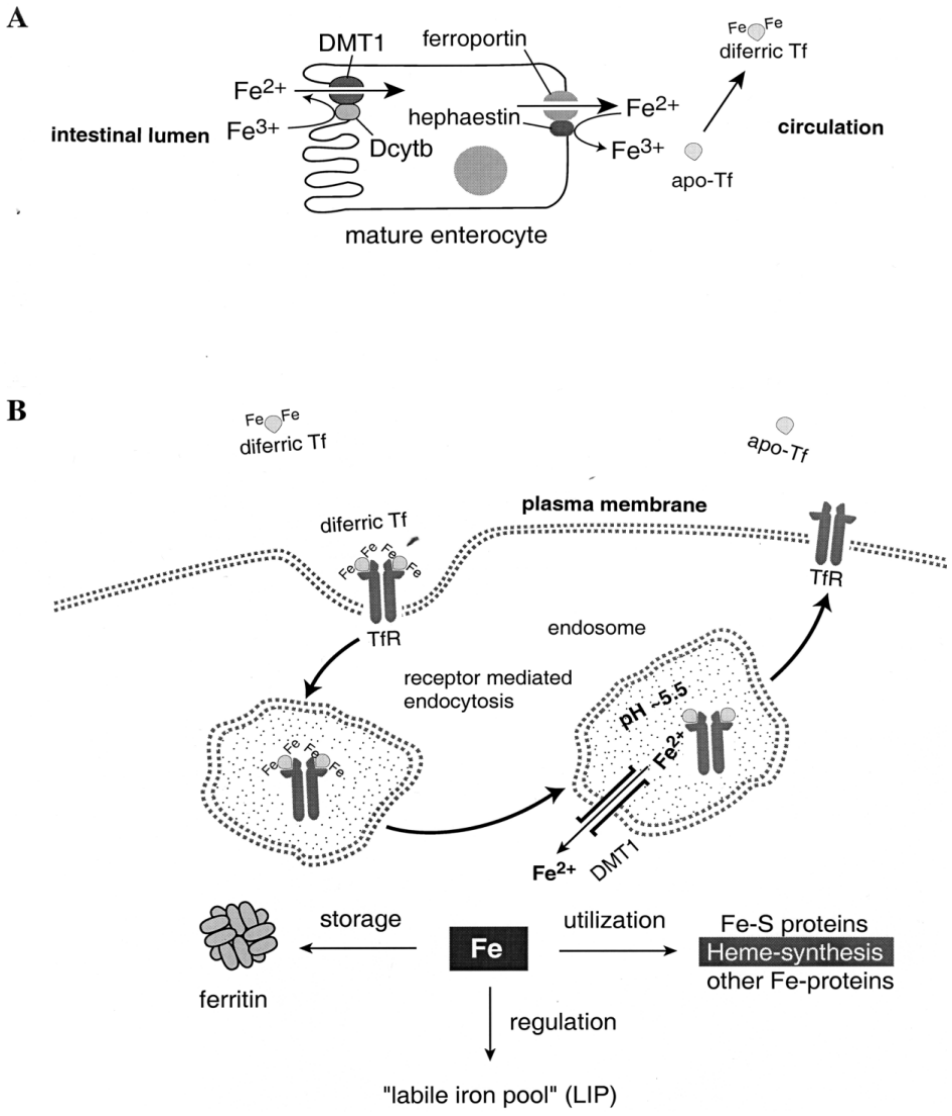

Figure 1. (A) Schematic representation of iron transport across duodenal epithelial cells. (B) Cellular iron uptake from transferrin (Tf) via receptor mediated endocytosis. ***(Pantopoulos 2004)***

Following its release from transferrin within endosomes, iron is thought to enter the labile iron pool (LIP) where it becomes available for intracellular use or for storage in ferritin (Andrews 2008). Another source of iron for this pool comes from the breakdown of nonheme- and heme- iron-containing proteins. It has been proposed that iron in this pool may form complexes with citrate, sugars, various amino acids, pyridoxal, or nucleotides, but the details regarding the regulation of this pool remain elusive (Kakhlon and Cabantchik 2002).

2.1.3 Regulation of systemic iron homeostasis

Iron homeostasis in mammals is regulated at the level of intestinal absorption, as there is no excretory pathway for iron. Hepcidin, a circulating peptide hormone, is the master regulator of systemic iron homeostasis, coordinating the use and storage of iron with iron acquisition (Hershko 2006). This hormone is primarily produced by hepatocytes and is a negative regulator of iron entry into plasma (Sela 2008). Hepcidin acts by binding to ferroportin, an iron transporter present on cells of the intestinal duodenum, macrophages, and cells of the placenta (Ramey, Deschemin et al. 2009). Binding of hepcidin induces ferroportin internalization and degradation resulting in reduced iron entry into plasma. Conversely, decreased expression of hepcidin leads to increased cell surface ferroportin and increased iron absorption. Plasma hepcidin levels are regulated by different stimuli, including cytokines, plasma iron, anemia, and hypoxia (Ganz 2003; De Domenico, Ward et al. 2007). Overexpression of hepcidin has been linked to the development of anemia, while low hepcidin is associated with hereditary hemochromatosis (De Domenico, Ward et al. 2007).

2.1.4 The IRP-IRE regulation of cellular iron homeostasis

The iron-responsive element, (IRE), is present in the mRNA of various iron regulatory proteins including ferritin and the transferrin receptor. Enlargement of the intracellular transit iron pool, in general, leads to a stimulation of ferritin synthesis and decrease in the expression of transferrin receptors (Pantopoulos 2004).

Iron-dependent regulation of both ferritin and transferrin receptors is mediated by virtually identical IREs. The IREs are hairpin structures recognized by iron-regulatory protein-1 (IRP1). When cellular iron becomes limiting, the IRP-1 becomes bound to the IRE located within the 5' UTR of the ferritin mRNA and this represses the translation of ferritin (Figure 2, upper panel). A similar mechanism regulates the expression of transferrin receptor. Under conditions of low iron, IREs within the 3' UTR of the transferrin receptor mRNA become bound by IRP-1, which in turn stabilizes the transcript against ribonuclease activity (Figure 2, lower panel). Together, these responses lead to increased iron uptake and reduced iron storage. Conversely, the expansion of the labile iron pool inactivates IRP-1, resulting in an efficient translation of ferritin mRNA and rapid degradation of transferrin receptor mRNA. These responses lead to decreased iron uptake and elevated iron storage (Ponka 1999; Munoz, Villar et al. 2009).

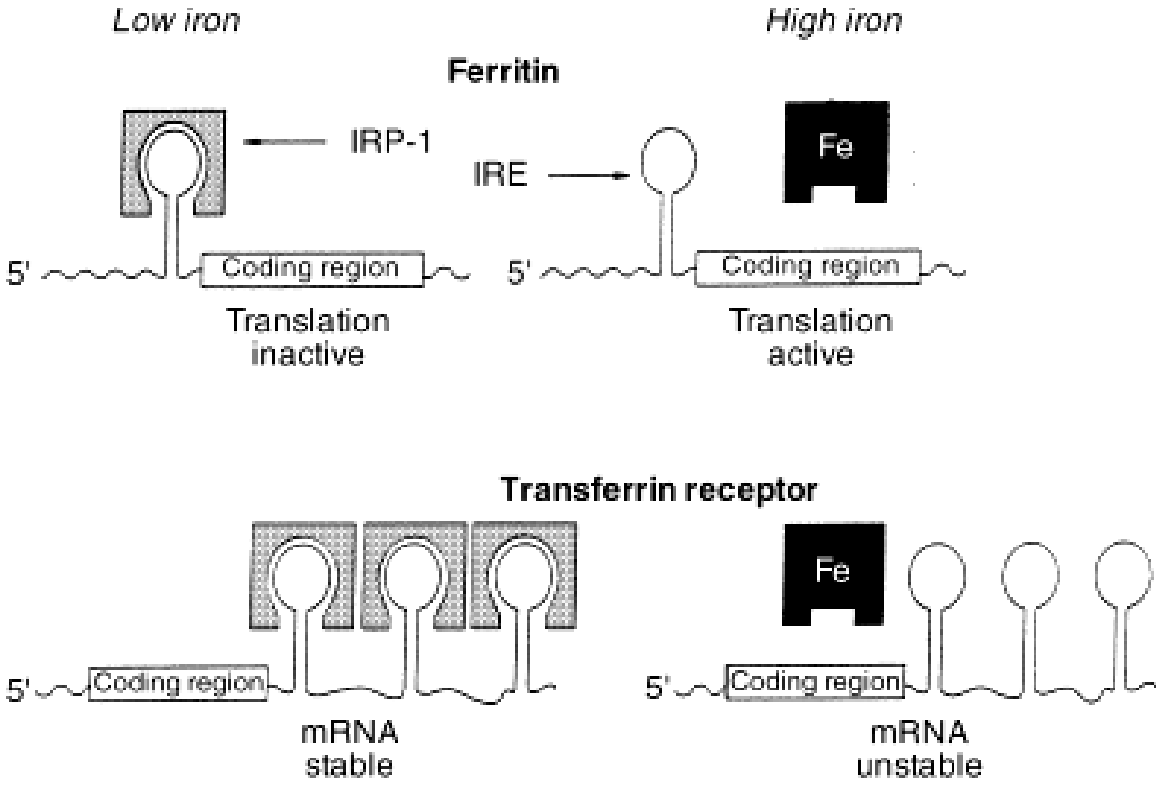

Figure 2. Role of cellular iron level in the regulation of ferritin and transferrin receptor expression via the IRE/IRP system. ***(Ponka 1999)***

2.2 DISORDERS OF IRON OVERLOAD

Iron overload is a group of disorders caused by the accumulation of iron in the body. These disorders can be either acute or chronic in nature (Heeney and Andrews 2004). Acute iron overload is typically caused by excess iron intake such as that seen after the accidental ingestion of large quantities of iron-containing multivitamins, or iron supplements in young children. Acute iron overload has been found to irritate the stomach lining, and is associated with nausea and vomiting. If the intake is excessive, damage to internal organs (e.g. brain and the liver), metabolic acidosis and death oftentimes result (Singhi, Baranwal et al. 2003). In contrast to that observed for acute iron overload, the manifestation of chronic iron overload appears to be more varied as

this disorder can be caused by primary (genetically determined) conditions or arise secondary to other conditions (Piperno 1998).

2.2.1 Primary iron overload (Hereditary hemochromatosis)

Hereditary hemochromatosis is caused by mutation of genes involved in regulation of iron homeostasis (Table 1). The majority depend on defined- HFE gene mutations discovered in 1996 and are referred to as “classical hemochromatosis” (Janssen and Swinkels 2009).

Table 1. Hereditary hemochromatosis; Classification and associated gene products

Classification	**Associated gene product**
Type I: "classical" hemochromatosis	HFE
Type IIA: Juvenile hemochromatosis	Hemojuvelin “HJV”
Type IIB: Juvenile hemochromatosis	Hepcidin antimicrobial peptide “HAMP”
Type III	Transferrin receptor-2 “TFR-2”
Type IV: African iron overload	Ferroportin
Neonatal hemochromatosis	Unknown
Aceruloplasminemia	Ceruloplasmin
Congenital atransferrinemia	Transferrin
GRACILE syndrome	BCS1L

Other gene mutations have been discovered later and are grouped together as "non-classical hereditary hemochromatosis" or "non-HFE hemochromatosis". Most types of hereditary hemochromatosis have autosomal recessive inheritance, while type IV has autosomal dominant inheritance (Janssen and Swinkels 2009).

While the genetic mutations causing several variants of hemochromatosis have been identified, the exact function of these genes is yet unknown. However, most genetic forms of iron overload seem to be associated with hepcidin deficiency resulting in increased intestinal absorption of iron (Lee and Beutler 2009). An exception is type IV hemochromatosis where ferroportin becomes mutated resulting in a deficiency in the action of hepcidin (Fernandes, Preza et al. 2009).

2.2.2 Secondary iron overload

Secondary iron overload may result from chronic blood transfusion, from increased gastrointestinal absorption of iron, or from some combination thereof (Kushner, Porter et al. 2001).

Chronic blood transfusion: An adequate transfusion program can sustain life in patients with severe chronic refractory anemia, but transfusion therapy alone produces a progressive accumulation of the iron contained in transfused red cells. In patients with severe congenital anemias, such as thalassemia major and the Blackfan-Diamond syndrome, regular transfusions can prevent death from anemia in infancy and permit normal growth and development during childhood but, if left uncontrolled, may result in severe iron overload by adolescence (Borgna-Pignatti, Rugolotto et al. 2004; Chen, Tseng et al. 2009). Treatment of acquired transfusion-dependent anemias, such as aplastic anemia, pure red cell aplasia, and hypoplastic or myelodysplastic disorders,

among others, may also result in the development of marked iron overload (Malcovati 2009). In addition, although sickling disorders (e.g., sickle cell anemia) are not transfusion-dependent, these patients may acquire a considerable iron load from repeated transfusions for the prevention of stroke, painful crises, and other recurrent complications (Ballas 2001).

About 200 to 250 mg of iron is added to the body iron load with each unit of transfused red cells. Most transfusion-dependent patients require 200 to 300 ml/kg of blood a year; for example, a 70 kg adult requires about two to three units of blood every 3 to 4 weeks, adding about 6 to 10 g of iron a year (Agarwal 2009). The severity of iron toxicity seems to be related to the magnitude of the body iron burden. Almost all patients who have been treated with transfusion alone and have received 100 or more units of blood (about 20 to 25 g of iron) develop cardiac iron deposits, often in association with signs of hepatic, pancreatic, and endocrine damage (Brittenham 2006)

Ineffective erythropoiesis: This disorder occurs in patients with congenital dyserythropoietic anemia, pyruvate kinase deficiency, thalassemia major, thalassemia intermedia, sideroblastic anemia, some myelodysplastic anemias, and other anemic disorders in which the incorporation of iron into hemoglobin is impaired (Sarnaik 2005; Rivella 2009). As a result of ineffective erythropoiesis, plasma iron turnover increases drastically, resulting in excessive production of growth differentiation factor 15 (GDF15) (Tanno, Bhanu et al. 2007). GDF15 is a member of the transforming growth factor-β (TGF-β) superfamily which, at high levels, is able to suppress hepcidin production, resulting in increased intestinal iron absorption and release of catabolic iron from macrophages (Gardenghi, Marongiu et al. 2007).

Chronic liver disease: Some patients with chronic liver disease, for example alcoholic cirrhosis, may experience minor or modest degrees of iron loading as a result of increased dietary iron absorption (Schulz and Sanft 1984; Duane, Raja et al. 1992). The mechanisms responsible for the increased gastrointestinal iron uptake have not been identified, although ineffective erythropoiesis and hyperferremia associated with alcohol-induced folate and sideroblastic abnormalities have been proposed as etiologic factors (Gentry-Nielsen, Preheim et al. 2001; Harrison-Findik 2007). Body iron stores are increased only to a minor degree, but in alcoholic cirrhosis, the higher the liver iron the shorter the survival.

Focal sequestration of iron: Focal iron sequestration is found in rare disorders, including idiopathic pulmonary hemosiderosis and renal hemosiderosis (Piperno 1998). Such abnormal iron deposition is also associated with neurologic abnormalities including Friedreich ataxia, in which decreased iron-sulphur-cluster and heme formation leads to mitochondrial iron accumulation primarily in sensory neurons, myocardium and endocrine glands (Boddaert, Le Quan Sang et al. 2007; Gucev, Tasic et al. 2009).

2.3 CLINICAL MANIFESTATION OF IRON OVERLOAD

Because humans lack a physiologic means of eliminating excess iron, iron progressively accumulates and eventually damages the liver, heart, pancreas, and other organs with death usually occurring as a result of cardiac failure (Hershko 2007). In younger patients, the iron burden results in growth failure and, in adolescence, delayed or absent sexual maturation (Nabavizadeh, Anushiravani et al. 2007; Safarinejad 2008). The precise manifestations of iron overload, however, depend on different factors

including, the underlying abnormality, body iron burden, the rate at which the increase in body iron has occurred and the distribution of the excess iron between storage sites (Kontoghiorghes, Pattichi et al. 2000; Wood, Skoien et al. 2009).

Initially, the deleterious effects of iron loading are not clinically significant, and manifest as discomfort in hand joints, increased skin pigmentation and fatigue (MacKenzie, Iwasaki et al. 2008). As tissue iron accumulates, liver damage ranging from fibrosis to cirrhosis can develop in affected individuals. In hereditary hemochromatosis, hepatomas develop almost exclusively in patients with hepatic cirrhosis and are the ultimate cause of death in 20% to 30% of these patients (MacKenzie, Iwasaki et al. 2008).

Iron overload also leads to iron deposition in the heart and endocrine tissues. Chronically elevated cardiac iron concentrations impair diastolic function, increase the propensity for arrhythmias, and, ultimately, cause end stage cardiomyopathy (Wood, Enriquez et al. 2005). Iron overload cardiomyopathy, defined as the presence of systolic or diastolic cardiac dysfunction secondary to increased iron deposition, is an important cause of heart failure and is the primary determinant of survival in patients with iron overload (Wood, Enriquez et al. 2005; Lekawanvijit and Chattipakorn 2009). Cardiomyopathy develops initially as a severe diastolic dysfunction; in the later stages however, heart failure progresses to severe systolic dysfunction and ventricular dilation. Death ensues promptly in the later stages due to cardiac failure and/or severe arrhythmias (Bartfay 1999). Other targets of iron deposition include pancreas (glucose intolerance, diabetes), posterior pituitary gland (secondary hypogonadism), joints (arthropathy), and neurons (neurological abnormalities) (Gamberini, De Sanctis et al. 2008) .

2.4 MECHANISMS OF IRON MEDIATED TOXICITY

2.4.1 Formation of non-transferrin bound iron

Iron toxicity results when iron in the circulation exceeds serum transferrin iron-binding capacity, leading to the appearance of non-transferrin-bound iron (NTBI) (Eaton and Qian 2002). The exact nature of NTBI is not clear, but it is believed to consist of labile low-molecular weight complexes of iron with plasma components such as albumin, citrate and phosphate (Cabantchik, Breuer et al. 2005). Unlike transferrin–bound iron, NTBI enters cells via a transferrin receptor-independent mechanism and at a rate exceeding the normal uptake of transferrin iron. NTBI uptake into cells bypasses the normal negative feedback regulatory mechanisms that control cellular iron uptake and metabolism. Once NTBI enters the cells, it is rapidly buffered by ferritin, limiting its potential for redox damage or other harmful interactions in the cell (Wood, Enriquez et al. 2005). Nonetheless, all buffering systems have limited capacity or can be disrupted by other factors. Thus, excess uptake of NTBI, combined with the lack of an effective iron excretory pathway, leads to the expansion of the labile intracellular iron pool (LIP), resulting in the formation of highly-reactive oxygen free radicals (Kruszewski 2003; Ozment and Turi 2009).

Ferritin molecules aggregate over time to form clusters, which are engulfed by lysosomes and degraded (Iancu et al. 1977, Bridges 1987). The end-product of this process, hemosiderin, is an amorphous agglomerate of denatured protein and lipid interspersed with iron oxide molecules (Wixom et al. 1980). Although the iron enmeshed in this insoluble compound constitutes an endstage product of cellular iron storage, it remains in equilibrium with soluble ferritin. Ferritin iron, in turn, is in equilibrium with iron complexed to low molecular weight carrier molecules (Konijn, Glickstein et al. 1999).

Therefore the introduction into the cell of an effective chelator captures iron from the low molecular weight "toxic iron" pool, draws iron out of ferritin, and eventually depletes iron from hemosiderin as well, though only very slowly (Crichton and Ward 2003).

2.4.2 Chemistry of iron and ROSs

The initial reactive oxygen intermediate produced in most cases of oxidative stress is superoxide ($O_2^{\cdot-}$) (Turrens 2003). Cellular sources of $O_2^{\cdot-}$ include mitochondria and lysosomes, with the production of this molecule exacerbated under conditions of hypoxia or ischemia. Once formed, superoxide is rapidly converted to H_2O_2 by the action of superoxide dismutases (SOD):

$$2O_2^{\cdot-} + 2H^+ \rightarrow H_2O_2 + O_2$$

Neither $O_2^{\cdot-}$ nor H_2O_2 are strong oxidizing agents, however when free iron ions are available, Fenton-type reaction takes place (Galaris and Pantopoulos 2008), producing the extremely reactive hydroxyl radical ($^{\cdot}HO$):

$$Fe^{2+} + H_2O_2 \rightarrow Fe^{3+} + OH^- + OH^{\bullet}$$

Superoxide anion may reduce Fe^{3+} back to Fe^{2+} (Haber-Weiss reaction), thus allowing iron to act as an autocatalyst of the reaction (Kell 2009):

$$Fe^{3+} + O_2^{\cdot-} \rightarrow Fe^{2+} + O_2$$

In addition, Fe^{2+} and certain Fe^{2+} chelates react with lipid hydroperoxides (LOOH), as they do with hydrogen peroxide, splitting the O–O bond. This gives rise to the alkoxyl radical (LO·), which can also abstract H· from polyunsaturated fatty acids and from hydroperoxides (Kell 2009):

$$LOOH + Fe^{2+} \rightarrow OH^{-} + LO^{\bullet} + Fe^{3+}$$

Alternatively, Fe^{3+} can initiate the reaction with lipid hydroperoxides (LOOH). The resulting peroxyl radicals (LOO·) can continue propagation of lipid peroxidation:

$$LOOH + Fe^{3+} \rightarrow H^{+} + LOO^{\bullet} + Fe^{2+}$$

Furthermore, elevated superoxide liberates free iron from ferritin, thereby providing a positive feedback loop where the increase in the amount of free iron catalyses the production of further hydroxyl radical formation (Keyer and Imlay 1996) (figure 3).

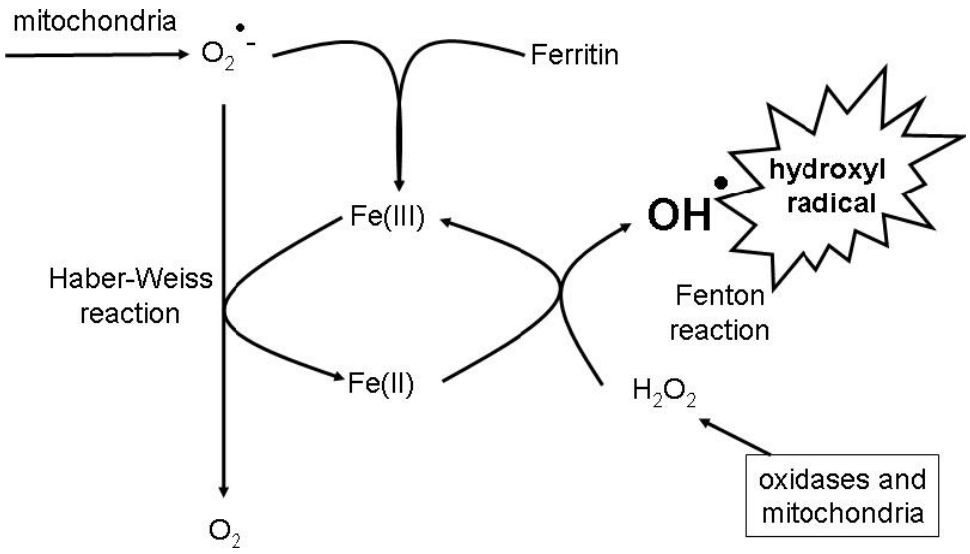

Figure 3. Catalysis and autocatalysis in the Haber-Weiss and Fenton reactions leading to the production of the hydroxyl radical, including the liberation by superoxide of free iron from ferritin. ***(Kell, 2009)***

2.4.3 Targets of iron-driven cellular damage

Given the tendency of transition metals such as iron to amplify oxidant damage, the fact that organs with very active mitochondria are targeted in iron overload disorders is probably no coincidence (Eaton and Qian 2002). The liver and heart have high steady-state production of $O_2^{\bullet -}$ and H_2O_2, largely derived from mitochondrial activity (Han, Williams et al. 2001). The pancreatic beta cell is also rich in mitochondria and is highly sensitive to oxidant-generating substances (Maiese, Chong et al. 2007). However, although the hepatic, cardiac, and pancreatic beta cell pathologies caused by iron overload probably involve an iron-driven oxidative component, the precise mechanisms through which reactive iron conspires with oxygen to amplify cellular oxidant damage remain unknown. The fundament of iron-mediated oxidant damage may be the tendency of free iron to associate with oxidizable targets within cells (e.g.,

polyunsaturated fatty acids, proteins, or DNA) and to engage in site-specific oxidation reactions (Lucesoli and Fraga 1995). These latter reactions have often been ascribed to the hydroxyl radical but more likely represent multiple reactions arising from complexes of iron bound to particular target molecules and oxidants which, upon reaction with the iron, form a highly oxidizing intermediate (ferryl or perferryl) (Eaton and Qian 2002).

Iron catalyzes the production of free radicals which can directly interact with many biological macro- and small molecules, leading to oxidative membrane damage throughout the cell (Galaris and Pantopoulos 2008). Excessive free radical generation leads to increased lipid peroxidation, protein oxidation, and gene modulation, triggering cellular damage and antioxidant depletion (Livrea, Tesoriere et al. 1996; Brown, Kinter et al. 1998; Bartfay, Dawood et al. 1999). Metal-catalyzed damage to proteins includes loss of histidine residues, bityrosine cross links, oxidative scission, the introduction of carbonyl groups (through, e.g., oxidative deamination), and the formation of protein-centered alkyl, alkylperoxyl, and alkoxyl radicals (Valko, Rhodes et al. 2006). Polymerization and denaturation of proteins and proteolipids form insoluble structures typically known as lipofuscin (Kell 2009). Elevated cellular iron levels also leads to DNA damage. Products of reactions between DNA, iron, and oxidants are not yet fully elucidated but include strand breaks, oxidatively modified bases, and DNA protein cross-links (Meneghini 1997; Gao, Campian et al. 2009). The relative importance of all these products in long-term iron-mediated DNA damage is not yet known. Alterations in gene expression and gene modulation have also been reported (Barouki and Morel 2001; Parkes and Templeton 2003); however, whether these changes represent

controlled interactions through iron response elements or nonspecific effects from redox damage is unclear.

Iron is preferentially taken up by mitochondria and lysosomes. In the mitochondria, iron accumulation results in peroxidation of polyunsaturated fatty acids (PUFA) within membrane phospholipids (Britton, O'Neill et al. 1990), disruption of mitochondrial respiratory enzymes (Bacon, O'Neill et al. 1993; Link, Saada et al. 1998) and mitochondrial DNA damage (Gao, Campian et al. 2009). Accumulation of iron within the cellular lysosomal compartment will sensitize the lysosomes to damage and rupture with release of damaging lysosomal digestive enzymes into the cytoplasm of the cell (Stal, Glaumann et al. 1990). Minimal release of lysosomal enzymes may induce transient reparative autophagocytosis, while moderate lysosomal rupture is followed by caspase activation and apoptosis (Kurz, Terman et al. 2008). Severe oxidative stress, resulting in massive lysosomal breakdown, is associated with necrosis (Kurz, Terman et al. 2008).

Iron can also directly interact with ion channels. For example, ferrous iron has similar size and charge to that of calcium ions and can permeate through cardiac L-type calcium channels (LTCC) (Oudit, Sun et al. 2003). Fe^{2+} slows Ca^{2+} current inactivation resulting in increase in the time integral of the Ca^{2+} current and net Ca^{2+} influx, which may possibly contribute to the impaired diastolic function observed during the early stages of iron overload (Oudit, Trivieri et al. 2006). With higher concentrations of ferrous iron there is a reduction in Ca^{2+} current due to competition with ferrous iron. This may contribute to the systolic dysfunction that is characteristic of more advanced iron-overload cardiomyopathy (Oudit, Trivieri et al. 2006) . Ferrous iron can also directly interact with the ryanodine sensitive calcium channel in the sarcoplasmic reticulum

(Kim, Giri et al. 1995). This channel is responsible for activation of contraction and also modulates calcium reuptake in the sarcoplasmic reticulum.

In addition to its effects on calcium homeostasis, intracellular iron impairs the function of membrane-bound fast-sodium channels as well as delayed rectifier potassium currents (Wood, Enriquez et al. 2005). The former channels are responsible for the rapid upstroke of the cardiac action potential. Channel blockage or other interference will slow cardiac conduction, and delay action potential spread across the myocardium (Wood, Enriquez et al. 2005). Hence it is not surprising that iron overload results in arrhythmias and poor cardiac function.

2.4.4 ROS and iron-mediated intracellular signaling

Mammalian cells exhibit a broad spectrum of responses toward oxidative stress, which is dependent on the severity of the stress encountered and the availability of catalytically active iron (Deb, Johnson et al. 2009). The members of mitogen-activated protein kinases (MAPKs), including ERK, JNK, and p38 subfamilies, have all been shown to be activated in response to oxidant injury and therefore could potentially contribute to influencing cell survival (Griendling, Sorescu et al. 2000). Each MAPK subtype is activated by phosphorylation on threonine and tyrosine residues by upstream dual-specificity kinases. In general, the ERK cascade appears to mediate signals promoting cell proliferation, differentiation or survival, whereas the p38 and JNK cascades appear to be involved in the cell responses to stresses (Martindale and Holbrook 2002). However, activation of distinct MAPK subtypes is dependent on the cell type and the stimuli. It was recently suggested that iron loading *in vitro* induces p38 and

ERK 1/2 phosphorylation associated with an increase in ROS levels (Antosiewicz, Ziolkowski et al. 2007).

Ferritin represents the main iron storage protein, and its concentration is mutually related with the cytosolic level of labile iron. Changes in iron availability regulate ferritin expression primarily at the translational level through specifically regulated protein-RNA interactions between IRPs and IREs as described earlier in this chapter. In iron overload conditions, serum ferritin expression is increased, which is used as one common diagnostic tool to reflect body iron status (Piperno 1998).

Other pathways that are clearly linked to ROS include the induction of programmed cell death (apoptosis) (Orrenius 2007). Apoptosis is a genetically controlled response to eliminate unwanted cells that is involved in the regulation of cell number under several physiological and pathological conditions. High levels of ROS can lead to necrotic cell death, whereas low levels of ROS have been shown to induce apoptotic cell death (Denecker, Vercammen et al. 2001). Apoptosis is regulated through different mechanisms, including the expression of the members of the Bcl-2 protein family consisting of pro- and anti-apoptotic peptides interacting with each other by forming homo- and heterodimers. Bcl-2 is thought to act as negative regulator of apoptosis and has been thought to protect cells from ROS (Li, Ueta et al. 2004), although the mechanism by which this latter event occurs remains unclear. Conversely, Bax has been implicated to promote or accelerate cell death with recent data showing that Bax may be able to induce apoptosis by both caspase-dependent and -independent mechanisms. Recent studies have suggested that iron induces cell apoptosis via the promotion of Bax translocation, cytochrome c release, and caspase-3 activation (Yajun 2005). Whether iron exerts its signaling effects independently or it simply participates in

reactions of ROS-mediated signaling is presently unknown and needs further investigation.

2.5 METHODS OF DETECTING BODY IRON

Both direct and indirect means for the assessment of body iron are available but no single indicator or combination of indicators is ideal for the evaluation of iron status in all clinical circumstances. As 90% of excess iron is deposited in the liver, measurement of hepatic iron stores provides the most quantitative means of assessing the body iron burden and may be considered the reference method for comparison with other techniques (Vermylen 2008). The invasive nature of the liver biopsy, however, means that other markers such as serum ferritin levels are frequently employed. Other approaches using biomagnetic susceptometry and magnetic resonance imaging (MRI) are also being assessed in order to identify an accurate, low-risk, and convenient approach to assessing patient iron status.

2.5.1 Indirect Assessment

Serum ferritin: Serum ferritin is easily measured using a commercially available kit. A ferritin level constantly below 2500 µg/L has been shown to reduce the risk of cardiac complications, but a target value of 1000 µg/L is recommended. Factors such as inflammation, ascorbate status, and hepatitis can affect serum ferritin levels (Olivieri, De Silva et al. 2000). Therefore, results should be interpreted with caution and a trend in the evolution of serial measurements is a better index than day-to-day variation. In patients with transfusion-dependent diseases, chelation should be initiated after 10–20 blood transfusions or when ferritin level rises above 1000 µg/L (Vermylen 2008).

24–hour deferoxamine-induced urinary iron excretion: This includes measuring the amount of chelated iron in the urine after a single intramuscular dose or prolonged subcutaneous infusion of deferoxamine. The usefulness of this method has several limitations in the accurate assessment of body iron burden (Olivieri and Brittenham 1997). Most important is the poor correlation between urinary iron excretion and hepatic iron concentration which develops, at least in part, because the relative amounts of iron excreted into stool and urine vary with the dose of deferoxamine administered, body iron burden, and erythroid activity (Olivieri and Brittenham 1997). Chelator-induced urinary iron excretion is also vulnerable to extraneous influences by infection, inflammation, the activity and effectiveness of erythropoiesis, extramedullary hematopoiesis, liver disease, and ascorbic acid deficiency.

Magnetic resonance imaging (MRI): MRI measures tissue iron concentration indirectly by detecting the paramagnetic influences of storage iron (ferritin and hemosiderin) on proton resonance behavior. Iron deposits act like little magnets when placed in a strong magnetic field, disrupting coherence among the emitted protons and darkening the image more quickly (Vermylen 2008). Liver iron content (LIC) determined using MRI shows excellent correlation with that obtained from liver biopsy (Papakonstantinou, Maris et al. 1995). Furthermore, MRI has the ability to evaluate the entire organ and gives more accurate measurement of LIC, particularly in patients with heterogeneous iron content (Li, Aisen et al. 2004). Although very promising, the widespread use of this method in many parts of the world may be hampered by the need for expensive equipment and trained personnel to perform the scan.

2.5.2 Direct assessment

Liver biopsy: The measurement of liver iron content is the most accurate method for assessing body iron and thus it is referred to as the “gold standard” as there is a high correlation between LIC and total body iron (Alustiza, Castiella et al. 2007). The procedure also provides information about the severity of the liver disease. Liver biopsy, however, is an invasive technique that is associated with some pain and risk of hemorrhage and infection. Thus, it is not indicated for routine assessment.

Superconducting quantum interference device (SQUID): SQUID provides a direct measure of tissue iron that is based on a fundamental physical property of ferritin and hemosiderin (Olivieri et al, 1997). SQUID is capable of measuring very small changes in magnetic flux. Iron stored as ferritin and hemosiderin is the only relevant paramagnetic material in the human body. The magnitude of paramagnetic response is directly related to the amount of iron in a certain volume of tissue (Vermylen 2008). This is a noninvasive method, with a linear correlation with LIC assessed by biopsy. However, equipment availability is extremely limited.

2.6 MANAGEMENT OF IRON OVERLOAD

Iron overload treatment is dependent on the underlying condition. Phlebotomy is currently the recommended iron overload treatment for most patients with hereditary excess iron, although iron chelation therapy could be an option for patients who cannot or choose not to undergo phlebotomy (Brissot 2009). For transfusional iron overload, iron chelation therapy is the first-line therapy (Cappellini 2005).

2.6.1 Phlebotomy

The treatment of choice for hereditary hemochromatosis is phlebotomy to reduce the body iron levels to normal or near-normal and maintain them in that range (Tavill 2001). In patients with hereditary hemochromatosis who develop cardiac failure, the use of both phlebotomy and chelation therapy has been suggested. Phlebotomy therapy should be started as soon as the diagnosis of the homozygous state for hereditary hemochromatosis has been established, as postponement is likely to increase the risk of organ damage from iron overload. The phlebotomy program should remove 500 ml of blood (containing 200 to 250 mg of iron) once weekly or, for heavily loaded patients, twice weekly until the patient is iron deficient (Brissot 2009).

In patients with hereditary hemochromatosis, prolonged treatment is often needed. For example, if the initial body iron burden is 25 g, complete removal of the iron burden with weekly phlebotomy may require 2 years or more. After the iron load has been completely removed, a lifelong program of maintenance phlebotomy is required to prevent reaccumulation of the iron burden (Tavill 2001). Typically, phlebotomy of 500 ml of blood every 3 to 4 months is needed. If phlebotomy therapy removes the iron load before diabetes mellitus or cirrhosis develops, the patient's life expectancy is expected to be normal. If cirrhosis develops, however, the risk of hepatocellular carcinoma is increased by more than 200-fold (Bacon 2001). Phlebotomy therapy is almost always indicated for patients with hereditary hemochromatosis, even when cirrhosis or organ damage is already present, as further progression of the disease can be stopped with the possibility of minimizing organ dysfunction (Brissot 2009).

2.6.2 Chelation therapy

For patients requiring regular blood transfusions, iron chelation may represent life-saving therapy. In patients with thalassemia major, the availability of chelation therapy led to one of the most marked improvements in morbidity and mortality associated with a genetic disease (Cianciulli 2008; Agarwal 2009). The major goal of iron chelation therapy is to bind NTBI and intracellular labile iron, thereby effectively eliminating toxic iron (Porter 2007). Due to the cumulative nature of iron loading, continuous (24-hour) control of NTBI levels is desirable (Ozment and Turi 2009).

Although the benefits of chelation therapy with regard to a reduction in morbidity and mortality may be apparent within a much shorter timeframe, it may take years for body iron levels to reach normal levels. The availability of effective iron chelation therapies has significantly extended the life expectancy of transfusion-dependent patients, and consistent therapy reduces the toxicity and organ damage associated with excess iron (Cario, Janka-Schaub et al. 2007).

For any given patient, reaching their target body iron levels depends to a large extent on their ability to comply with long-term therapy, which itself is largely determined by the side effects, tolerability, perceived efficacy and convenience of the iron-chelating agent (Cohen 2006). Unfortunately, the survival and health benefits of current iron chelation agents decline measurably with even minimal reductions in compliance. Therefore, optimal compliance requires that patients both understand the nature of the threat of iron overload, and receive psychological and social support for continuing both blood transfusions and iron chelation therapy (Cohen 1990).

Three approved iron chelation agents are available currently: Deferoxamine, deferiprone, and deferasirox, with the approval and availability of these agents largely country specific (Cohen 2006). These three compounds are compared in table 2 to the properties of an ideal chelator.

Deferoxamine (DFO)

DFO, a hexadentate siderophore (Figure 4) isolated from Streptomyces pilosus, has been the clinical chelator of choice for the treatment of iron overload diseases since the 1970s (Brittenham 2003). The high affinity of this siderophore for Fe(III) renders iron bound in the resulting 1:1 complex metabolically inactive, preventing the production of ROS. Consequently, DFO is able to decrease oxidative stress, alleviating the symptoms associated with iron overload disease (Olivieri and Brittenham, 1997). However, the DFO-iron chelate is charged and does not readily enter and leave cells. The high hydrophilic nature of DFO limits the membrane permeability and efficiency of this ligand, imparting poor absorption from the gastrointestinal tract and a short plasma half-life of 12 minutes due to rapid drug metabolism (Aouad et al. 2002). As a result, DFO must be administered via subcutaneous infusion for extensive periods to achieve a negative iron balance, ranging from 8 to 12 h, five to seven times per week at a daily dosage of 20 to 60 mg/kg (Hershko et al. 2003). Apart from the cumbersome administration route and high cost, a third of patients treated with DFO experience pain and swelling at the injection site, cumulatively leading to poor patient compliance (Olivieri and Brittenham, 1997; Wong and Richardson, 2003). Irrespective of its shortcomings, it should be noted that DFO use has been credited with producing dramatic strides in survival of thalassemia patients.

Given the potential problems associated with the prolonged use of DFO, there have been numerous attempts to improve its efficacy. These include the generation of a high molecular weight form of the chelator coupled to hydroxyethyl starch, lipophilic DFO analogs, and libraries of structural DFO analogs (Kalinowski and Richardson 2005). Unfortunately, the evolution of DFO analogs has not resulted in chelators with advantages over the original siderophore. Hence, other orally active alternatives have been sought in the quest to develop effective and specific iron chelators.

Deferiprone

Deferiprone is an orally active hydroxypyridineone (Figure 4) first used in humans in 1987. An advantage of this compound is that the iron(III) chelate of deferiprone carries no net charge and therefore can penetrate membranes easily, allowing removal of potentially toxic iron from tissues (Neufeld 2006). Deferiprone is available in Europe and some other countries but not the United States (Kontoghiorghes et al. 2004). The reasons for this difference in availability between countries is not entirely understood but may be due to conflicting clinical trials related to the safety and iron clearing efficiency of this ligand (Richardson, 2001).

As deferiprone is bidentate, three molecules are necessary to occupy the coordination sites of iron. In biological systems, deferiprone appears to exhibit incomplete coordination of iron which would enable access of reductants to the iron core and may potentially lead to ROS production (Kalinowski and Richardson 2005). Such findings could question the safety of deferiprone, and to overcome this problem combination therapy with DFO has been assessed. Deferiprone often causes gastrointestinal symptoms and idiosyncratic side effects including erosive arthritis

(common in patients in South Asian countries, 5%-20% of patients), neutropenia (up to 5% of patients), and severe agranulocytosis (up to 0.5% of patients) (Neufeld 2006). Thus, close monitoring is required.

To maintain a negative iron balance in overload patients, deferiprone must be administered at a high daily dosage (75 mg/kg/d in 3 divided doses, up to 100 mg/kg) (Balfour and Foster, 1999). The limited efficiency of deferiprone is due mainly to extensive phase II drug metabolism in the liver where the hydroxyl group, essential for chelation and iron clearance, undergoes glucuronidation (Liu and Hider 2002). The metabolic inactivation of deferiprone has sparked research into the synthesis of other hydroxypyridinones that do not undergo this form of modification *in vivo*.

Deferasirox

Deferasirox (ICL670, Exjade) belongs to a new class of oral tridentate chelators N-substituted bis-hydroxyphenyltriazoles (Figure 4), that uses a triazolyl nitrogen and two phenolic oxygens as donor groups. This ligand represents one of > 700 compounds designed through computer modeling intended for the treatment of transfusional iron overload (Nick et al. 2003). Deferasirox is selective for iron (as Fe^{3+}) and binds iron with high affinity in a 2:1 ratio. Although deferasirox has very low affinity for zinc and copper, there are variable decreases in the serum concentration of these trace metals after the administration of deferasirox. The clinical significance of these decreases is uncertain. Deferasirox is orally active with 70% bioavailability and is marketed in the form of tablets for oral suspension (Exjade®). It is highly (~99%) protein bound almost exclusively to serum albumin and is mainly metabolized in the liver by glucuronidation. With a plasma half-life of 8 to 16 hours, once-daily dosing permits circulating drug at all times to

scavenge NTBI (Cappellini and Pattoneri 2009). Deferasirox-iron complexes undergo enterohepatic recycling and are mainly excreted in the feces (84% fecal, 8% renal). Females have a moderately lower apparent clearance (by 17.5%) for deferasirox compared to males.

In addition to its ability to remove NTBI, a recent study has shown that deferasirox can also cross the plasma membrane and enter the cell using unknown carriers (Glickstein, El et al. 2005; Glickstein, El et al. 2006). Clinical studies have demonstrated that after one year , deferasirox produced significant reduction in liver iron concentration (Cappellini 2008). In animal models, deferasirox has been shown to be 5 times more potent than deferoxamine and 10 times more potent than deferiprone (Choudhry and Naithani 2007).

Deferasirox is indicated for the treatment of chronic iron overload due to blood transfusions (transfusional hemosiderosis) in patients 2 years of age and older. The recommended initial daily dose of deferasirox is 20 mg/kg body weight. Doses of deferasirox should not exceed 30 mg/kg per day since there is limited experience with doses above this level. The decision to remove accumulated iron should be individualized based on anticipated clinical benefit and risks of deferasirox therapy. In patients who are in need of iron chelation therapy, it is recommended that therapy with deferasirox be started when a patient has evidence of chronic iron overload, such as the transfusion of approximately 100 mL/kg of packed red blood cells (approximately 20 units for a 40-kg patient) and a serum ferritin consistently >1000 µg/L.

The most frequently occurring adverse events in the therapeutic studies of deferasirox were abdominal pain, nausea, vomiting, diarrhea, and skin rashes. Some deferasirox-treated patients also experienced dose-dependent increases in serum

creatinine, though most of the creatinine elevations remained within the normal range (Cappellini 2005). Serum creatinine should be assessed in duplicate before initiating therapy to establish a reliable pretreatment baseline and monitored monthly thereafter.

Table 2. Comparison of the main available iron chelators to an ideal chelating drug. ***(modified from Neufeld, 2006)***

	Ideal Chelator	Deferoxamine 1970	Deferiprone 1987	Deferasirox 2005
Route of administration	Oral	S/C, IV	Oral	Oral
Plasma t1/2	Long enough to prevent NTBI	Short (minutes); requires constant delivery	Moderate (<2 hr); required t.i.d dosing	Long (8-6 hr); remains in plasma 24 hr
Therapeutic index	High	High	Idiosyncratic side effects	High
Chelating efficacy/ charge	High Uncharged	High Charged	Low Uncharged	Moderate Uncharged
Side effects	None	Auditory and retinal toxicity, effects on bone and growth, lung toxicity, local skin reactions	Agranulocytosis, neutropenia, abdominal discomfort, erosive arthritis	Abdominal discomfort rash, mild diarrhea
Ability to chelate intracellular cardiac & other tissue iron	High	Lower than deferiprone and deferasirox	High in clinical and *in vitro* studies	Insufficient clinical data Promising laboratory studies

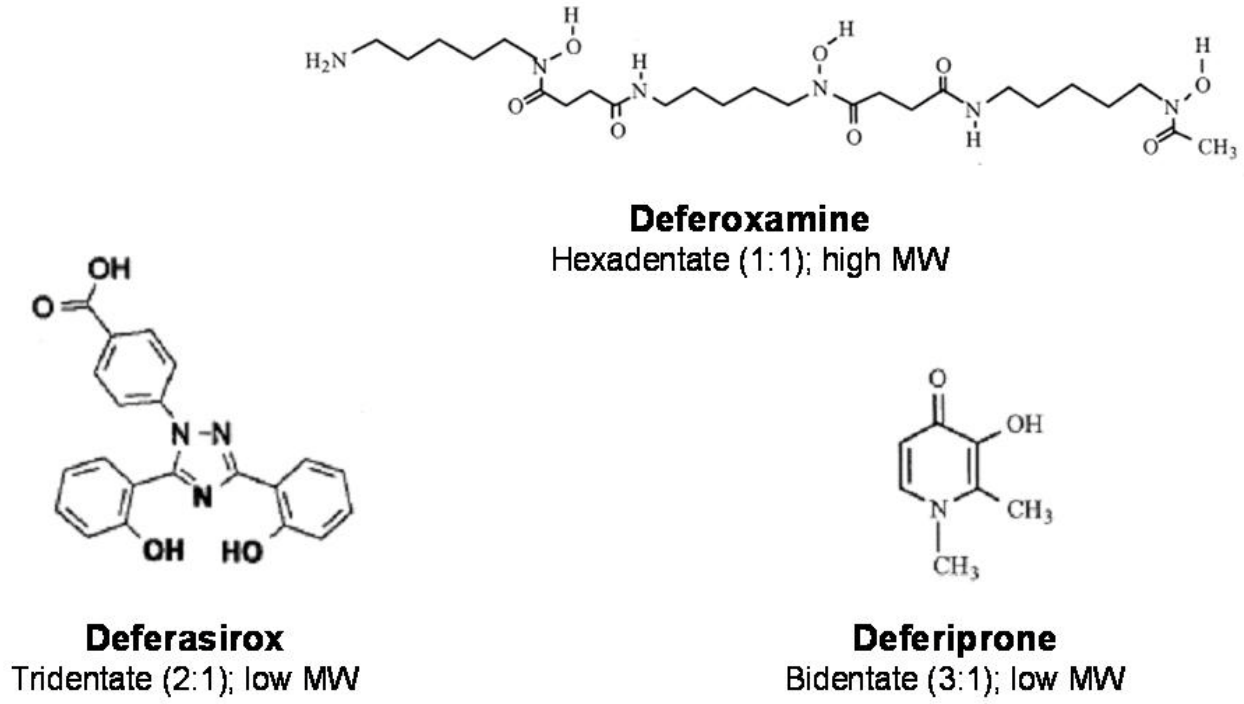

Figure 4. Chemical structure of the iron chelating agents in clinical use and their corresponding iron binding ratio.

2.7 ANIMAL MODELS OF IRON OVERLOAD

Past efforts to study iron overload and its associated toxicity have been hampered by the lack of a suitable experimental model of human iron overload; most animal species have a far greater capacity to excrete iron than humans. Recently, the Mongolian gerbil (Meriones unguiculatus) was developed as a model of iron overload using weekly subcutaneous injections of iron dextran (Carthew, Dorman et al. 1993). Studies using the gerbil model have reported that cardiac and hepatic iron content was

increased to amounts within the range reported in patients with iron overload (Kuryshev, Brittenham et al. 1999). In addition, the gerbil model tends to reproduce critical features of the cardiomyopathy found in human iron overload as the gerbil seems unable to excrete iron as effectively as other rodents. In one study, gerbils treated with repeated injections of iron dextran over a period of months developed a cardiomyopathy that resembles the cardiomyopathy that develops over a period of years in patients with chronic iron overload (Kuryshev, Brittenham et al. 1999). Similarly, the accumulation of iron in the gerbil heart has been associated with myocyte degeneration and intracellular calcification, whereas in the hearts of mice treated identically with iron-dextran that had accumulated comparable cardiac iron levels, similar evidence of myocyte damage was absent (Yang, Dong et al. 2002). These results suggest that the gerbil model would be useful in studying the progression of end organ damage associated with iron-overload.

CHAPTER III

MATERIALS AND METHODS

This chapter outlines the procedures used for data collection and analysis in the present study. The adult male Mongolian gerbil (*Meriones unguiculatus*) model of iron overload was used. Iron overload was achieved by multiple intraperitoneal injections of iron-dextran. Deferasirox treatment was administered orally at different time points after the completion of iron loading. Electrocardiographic and echocardiographic measurements were conducted at baseline (before iron loading) and every three months thereafter. After the completion of deferasirox treatment, gerbils were sacrificed and heart, aorta, liver, kidney and pancreas were excised. Examination for changes in tissue iron concentration, expression of ferritin, and cardiac morphology followed.

3.1 Animal selection and care

All experiments were conducted using male Mongolian gerbils. Adult male Mongolian gerbils (*Meriones unguiculatus*) were obtained from Charles River Laboratories and housed four per cage in an AALAC approved vivarium. Housing conditions consisted of a 12h: 12h dark-light cycle with temperature maintained at 22 ± 2° C. Animals were provided food and water *ad libitum*. Gerbils were allowed to acclimate to the housing facilities for at least two weeks before experimentation began. During this time, the animals were carefully observed. None of the animals exhibited signs of failure to thrive, such as precipitous weight loss, disinterest in the environment, or unexpected gait alterations. Animal care and procedures were conducted in accordance with the Institutional Animal Care and Use Committee of Marshall University

using the criteria outlined by the American Association of Laboratory Animal Care (AALAC) as proclaimed in the Animal Welfare Act (PL89-544, PL91-979, and PL94-279).

3.2 Iron loading and chelation

Gerbils were divided into Control (Ctrl), Iron overload (IO), and iron overload followed by deferasirox treatment (IO+DFR). Iron treated animals received 15 subcutaneous injections of iron dextran (Sigma Chemical, St. Louis, Mo) at a dose of 100 mg/kg every 5 days for 10 weeks. Deferasirox was administered for one, three, or nine months post iron loading. For each treatment group, an age-matched Ctrl and IO group was maintained for comparison (Table 3).

To avoid the stress of chronic, repeated gavage feeding, deferasirox was homogenously mixed in plain peanut butter (vehicle) for oral feeding via a 1-mL syringe. Deferasirox powder was carefully blended or mixed with creamy, low-fat peanut butter and the mixture placed into conical bakery squeeze applicators and delivered into 15-mL plastic syringes which have had tips cut off. The mixture was then delivered into 1-mL syringes with tips removed from which small volumes of the mixture containing the desired quantity of drug was carefully introduced into the animal mouths and eaten. We have found that animals acquire a taste for peanut butter after a few days of feeding and thereafter eagerly consume the peanut butter. Therefore, the animals were adjusted to peanut butter prior to administration of deferasirox-peanut butter mixtures. This method of administration is equivalent to giving the drug with food or in formulations of drug with filler material.

Deferasirox treatment was started 1-week after the last iron dextran injection and was given at a single daily dosage of 100 mg/kg. This dosage is based on a previously determined dose-response curve of deferasirox in iron overloaded gerbils and represents 67% of human values when normalized for body surface area (Wood, Otto-Duessel et al. 2006). Oral chelator administration gave the animals approximately 0.15 mL of peanut butter per day. Control and iron overload groups received plain peanut butter (vehicle) and were housed, fed, and maintained under identical conditions.

Table 3. Deposition of gerbils in the experimental groups

Interval	Groups n = 10/ group	Treatment
Baseline	Ctrl	10 wk Saline
	IO	10 wk iron
1 months	Ctrl	10 wk Saline + 1 mo vehicle
	IO	10 wk iron + 1 mo vehicle
	IO+ DFR	10 wk iron + 1 mo DFR
3 months	Ctrl	10 wk Saline + 3 mo vehicle
	IO	10 wk iron + 3 mo vehicle
	IO+ DFR	10 wk iron + 3 mo DFR
9 months	Ctrl	10 wk Saline + 9 mo vehicle
	IO	10 wk iron + 9 mo vehicle
	IO+ DFR	10 wk iron + 9 mo DFR

3.3 Electrocardiographic procedures

Gerbils were anesthetized with a ketamine (100 mg/ml)/xylazine (20 mg/ml) mixture. EKG recording was performed using standard limb lead system (Biopac)®. To emulate lead II, we utilized subcutaneously placed electrodes located in the line with the long access of the heart. One electrode (anode) is placed in the upper right quadrant of the chest and the other (cathode) in the lower left abdominal wall, just cranial to the

groin area. Lead I configuration was performed by placing the cathode and the anode in the upper right, and left quadrants of the chest, respectively. Lead III configuration was performed by placing the cathode in the upper left quadrant of the chest, while the anode was placed in the lower left abdominal wall.

3.4 Transthoracic echocardiography

Echocardiography is a noninvasive ultrasound procedure in which harmless, high-frequency sound waves (frequency >20,000 cycles/sec) are emitted from a piezoelectric crystal or transducer, beamed in particular directions, and reflected back (echo) by small structures in the mm and sub-mm range. These waves are beamed toward and penetrate the heart and are reflected back to the transducer as a series of echoes, which are amplified and displayed on a cathode ray tube. It is used to evaluate the position, size, and movement of cardiac valves, heart wall structure and function, and directional flow of blood within cardiac chambers (Walker, Epling et al. 2007). Animals were anesthetized with ip injections of a 2:1 mixture of ketamine HCl (100 mg/ml) and xylazine (20 mg/ml). Echocardiographic recordings were performed at the Cabell Huntington Hospital, Huntington, WV. Gerbils were shaved in the chest area for adequate sonic transference, an ultrasonic transmission gel was applied to the chest area, and the animals were positioned on their left sides or backs. Two-dimensional echocardiographic measurements, two-dimensional guided M-mode, Doppler M-mode, and other recordings from parasternal long- (PLAX) and short-axis (PSAX) views were obtained using a Phillips 5500 ECHO system with a 12 MHz transducer. Two-dimensional measurements were used to image cardiac structures in the parasternal long- and short-axis views. The echocardiographic views were then used to position the

M-mode echocardiographic line. In the long-axis procedures, the probe was oriented toward the base of the heart projecting toward the apex (x-axis) with depth along the y-axis, thus allowing pulse wave Doppler evaluation of valvular blood flow velocities. In the short-axis procedures, the probe was oriented toward the left ventricle and across the heart for evaluation of wall structure, which was utilized in the calculation of ejection fraction and fractional shortening during systole. M-mode displays were analyzed by a digital echocardiographic analysis system. Six measurements were selected for each assessment of cardiac structure and function. The structural parameters included diastolic (LVSd) and systolic (LVSs) left ventricular septal thickness, diastolic (LVIDd) and systolic (LVIDs) left ventricular internal dimension, diastolic (LVPWd) and systolic (LVPWs) left ventricular posterior wall thickness, and right ventricular diastolic internal dimension (RV). Functional measurements included left ventricular ejection fraction (EF), left ventricular fractional shortening during systole (FS), maximal aortic (AVmax), pulmonary (PVmax), mitral (MVmax), and tricuspid (TVmax) valvular blood flow velocity. Left ventricular ejection fraction (EF), and fractional shortening (FS) were used to evaluate systolic function.

3.5 Tissue collection

Prior to sacrifice, gerbils were anesthetized with a ketamine-xylazine (4:1) cocktail (50 mg/kg i.p.) and supplemented as necessary to achieve loss of reflexive response. Loss of toe pinch and eye blink reflexes was assessed prior to the initiation of any experimental manipulations. Every effort was made to minimize stress and discomfort to the animals.

After midline laparotomy, heart, liver, pancreas and aorta were removed and placed in Krebs-Ringer bicarbonate buffer (KRB) containing: 118 mM NaCl, 4.7 mM KCl, 2.5 mM $CaCl_2$, 1.2 mM KH_2PO_4, 1.2 mM $MgSO_4$, 24.2 mM $NaHCO_3$, and 10 mM α-D-glucose (pH 7.4) equilibrated with 5% CO_2/ 95% O_2 and maintained at 37°C. Isolated tissues were quickly cleaned of connective tissue, weighed, and immediately snap frozen in liquid nitrogen.

3.6 Tissue iron assessment

After sacrifice, portions of the heart, liver, kidney, pancreas, and aorta were isolated, weighed, and sent for quantitative iron (total, heme plus non-heme, tissue iron) determination (University of Tampa, Tampa, FL) by inductively coupled plasma-atomic emission spectrometry (ICP-AES) (Walker, Epling et al. 2007). Briefly, digestions were performed using commercially available trace metal grade HNO_3 (ThermoFisher Scientific). Dilutions were made with 2% (vol.) HNO_3 (trace metal grade) prepared with deionized water. All digestion tubes, volumetric pipettes, and volumetric glassware were soaked for 24 hours in 2% (vol.) HNO_3 (trace metal grade), rinsed four times with deionized water, and air dried prior to use. Approximately 300 mg (wet weight) of sample was weighed into a glass digestion tube and 6.0 ml of concentrated trace metal grade HNO_3 added. A 1000 mg/L Yttrium solution in 2% HNO_3 (Perkin Elmer), used as an internal standard (final concentration 1.67 mg/L), was added to each tube. Samples were heated at 37°C for 1 hour and then at 110°C for 2 hours. After digestion, 5.0 ml of the clear solution was transferred to a 50 ml volumetric flask and brought to volume with 2% (vol) HNO_3 (trace metal grade). Solutions were filtered through a 0.22 μm syringe driven filter unit (Millipore) and analyzed by ICP-AES. A 1.67 mg/L iron solution was

used as a control for the digestion procedure. Analyses were performed on a Perkin Elmer ICP-AES (Optima 2100 DV) using a 0 to 1 mg/L, 0 to 10 mg/L, or 0 to 100 mg/L (for iron only) standard curve, depending upon iron concentration. Calibration and control solutions for the 0 to 1 mg/L and 0 to 10 mg/L standard curves were prepared from a multi-element standard (ICP Multi-element Solution 2, Spex Chemicals, 10 mg/L). Calibration and control solutions for the 0 to 100 mg/L standard curve were prepared from a 1000 mg/L iron standard solution (Perkin Elmer). All calibrators and controls contained an internal Yttrium standard. The measurements for iron (238.204 nm) were conducted in the axial mode. Sample concentrations were determined from standard curves generated by linear regression analysis. The minimal detectable concentration for each metal was determined using the mean plus the three-fold standard deviation obtained from 10 blank digestions.

3.7 Histological analysis

Whole hearts (breadloaf sectioned) and representative sections of liver, pancreas, and aorta were fixed in 10% buffered formalin solution, and processed into paraffin blocks by routine procedures. Samples were then sectioned (8 μm) with a cryostat and sections were mounted on poly-lysine (Sigma, St. Louis, MO) coated slides. Sections were stained with Prussian blue iron stain. Slides were evaluated by light microscopy and images were taken at 200X, or 400X. This data was collected and reviewed in a blinded fashion.

3.8 SDS-PAGE and immunoblotting

Tissue was pulverized in liquid nitrogen using a mortar and pestle until a fine powder was obtained. After washing with ice cold PBS, samples were lysed on ice for 15 minutes in T-PER (2 mL/1 g tissue weight) and centrifuged for 10 minutes at 12000 x g. The supernatant was collected and the protein concentrations of homogenates were determined in triplicate via the Bradford method (Pierce) using bovine serum albumin as a standard. Samples were solubilized at a concentration of 3 mg/ml in SDS-loading buffer and boiled for 5 minutes. Sixty µg of protein from each sample was separated on 10% SDS-PAGE gels and then transferred onto Hybond nitrocellulose membranes using standard conditions. To verify transfer of proteins and equal loading of lanes, the membranes were stained with Ponceau S. Membranes were blocked in buffer (5% nonfat dry milk in tris-buffered saline with 0.1% Tween-20 (TBST) for 1 hour at room temperature, washed (TBST, 3 X 5 minutes), and incubated in primary antibody (1:1000 dilution) in TBST with 5% milk overnight at 4ºC. After washing (TBST, 3 X 5 minutes), membranes were incubated in horseradish peroxidase HRP-linked anti-biotin and the appropriate secondary antibody (1:1000 dilution) in TBST with 5% milk for 1 hour at room temperature, then rewashed (TBST, 3 X 5 minutes). Proteins were visualized by ECL and quantified by densitometry. Exposure times were adjusted to keep the integrated optical densities (IOD) of the film within a linear and nonsaturated range. Specificity of the bands was assessed by comparison of molecular weight markers and positive controls. To allow direct comparisons to be made between the expression levels of different signaling molecules and the amount of protein present, immunoblots were stripped with Restore western blot stripping buffer and reprobed as detailed by the manufacturer. After verifying the absence of residual HRP activity, membranes were

washed and reprobed for other proteins. All membranes were probed for GAPDH for analysis and loading control.

3.9 Oxidative fluorescent microscopy

Cardiac or hepatic specimens were serially sectioned (8 μm) using an IEC Minotome cryostat and collected on poly-lysine coated slides. Hydroethidine (HE), an oxidative fluorescent dye, was used to visualize superoxide (O_2•–) production *in situ* (Miller, Gutterman et al. 1998; Lund, Faraci et al. 2000). Hydroethidine freely permeates the cells and, in the presence of O_2•–, is oxidized to ethidium bromide, which is trapped by intercalating with the DNA (Rothe, Emmendorffer et al. 1991). Because ethidium bromide is impermeable to cell membranes, extracellular O_2•– would not be expected to contribute significantly to the observed cellular fluorescence. Neither hydroxyl radical, nitric oxide radical, peroxynitrite, hydrogen peroxide, hypochlorite, nor singlet oxygen significantly oxidize hydroethidine; as such, an increase in ethidium bromide fluorescence is thought to indicate O_2•– generation specifically within the fluorescing cell. Heart sections were stained with hydroethidine and visualized under fluorescence as described previously (Rice, Preston et al. 2006). The intensity of fluorescent ethidium bromide-stained nuclei was calculated by digitizing images and then determining the average pixel intensity of six randomly positioned regions (1000 μm^2) per cross section. Morphometric evaluation was performed with the use of a computerized imaging analysis system (Olympus MicroSuite™ Basic).

3.10 Oxidized Protein Analysis

Cardiac and hepatic protein isolation was conducted as described above. To identify carbonyl groups that are introduced into the amino acid side chain after oxidative deamination of proteins, oxyblot analysis was performed. The level of protein oxidation was determined by an Oxidized Protein Detection Kit (Oxyblot, Chemicon Cat# S7150-Kit). Oxyblot kit derivatizes carbonyl groups to a 2, 4-dinitrophenylhydrazone (DNP) moiety. The DNP moiety can then be detected using anti-DNP antibodies and is a method to assay for one form of oxidative damage to a protein. The proteins are derivatized as per the protocol given in the kit. These proteins are separated on 10% SDS-PAGE gels and transferred onto nitrocellulose membrane. After the transfer, membranes were blocked with 2.5% BSA in Tris Buffered Saline (TBS) with 0.2% Tween-20 for 1 hour at room temperature. The nitrocellulose membrane was exposed to a primary rabbit anti-DNPH protein antibody from Chemicon Oxyblot (1:200 working dilution) for 1 hour, and then to a secondary antibody (Goat Anti-Rabbit IgG (HRP-conjugated) diluted in the blocking solution 1:500 for 1 hour at room temperature. Membranes were washed after every step in washing buffer (TBS with 0.2% Tween-20). Protein bands were visualized with ECL (Amersham Biosciences). Band signal intensity was quantified by densitometry using a flatbed scanner (Epson Pefection 3200 PHOTO) and Imaging software (AlphaEaseFC).

3.11 In situ cell death detection (TUNEL)

Liver samples were cut into serial 8μm sections using an IEC Minotome Cryostat. After fixing with 4% paraformaldehyde, sections were washed with phosphate-buffered saline (PBS, pH7.4), and then permeabilized with 0.1% sodium citrate and 0.1% Triton

X-100. DNA fragmentation was determined by TdT-mediated dUTP nick end labeling (TUNEL) as suggested by the manufacturer's recommendations. Cross-sections from each liver were treated with DNase I to induce DNA fragmentation as a positive control. Three randomly selected regions from each cross section were visualized by epifluorescence using an Olympus fluorescence microscope (Melville, NY) fitted with a 40X objective. Images were recorded digitally using a CCD camera (Olympus, Melville, NY), and the samples were analyzed by counting positively stained nuclei with DAPI nuclear staining for contrast.

3.12 Statistical analysis

Results are presented as mean ± SEM. Data were analyzed by using SigmaStat 3.0 computer software. One-way (or two-way) analysis of variance (ANOVA) was used for overall comparisons where appropriate with the Student-Newman-Keuls post hoc test used to determine statistical significance. The level of significance accepted *a priori* was $P \leq 0.05$.

3.13 Materials

Deferasirox powder used in the study was provided by Novartis Pharmaceuticals (East Hanover, NJ). Primary antibodies against P-ERK1/2 MAPK (Thr202, Tyr204) (cat #9106), p-p38 MAPK (Thr180, Tyr182) (cat#9216), p-JNK (Thr183, Tyr185) (cat #9251), ERK1/2 MAPK (cat #9102), p38 MAPK (cat #9218), JNK (cat #9252), caspase-3 (#9662), anti-biotin as well as anti- mouse and -rabbit secondary antibodies, and NIH 3T3 cell lysates were obtained from Cell Signaling Technology (Beverly, MA). Anti-Bax (N-20) (sc-492), Bcl-2(C-2) (sc-7382), and Bad (H-168) (sc-7869), ferritin heavy chain

(H-53) (cat #25617) and anti-goat secondary antibodies were from Santa Cruz Biotechnology (Santa Cruz, CA). The TUNEL assay kit was purchased from Roche Diagnostics Corporation (Indianapolis, IN). Precast 10% and 15% SDS-PAGE gels were procured from Cambrex Biosciences (Baltimore, MD) while the enhanced chemiluminescence (ECL) Western blot detection reagents, Hyperfilm, and Hybond nitrocellulose membranes came from Amersham Biosciences (Piscataway, NJ). Restore western blot stripping buffer and T-PER tissue lysis buffer were obtained from Pierce (Rockford, IL). Dual Color molecular weight markers were from BioRad (Hercules, CA). All other chemicals were purchased from Sigma (St. Louis, MO).

CHAPTER IV

RESULTS

The results chapter will be subdivided into three articles. Each article will deal specifically with a specific aim of the dissertation project.

Note: The method section has been omitted from these articles to avoid redundancy. Please refer to Chapter III for detailed materials and methods.

Article #1: Corresponds to Specific Aim #1

> To determine if deferasirox is able to reduce cardiac iron content, iron-induced ferritin upregulation, and iron-related increases in indices of oxidative stress such as superoxide overproduction, protein oxidation, and the phosphorylation of the extracellular regulated kinase 1/2 (ERK1/2)-, p38-, and c-Jun N-terminal kinase (JNK)-mitogen activated protein kinases (MAPKs).

DEFERASIROX REMOVES CARDIAC IRON AND ATTENUATES OXIDATIVE STRESS IN THE IRON-OVERLOADED GERBIL

Rabaa M. Al-Rousan[1], Satyanarayana Paturi[2,3], Joseph P. Laurino[4], Sunil K. Kakarla[1, 3], Anil K. Gutta[2, 3], Ernest M. Walker[3, 5], and Eric R. Blough[1, 2]

[1]Department of Pharmacology, Physiology, and Toxicology, Joan C. Edwards School of Medicine, Marshall University, Huntington, WV; [2]Department of Biological Sciences, Marshall University, Huntington, WV; [3] Cell Differentiations and Development Center, Marshall University, Huntington WV; [4]Department of Chemistry, University of Tampa, Tampa, FL; [5]Department of Pathology, Joan C. Edwards School of Medicine, Marshall University, Huntington, WV

American Journal of Hematology, 84:565–570, 2009.

Abstract

Iron-induced cardiovascular disease is the leading cause of death in iron-overloaded patients. Deferasirox is a novel, once daily oral iron chelator that was recently approved for the treatment of transfusional iron overload. Here, we investigate whether deferasirox is capable of removing cardiac iron and improving iron-induced pathogenesis of the heart using the iron overload gerbil model. Animals were randomly divided into three groups: control, iron overload, and iron overload followed by deferasirox treatment. Iron-dextran was given 100 mg/kg per 5 days i.p for 10 weeks. Deferasirox treatment was started post iron loading and was given at 100 mg/kg/day p.o for 1- or 3- months. Cardiac iron concentration was determined by inductively coupled plasma atomic emission spectroscopy. Compared with the untreated group, deferasirox treatment for 1- and 3- months decreased cardiac iron concentration 17.1% ($P = 0.159$) and 23.5% ($P < 0.05$), respectively. These treatment-associated reductions in cardiac iron were paralleled by decreases in tissue ferritin expression of 20% and 38% at 1 and 3 months, respectively ($P < 0.05$). Using oxyblot analysis and hydroethidine fluorescence, we showed that deferasirox significantly reduces cardiac protein oxidation and superoxide abundance by 47.1% and 36%, respectively ($P < 0.05$). Iron-induced increase in oxidative stress was also associated with increased phosphorylation of ERK1/2-, p38-, and JNK-mitogen-activated protein kinases (MAPKs). Interestingly, deferasirox treatment significantly diminished the phosphorylation of all three MAPK subfamilies. These results suggest that deferasirox may confer a cardioprotective effect against iron induced injury.

Introduction

Excessive body iron or iron overload in thalassemia and other conditions is a serious health issue the world over (Hershko 2007). Increased cardiac iron deposition is the leading cause of morbidity and mortality in transfusion-dependent patients as these conditions are oftentimes associated with diastolic dysfunction, arrhythmias, and dilated cardiomyopathy (Walker, Epling et al. 2007). The mechanism(s) by which increased iron affects cellular function are not well understood; however, increases in reactive oxygen species (ROS) have been posited to be involved as current data has suggested a strong link between elevations in cardiac ROS levels and cardiac dysfunction (Oudit, Trivieri et al. 2004).

In the past, iron overload was treated with deferoxamine and deferiprone, although effective, treatment compliance was frequently compromised as the administration of these compounds is often burdensome or associated with serious side effects (Hershko, Link et al. 2005; Neufeld 2006). Deferasirox is a recently approved, orally administered tridentate iron chelator that is administered on a once-daily regimen (Vichinsky 2008). Initial findings regarding the use of deferasirox have suggested that this chelator is very effective in removing liver iron, while other data have suggested that deferasirox may be effective in diminishing cardiac iron (Rachmilewitz, Weizer-Stern et al. 2005; Pennell, Porter et al. 2008; Pennell, Sutcharitchan et al. 2008). The primary objective of this investigation was to determine if chronic administration of deferasirox is capable of removing excess iron from the heart in the gerbil model of iron overload. We hypothesized that deferasirox would reduce cardiac iron content and that this reduction, if present, would be associated with diminished cardiac ROS.

Results

Characterization of animals

Total body and liver weights were obtained and compared. All animals tolerated the iron loading and chelation without any apparent ill effects. The body weights of iron overloaded gerbils were similar to controls, indicating that the injection of iron dextran did not result in debilitation or weight loss. Heart/ body weight ratio was ~20% higher in the IO group compared to the Ctrl group ($P < 0.05$) (Table 4). No significant difference was observed after one or three months of follow up or with deferasirox treatment.

Table 4. Deposition of gerbils in the experimental groups and heart/body weights.

Interval	Groups n = 10/ group	Treatment	Heart/ body wt (%)
Baseline	Ctrl	10wk saline	0.41 ± 0.04
	IO	10wk iron	0.49 ± 0.02*
1 months	Ctrl	10 wk saline + 1mo vehicle	0.42 ± 0.01
	IO	10 wk iron + 1 mo vehicle	0.43 ± 0.01
	IO+ DFR	10 wk iron + 1 mo DFR	0.42 ± 0.01
3 months	Ctrl	10 wk saline + 3 mo vehicle	0.38 ± 0.01
	IO	10 wk iron + 3 mo vehicle	0.39 ± 0.01
	IO+ DFR	10 wk iron + 3 mo DFR	0.38 ± 0.01

An asterisk (*) indicates significant difference from age matched control

Cardiac iron levels

Cardiac iron levels were measured using inductively coupled plasma atomic emission spectrometry (ICP-AES). Compared to hearts obtained from control animals, iron overload increased cardiac iron level by 10.4 fold ($P < 0.05$). Cardiac iron levels were 8.1- and 7.4-fold higher than that of the corresponding age-matched controls at

one and three months of follow up, respectively ($P < 0.05$). Compared to the 3 month-IO group, deferasirox treatment decreased cardiac iron levels by 23.5% ($P < 0.05$) (Figure 5). Prussian blue staining demonstrated elevated iron deposition in cardiac sections from gerbils in the 3 month-IO group (Figure 6). Iron deposition exhibited a nonhomogenous distribution with a higher deposition in the ventricle compared to atria. In the left ventricular wall, iron accumulation was higher in the epicardium and endocardium, and was the least in the myocardium. Within the myocardium, iron tended to accumulate in the interstitium although deposition was clearly visible inside the myocytes. Deferasirox treatment for three months produced a notable decrease of stainable iron visible in all regions of the heart (Figure 6).

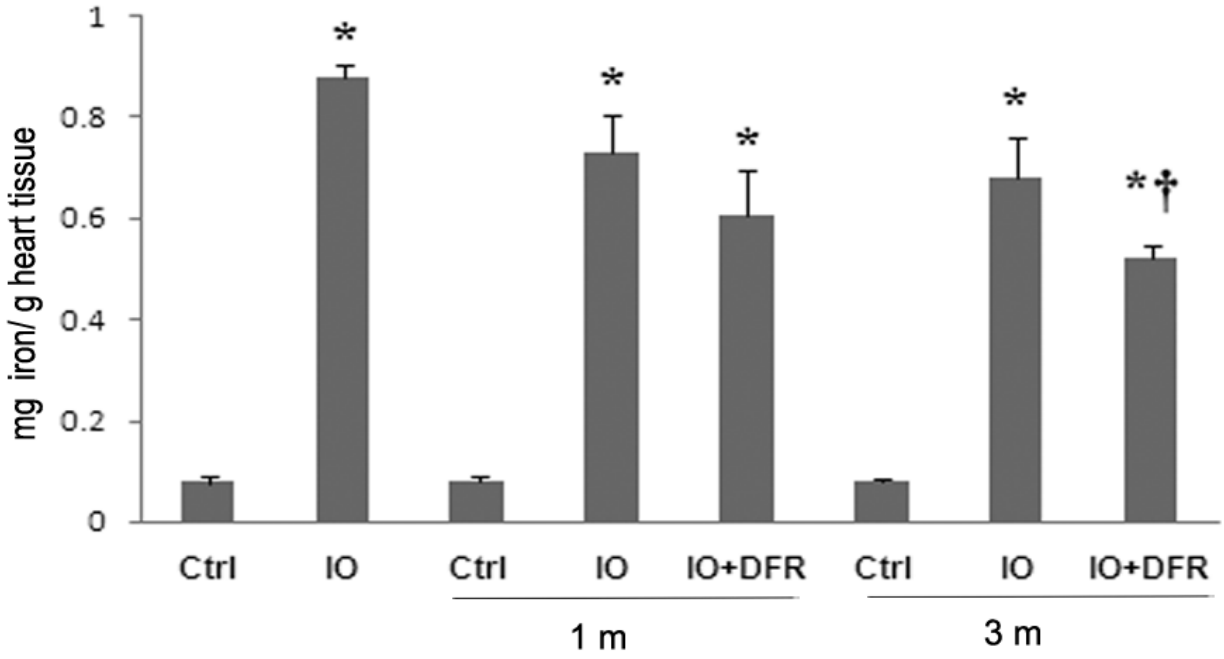

Figure 5. Average iron levels in mg/g tissue weight in cardiac tissue of gerbils in the experimental groups. Ctrl: control, IO: Iron overload, IO+ DFR: Iron overload followed by deferasirox treatment, 1m: 1 month interval, 3m: 3 months interval. (*) indicates significant difference from control, (†) indicates significant difference from iron overload group ($P < 0.05$).

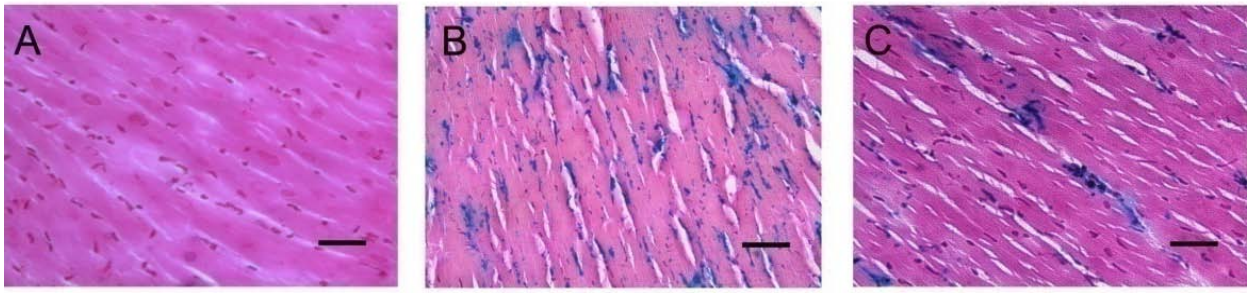

Figure 6. Histological examination of left ventricular myocardium of Ctrl (A), IO (B), and IO+DFR (C) gerbils followed for 3 months. Ferric iron was detected by Prussian blue staining. No apparent iron deposition was observed in control gerbils. Iron overload resulted in iron accumulation in endothelial cells in cardiac interstitium and to a lesser extent in cardiac myocytes. Deferasirox treatment diminished iron deposition from all regions of cardiac tissue. Bar represents 100 µm, Images were taken at 400X original magnification.

Ferritin protein expression

Cardiac ferritin protein levels were analyzed by immunoblot using total protein isolates from each of the experimental groups. Compared to control animals, ten weeks of iron overload increased ferritin protein by 1.9 fold ($P < 0.05$) (Figure 7). After completion of iron loading ferritin levels remained elevated and were 1.7 and 1.6 fold higher than that of the corresponding age-matched control after one and three months of follow up, respectively ($P < 0.05$). Deferasirox treatment significantly reduced cardiac ferritin expression by 20% and 38% after one (1m-IO+DFR) and three months (3m-IO+DFR) of treatment, respectively ($P < 0.05$).

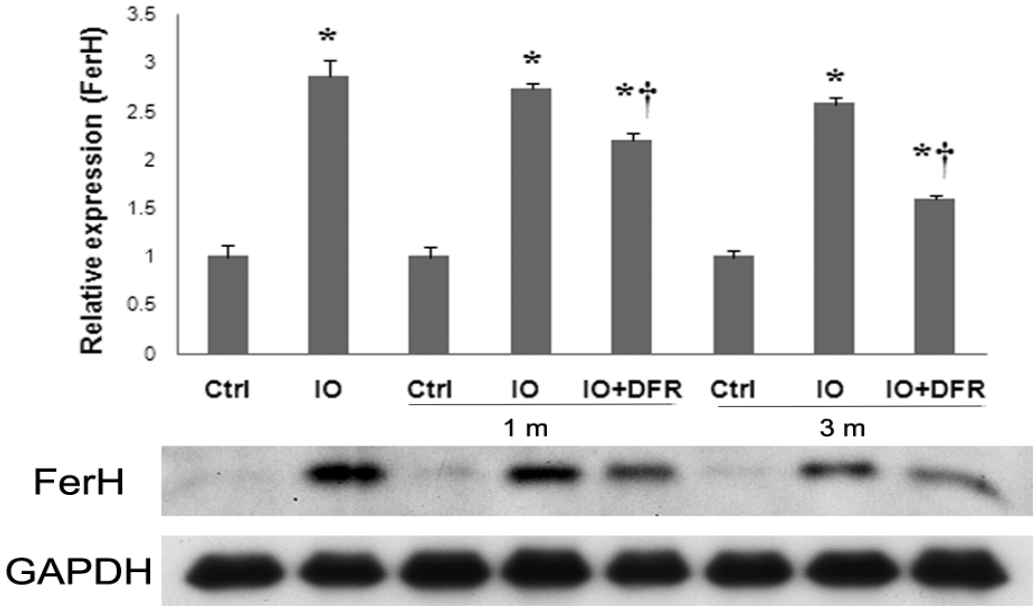

Figure 7. Effect of iron overload and iron chelation on ferritin heavy chain (FerH) protein expression in cardiac tissue of gerbils in the experimental groups. (Upper panel) Results were obtained from six experiments in each group and expressed as a percentage of the corresponding age matched control value. (Lower panel) Representative Western blot analysis. Ctrl: control, IO: Iron overload, IO+ DFR: Iron overload followed by deferasirox treatment, 1m: 1 month interval, 3m: 3 months interval. (*) indicates significant difference from control, (†) indicates significant difference from iron overload group ($P < 0.05$).

Superoxide abundance

Because increased iron accumulation has been found to be associated with increased oxidative stress, we examined cardiac tissue sections from Ctrl, IO, and IO+DFR groups from 3 months interval for superoxide generation using HE fluorescence. Compared to 3 months-Ctrl, a 101% increase in HE fluorescence was observed in the 3 months-IO groups ($P < 0.05$). Three months of deferasirox treatment (3mIO+DFR) resulted in 36% reduction in HE fluorescence ($P < 0.05$) (Figure 8). The overall distribution of superoxide abundance appears to be similar in all regions of the cardiac myocardium (Figure 8).

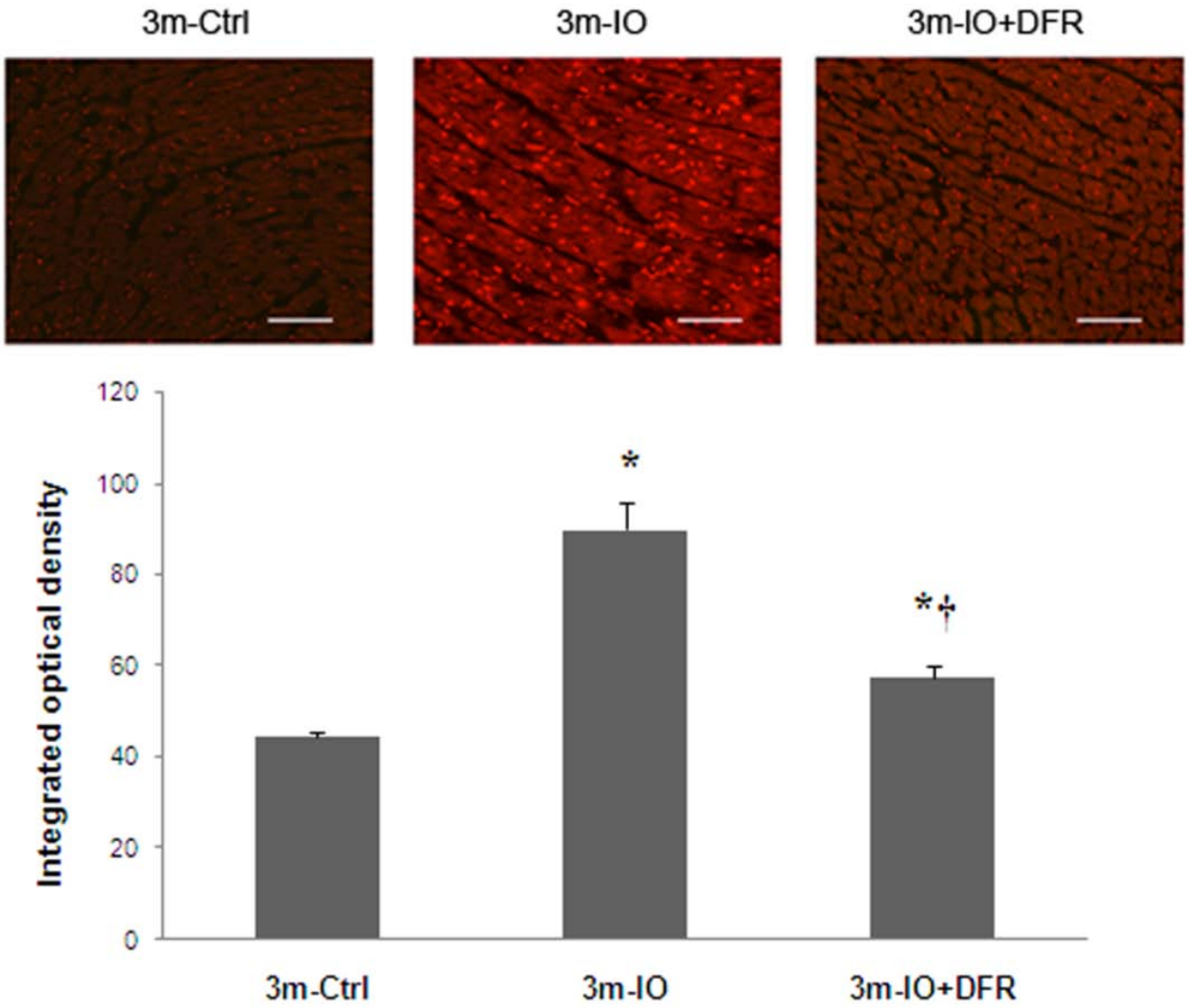

Figure 8. Detection of cardiac superoxide by dihydroethidium in Ctrl, IO, and IO+DFR groups. (Upper panel) The increase in superoxide involves all layers of ventricular wall. Bar represents 100µm, images were taken at 400X original magnification. (Lower panel) Quantification of cardiac superoxide as determined by intensity of fluorescent ethidium bromide-stained nuclei from six animals in each group. 3m = 3 months interval. An asterisk (*) indicates significant difference from control animals, (†) indicates significant difference from iron overload ($P < 0.05$).

Protein oxidation

To investigate whether iron overload modifies cardiac proteins, we next examined protein isolates obtained from the hearts of Ctrl, IO, and IO+DFR for three months for the presence of carbonylated protein using OxyBlot™ detection kit. Protein

carbonylation was increased by 114% in the 3 month-IO group compared to that of 3months-Ctrl (*P* < *0.05*). These levels were reduced by 47% after three months of deferasirox treatment (3mIO+DFR) (*P* < *0.05*) (Figure 9).

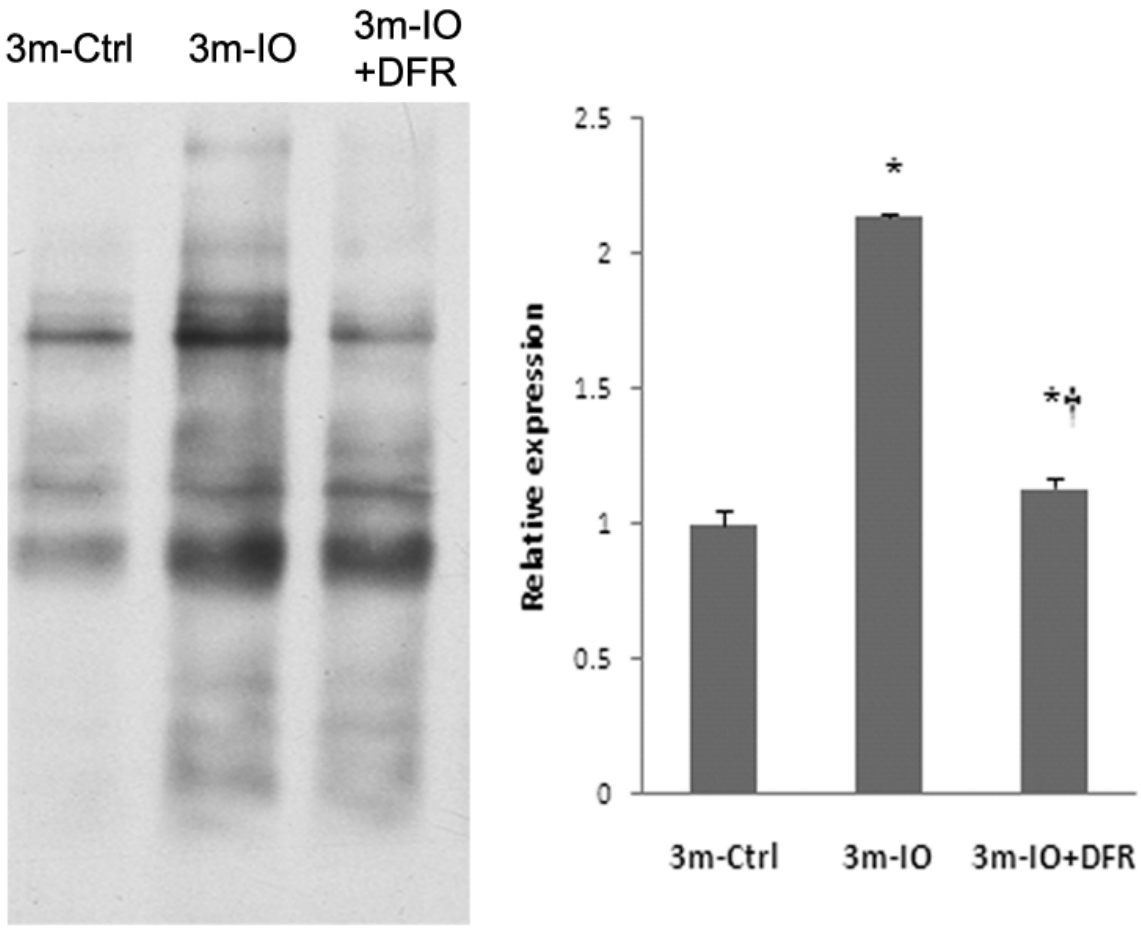

Figure 9. Effect of iron overload or deferasirox treatment on cardiac protein carbonylation. (Left) Representative oxyblots of cardiac protein isolates from ctrl, IO, and IO+DFR from 3 months interval. (Right) Quantification of oxidatively modified proteins in the corresponding groups. 3m = 3 months interval. An asterisk (*) indicates significant difference from control animals, (†) indicates significant difference from iron overloaded animals (*P* < 0.05).

Determination of ERK1/2-, p38-, and JNK-MAPK phosphorylation

The MAPK pathway has been identified as an important signaling cascade involved in the control of cell growth, differentiation, and adaptation whose activity is thought to be regulated, at least in part by cellular ROS levels (Martindale and Holbrook 2002). No significant difference in ERK1/2, P38, or JNK-MAPK protein expression was observed between groups. ERK1/2-MAPK phosphorylation was 67%, 50%, and 58% higher in the IO, 1 month-IO, 3 months-IO groups compared to the corresponding age matched control, respectively *($P < 0.05$)*. Deferasirox treatment for one or three months significantly reduced ERK1/2 phosphorylation by 13% and 32%, respectively *($P < 0.05$)* (Figure 10A). p38-MAPK phosphorylation was 164%, 218%, and 134% higher in the IO, 1 month-IO, 3 month-IO groups compared to the corresponding age-matched control, respectively. Similar to our findings for ERK1/2, the phosphorylation of p38-MAPK was decreased 33% and 46% after one and three months of deferasirox treatment, respectively (Figure 10B). Likewise, JNK-MAPK phosphorylation, was 52%, 50%, and 98% higher in the IO, 1 month-IO, 3 month-IO groups compared to the corresponding age-matched control, respectively *($P < 0.05$)* (Figure 10C). Deferasirox treatment significantly reduced the phosphorylation of JNK-MAPK by 27%, and 47% after one and three months of chelation, respectively *($P < 0.05$)* (Figure 10C).

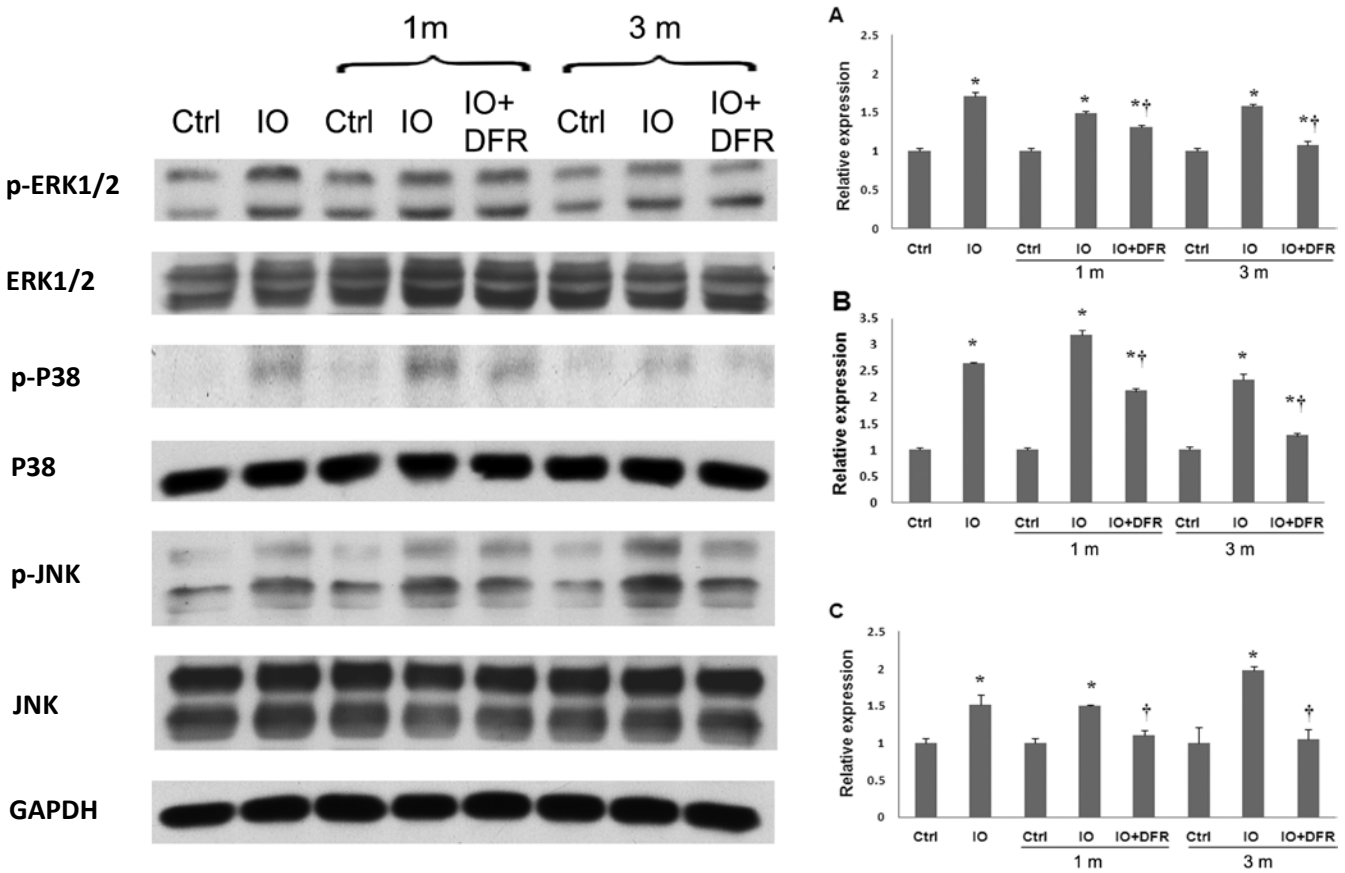

Figure 10. Effect of iron overload or deferasirox treatment on the expression of total and phosphorylated ERK1/2-, P38-, and JNK-MAPKs. (Left) Representative western blot demonstrating the expression of total and phosphorylated ERK1/2-, P38-, and JNK-MAPK in the hearts in the experimental groups. (Right) Quantification of protein expression of p-ERK1/2- (A), p-P38- (B), p-JNK-MAPKs (C) in the corresponding groups. Results are expressed as a percentage of the corresponding age matched control value. Ctrl: control, IO: Iron overload, IO+ DFR: Iron overload followed by deferasirox treatment, 1m: 1 month interval, 3m: 3 months interval. (*) significantly different from control group; (†) significantly different from iron overload group ($P < 0.05$).

Discussion

The accumulation of cardiac iron is a complication of iron overload in transfusion-dependent patients that if allowed to proceed unchecked can lead to cardiac arrhythmias and heart failure (Wood, Otto-Duessel et al. 2006). This study demonstrated that oral deferasirox administration significantly reduces cardiac iron

levels in the iron-overloaded Mongolian gerbil. In addition, our data demonstrates that these deferasirox-induced decreases in cardiac iron were associated with diminished indices of cardiac reactive oxygen species (ROS), and decreased activation of MAPK signaling.

Deferasirox decreases cardiac iron and ferritin levels in the iron overloaded gerbil

The similarities of iron accumulation, distribution, and associated pathology in gerbil and human hearts have suggested that the Mongolian gerbil iron-overload model may mimic many of the events seen in the iron-overloaded human (Kaiser, Davis et al. 2003). Our findings demonstrated that iron loading for ten weeks resulted in a 10.4 fold increase in cardiac iron concentration (Figure 5). Although decreasing slightly, tissue iron concentration in the iron overloaded animals remained elevated one- (8.1 fold) and three- (7.4 fold) months following discontinuation of iron administration. Three months of oral deferasirox treatment significantly reduced cardiac iron concentration by 23.5% compared to the corresponding untreated group (Figure 5). This decrease in tissue iron levels with treatment was consistent with previous reports that have used a similar duration of iron loading and deferasirox treatment (Wood, Otto-Duessel et al. 2006; Otto-Duessel, Aguilar et al. 2007; Walker, Epling et al. 2007). For example, Wood and colleagues (2006) have demonstrated that deferasirox treatment for 12 weeks reduced cardiac iron content 20.5%. In an effort to expand upon these findings, we also performed Prussian blue iron staining of cardiac tissue sections. As expected, and similar to previous studies (Otto-Duessel, Aguilar et al. 2007; Otto-Duessel, Brewer et al. 2008), we observed increases in cardiac iron deposition with iron overload and what

appears to be a similar reduction in the amount of tissue iron following deferasirox treatment (Figure 6).

To explore the effect of deferasirox on iron overload further, we also examined the regulation of ferritin protein levels in the heart. Ferritin is the major iron-storage protein at the cellular and organismal level. The ferritin protein is typically increased with iron overload (Tran, Eubanks et al. 1997) as this molecule is thought to be responsible for the sequestration of potentially harmful, reactive iron (de Valk and Marx 1999). Using immunoblotting, we demonstrate that iron-overload was associated with a robust induction of ferritin protein in the heart (Figure 7). As predicted from our ICP-AES data, we further demonstrate that deferasirox treatment significantly decreased cardiac ferritin levels (Figure 7). Taken together, these results are consistent with the notion that oral deferasirox administration is capable of reducing cardiac iron.

Reduced cardiac iron levels are associated with decreases in tissue ROS

Excess "labile iron" is potentially detrimental to the cell because of its propensity to participate in oxidation-reduction reactions that generate harmful free radicals (Deb, Johnson et al. 2009). In addition, it is also thought that a chronic elevation in tissue iron levels can lead to depletion of antioxidants which, if not restored, can by itself lead to further ROS elevation and provide a mechanism for further dysfunction (Eaton and Qian 2002; Oudit, Trivieri et al. 2004). Whether exogenous antioxidant supplementation can be used to prevent such changes remains to be determined. For example, previous reports using selenium and vitamin E, but not taurine, failed to show improvement in indices of oxidative stress in gerbil (Otto-Duessel, Aguilar et al. 2007). Although the physiological effects of reduced superoxide levels following iron chelation were not

investigated in the present study, it has been previously demonstrated that excess superoxide can result in the production of iron-catalyzed hydroxyl radicals (Bartfay, Dawood et al. 1999; de Valk and Marx 1999) and mitochondrial dysfunction (Afanas'ev 2005). Whether these events are occurring in the current study and if they are diminished by iron chelation is not clear.

To explore other ROS-related effects of iron overload and iron chelation, we also examined protein oxidation by determining the amount of protein carbonylation. Our data demonstrate that iron-overload was associated with increased levels of protein oxidation in the heart (Figure 9) and importantly, that deferasirox treatment is capable of decreasing the amount of oxidized proteins in the iron overloaded gerbil heart. Although the physiological effects of protein oxidation in the heart are not entirely elucidated, recent work has suggested that protein oxidation can alter protein function and conformation (Crowder and Cooke 1984; Hertelendi, Toth et al. 2008).

Reduced cardiac iron levels are associated with decreases in iron-associated MAPK phosphorylation

Recent data has suggested that increased ROS levels can trigger the activation of multiple signaling pathways including mitogen-activated protein kinases (MAPKs) (Martindale and Holbrook 2002). In addition, several lines of evidence have indicated that the MAPK proteins may be involved in cardiovascular remodeling and that the phosphorylation (activation) of these proteins is associated with the development of cardiac hypertrophy (Molkentin 2004; Wenzel, Muller et al. 2005). Here, we demonstrate that iron overload was associated with increased MAPK phosphorylation and that this effect was reversed following deferasirox treatment (Figure 10). These

data are consistent with previous work of Dai and colleagues who demonstrated in primary hepatocytes that increased intracellular iron was associated with increased ERK1/2- and p38-MAPK phosphorylation (Dai, Huang et al. 2004). Whether the observed changes in MAPK phosphorylation are directly related to changes in tissue iron concentration, indices of tissue ROS or other factors is not known and cannot be determined from the present study design. Nonetheless, it is interesting that tissue iron levels appeared to affect each of the MAPK proteins differently. For example, phosphorylated ERK1/2 levels appeared to be maximal directly after completion of the iron loading while conversely, the phosphorylation of the p38- and JNK-MAPK proteins was not maximal until one and three months of iron overload, respectively. Furthermore, the magnitude of p38-MAPK phosphorylation appears to be greater than that seen for either ERK1/2- or JNK-MAPK, possibly suggesting that p38-MAPK phosphorylation in the heart may be more sensitive to increased iron (or stress) than either the ERK1/2 or JNK proteins.

In summary, the present study demonstrates an important *in vivo* association between iron chelation, oxidative stress, and MAPK phosphorylation. Whether the observed changes may relate or contribute to complications seen in transfusional iron overload is currently unclear. Further, the effect of alternative treatment regimens is not clearly understood. Otte-Duessel et al. (2007) have suggested that twice-daily dosing of deferasirox appears to improve cardiac iron elimination compared to that observed using single daily dosing protocol. In addition, the administration of deferasirox in combination with deferoxamine produced no additive effect on the cardiac iron levels above that observed with deferasirox alone (Otto-Duessel, Aguilar et al. 2007). Whether this effect is due to limitations in the gerbil model itself (Otto-Duessel, Aguilar et al.

2007) or is applicable to other models remains to be determined. As such, clinical implications have to be evaluated carefully. Better understanding of the how cardiac iron levels may affect tissue ROS and function will no doubt be useful to improving clinical guidelines for cardioprotection.

Article #2: Corresponds to Specific Aim #2

To determine if deferasirox is able to reduce hepatic iron content, iron-induced ferritin upregulation, and iron related increases in indices of oxidative stress and the effect of these changes, if present, on the incidence of iron-related changes in cell death and apoptotic signaling.

DEFERASIROX PROTECTS AGAINST IRON-INDUCED HEPATIC INJURY IN MONGOLIAN GERBIL

Rabaa AL-Rousan[a], Kevin M Rice[a], Anjaiah Katta[a], Joseph Laurino[c], Ernest M. Walker[d], William E. Triest[e], and Eric R. Blough[a,b]

[a] Department of Pharmacology, Physiology, and Toxicology, Joan C. Edwards School of Medicine, Marshall University; [b]Department of Biological Sciences, Marshall University; [c]Department of Chemistry, University of Tampa; [d]Department of Anatomy and Pathology, Joan C. Edwards School of Medicine, Marshall University; [e]Huntington Veterans Administration Medical Center, Huntington, WV.

Abstract

Iron overload is associated with an increased risk of developing liver complications including fibrosis, cirrhosis, and hepatocellular carcinoma. Deferasirox is a novel oral chelator with high iron-binding potency and selectivity. Here, we investigate the ability of deferasirox to remove excessive hepatic iron and prevent or reverse iron induced hepatic injury. Adult male Mongolian gerbils were randomly divided into three groups: control, iron overload, and iron overload followed by deferasirox treatment. Iron overload animals received iron dextran 100 mg/kg i.p /5 d for 10 wks while deferasirox was given 100 mg/kg/d p.o for 1 or 3 months. Compared to the non-treated iron overload group, deferasirox treatment reduced hepatic iron levels by 43.5% after three months of treatment ($P < 0.05$). Histological analysis detected frequent iron deposition, evidence of hepatic damage, and lipid accumulation in hepatic tissue of the iron overloaded group. Iron deposition was significantly diminished with deferasirox treatment and no evidence of lipid accumulation was observed. Immunoblotting demonstrated that iron overload caused about a two fold increase in hepatic ferritin expression ($P < 0.05$), which was reduced by 47.5% following three months of deferasirox treatment ($P < 0.05$). In addition, deferasirox significantly reduced hepatic protein oxidation and superoxide abundance. The percentage of TUNEL-positive nuclei in the deferasirox treated livers was 41.0% lower than that of the iron overloaded group ($P < 0.05$). Similarly, iron related increase in the expression of Bax/Bcl-2, Bad, and caspase-3 were significantly lower following deferasirox treatment. These findings suggest that deferasirox may confer protection against iron induced hepatic toxicity.

Introduction

Iron overload is associated with liver, pancreatic, and cardiac dysfunction and is potentially deadly if improperly managed (Gordeuk, Bacon et al. 1987). The incidence of iron overload appears to be increasing, and it has been estimated that this disorder now afflicts over 100 million worldwide (Kontoghiorghes 2006). Most often, iron overload is seen in those with hereditary hemochromatosis and in individuals that must undergo frequent blood transfusions (Gordeuk, Bacon et al. 1987). The etiology of iron overload is thought to be governed by the magnitude of the body iron burden, the rate at which the increase in body iron has occurred, and the distribution of the excess iron within the body (Kushner, Porter et al. 2001). The management of iron overload may be achieved by pharmacologic chelating agents such as deferoxamine, deferiprone, and Deferasirox (Olivieri and Brittenham 1997). Deferoxamine (Desferal^{R}) is presently the standard of care for the first-line treatment of transfusional iron overload (Brittenham, Griffith et al. 1994). Although effective in removing iron, treatment compliance is oftentimes compromised given that deferoxamine administration requires overnight subcutaneous infusions, 5-7 nights/week (Hershko, Link et al. 2005; Neufeld 2006). In contrast to the burden associated with deferoxamine treatment, deferasirox (Exjade^{R}, ICL670) is given orally using a once-daily regimen. Although initial findings have been very promising, information regarding the effect of deferasirox on hepatic iron handling is lacking.

It is thought that the toxic effect of iron is due, at least in part, to the generation of reactive oxygen species (ROS) through the Fenton reaction where iron mediates the oxidation of free radical intermediates such as superoxide anion ($O^{2\bullet-}$) or hydrogen peroxide (H_2O_2) to highly toxic free radicals such as hydroxyl radical ($HO^{\bullet}$) (Storz and Imlay 1999). Here, we investigate whether deferasirox is capable of removing excess

iron from liver and the effect of iron removal, if present, on hepatic ROS. We hypothesized that deferasirox treatment would reduce hepatic iron content and that this decrease in iron would be associated with decreases in ROS that will, in turn, be strongly associated with the reversal or reduction of iron-induced changes in hepatic structure and function.

Results

Characterization of animals

Total body and liver weights were obtained and compared . All animals tolerated the iron loading and chelation without any apparent ill effects. The body weights of iron overloaded gerbils were similar to controls, indicating that the injection of iron dextran did not result in debilitation or weight loss. Liver weights were increased 52% after 10 weeks of iron overload and remained elevated after one and three months follow up *(P* < 0.05*)* (Table 5). Deferasirox treatment was effective in reducing iron-associated increases in whole liver weight (Table 5).

Table 5. Deposition of gerbils in the experimental groups and liver/body weights.

Interval	Groups n = 10/ group	Treatment	Liver/ body wt (%)
Baseline	Ctrl	10wk saline	3.10 ± 0.17
	IO	10wk iron	4.72 ± 0.21*
1 months	Ctrl	10 wk saline + 1mo vehicle	3.71 ± 0.14
	IO	10 wk iron + 1 mo vehicle	5.77 ± 0.21*
	IO+ DFR	10 wk iron + 1 mo DFR	5.20 ± 0.17*+
3 months	Ctrl	10 wk saline + 3 mo vehicle	3.63 ± 0.08
	IO	10 wk iron + 3 mo vehicle	5.47 ± 0.20*
	IO+ DFR	10 wk iron + 3 mo DFR	4.51 ± 0.15*+

An asterisk (*) or cross (+) indicates significant difference from age matched control or iron overload groups, respectively.

Hepatic iron levels

Hepatic iron levels were elevated 90 fold compared to age matched controls after iron overload injections ($P < 0.05$). Hepatic iron levels exhibited gradual reduction to 76.5 and 57.8 fold at one month and three months post overload, respectively ($P < 0.05$). Deferasirox treatment decreased hepatic iron level by 43.5% after three months of treatment ($P < 0.05$) (Figure 11). These observations were consistent with hepatic Prussian blue staining results in which iron overloaded hepatic tissue exhibited frequently elevated iron deposits in all regions of the hepatic plate but especially concentrated in the periportal region (Figure 12, C). Interestingly, deferasirox produced striking hepatocyte clearing from all regions of hepatic plate (Figure 12, D).In addition, we observed an increase in lipid accumulation as vacuoles in the hepatocytes of the iron overloaded group (Figure 12, B). These vacuoles were not apparent in hepatic tissue from either control or deferasirox treated groups.

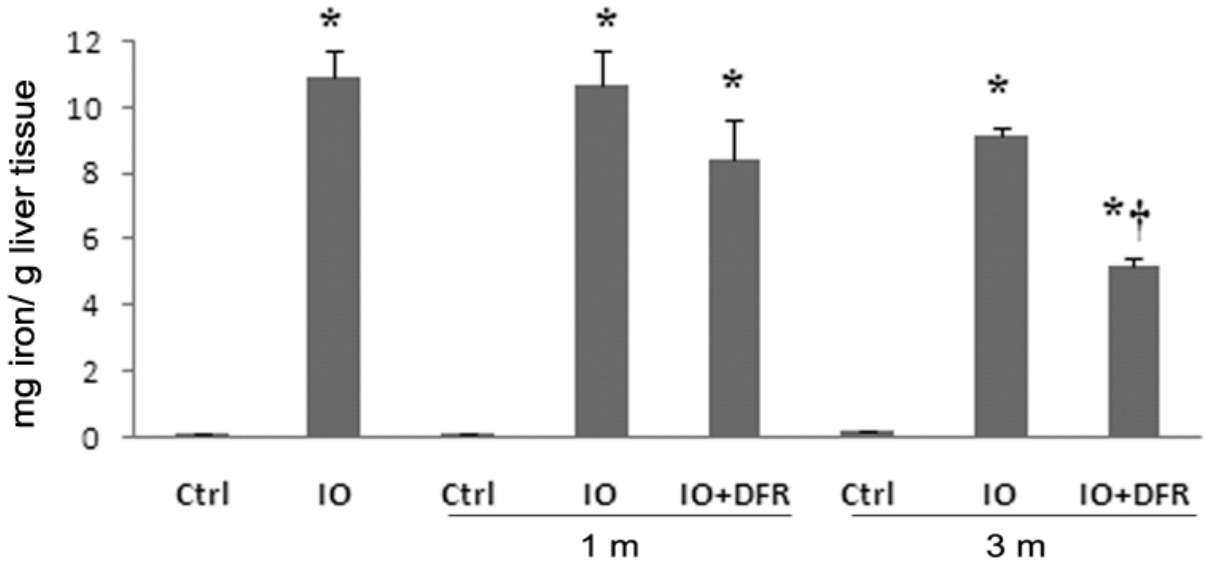

Figure 11. Average iron levels in mg/g tissue weight in hepatic tissue of gerbils in the experimental groups. Ctrl: control, IO: Iron overload, IO+ DFR: Iron overload followed by deferasirox treatment, 1m: 1 month interval, 3m: 3 months interval. (*) indicates significant difference from control, (†) indicates significant difference from iron overload group ($P < 0.05$).

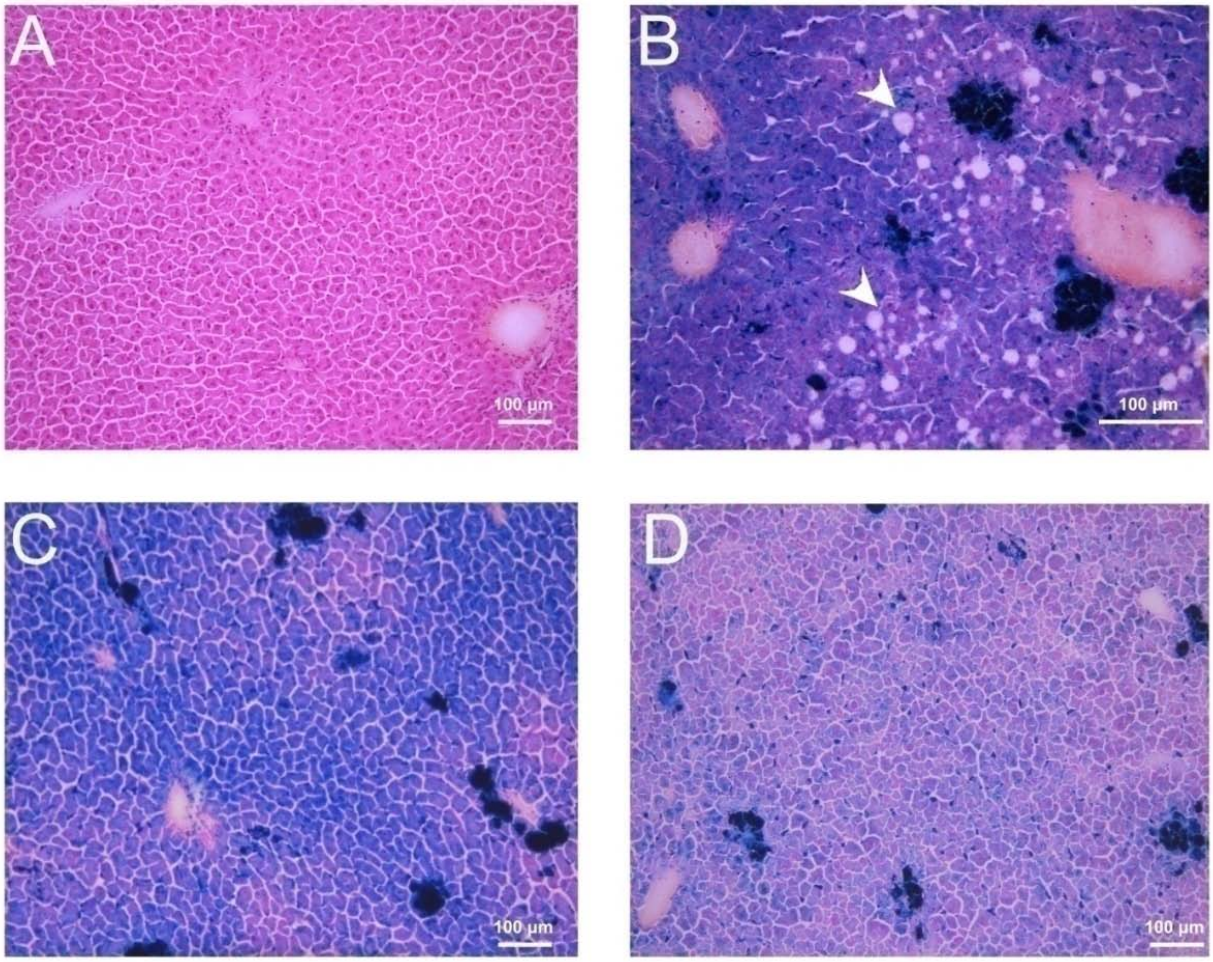

Figure 12. Iron deposition in hepatic tissue of Ctrl (A), IO (B,C), and IO+DFR(D) gerbils followed for 3 months. Ferric iron was detected by Prussian blue staining. (A) demonstrates no apparent iron deposition in the liver of control gerbils (200X). (B) depicts iron induced damage and lipid accumulation in hepatocytes as vacuoles (Arrow, 400X). (C) shows iron accumulation in all areas of hepatic plate, but especially concentrated in the periportal region (200X). Large, intensely stained lobular masses represent macrophages. (D) demonstrates decreased iron deposition in all areas of deferasirox treated hepatic tissue (200X). Iron accumulation manifests as blue background staining at this magnification but is discernible as discrete deposits “dots” at higher power

Ferritin protein expression

We investigated whether the elevation in hepatic iron levels with iron overload is associated with an increase in hepatic ferritin protein expression using Western blot analysis. As expected, ferritin protein expression was 2.4 fold higher after ten weeks of iron overload. Ferritin levels decreased slowly over time, and it was 2.2 fold, and 2.1 fold at one and three months follow up. Interestingly, one and three months of deferasirox treatment resulted in 23%, and 47.5% reduction in ferritin protein expression compared to that of the age matched iron overload value (Figure 13).

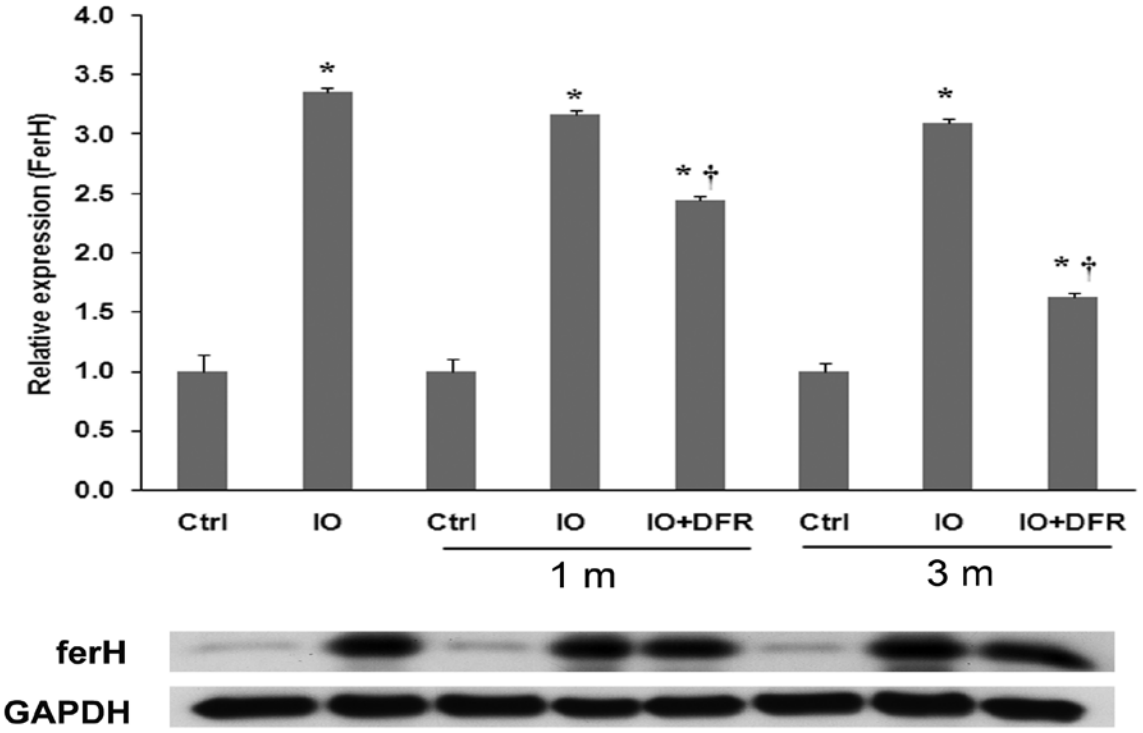

Figure 13. Western blot analysis of ferritin heavy chain (ferH) protein expression in hepatic tissue of gerbils in the experimental groups. Effects of iron overload and deferasirox treatment on ferritin protein expression were analyzed. Results were obtained from six experiments and expressed as a percentage of the corresponding age matched control value (upper panel). Representative Western blot (lower panel). 1m: 1 month interval, 3m: 3 months interval. (*) indicates significant difference from control, (†) indicates significant difference from iron overload group ($P < 0.05$)

Superoxide abundance

Liver specimens were evaluated for $\cdot O_2^-$ generation within tissue sections utilizing HE fluorescence. Iron overload induced a 167.0% increase in fluorescent staining in hepatic tissue three months after iron injections ($P < 0.05$). This increase was reduced by 48.6% with deferasirox treatment in hepatic tissue when compared to age-matched control ($P < 0.05$) (Figure 14).

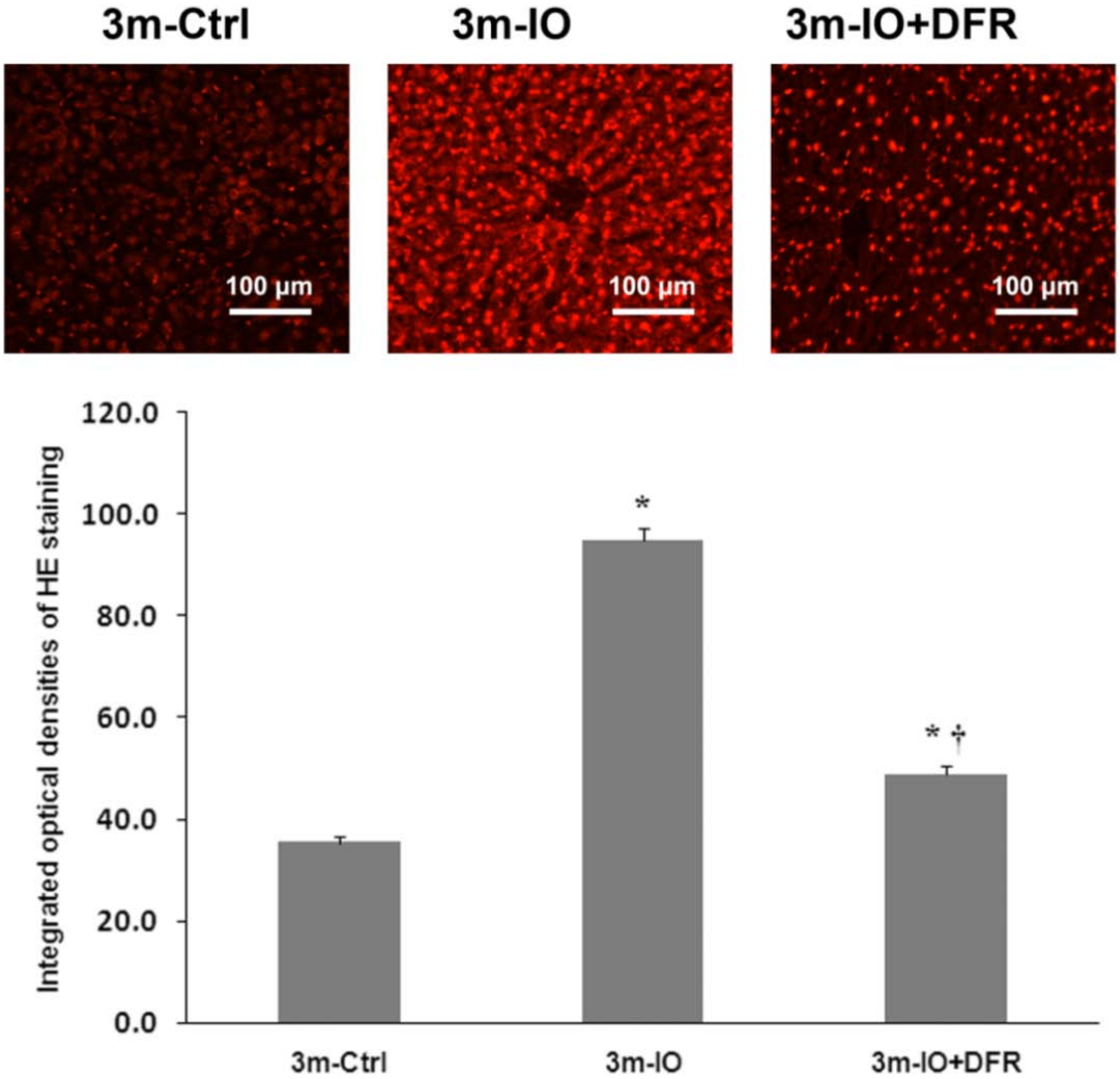

Figure 14. Detection of hepatic superoxide by hydroethidine in Ctrl, IO, and IO+DFR. The increase in superoxide involves all regions of the hepatic plate (Upper panel). Quantification of hepatic superoxide as determined by intensity of fluorescent ethidium bromide-stained nuclei (Lower panel). 3m: 3 months interval. An asterisk (*) indicates significant difference from control animals, (†) indicates significant difference from iron overload ($P < 0.05$).

Protein oxidation

Iron catalyzed oxidation of proteins introduces carbonyl groups at lysine, arginine, proline, and threonine residues in a site specific manner. Protein modification by oxygen free radicals and other reactive species were analyzed in hepatic cells from control, iron overloaded, and deferasirox treated groups utilizing an OxyBlot™ detection kit. Interestingly, iron overload induced 1.6 fold increase in protein oxidation at 3 months. Protein oxidation was reduced by 50.2% after three months of deferasirox treatment ($P < 0.05$) (Figure 15).

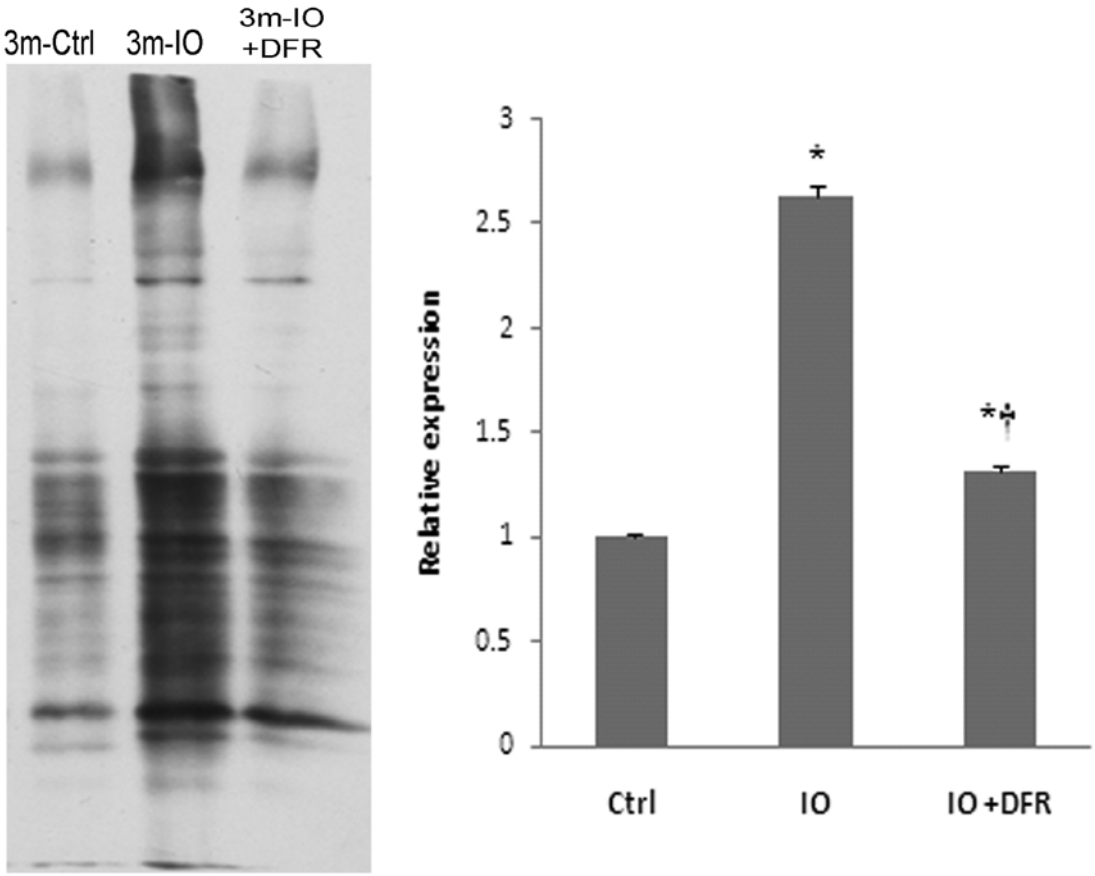

Figure 15. Effect of iron overload or deferasirox treatment on hepatic protein carbonylation. (Left) Representative oxy-blots of hepatic protein isolates from Ctrl, IO, and IO+DFR. (Right) Quantification of oxidatively modified proteins in hepatic protein

isolates obtained from the corresponding groups. 3m: 3 months interval. An asterisk (*) indicates significant difference from control animals, (†) indicates significant difference from iron overloaded animals ($P < 0.05$).

Cell death

To investigate whether iron overload induced alterations in oxidative stress are related to hepatic cell death, we examined the number of nuclei staining positively for DNA fragmentation by TUNEL assay. The apoptotic index in the hepatocytes of iron overloaded gerbils increased 7.5 fold compared to age-matched control 3 months post iron overload, while deferasirox treatment demonstrated a 41.0% reduction in the apoptotic index when compared to this iron overload induced increase ($P < 0.05$) (Figure 16).

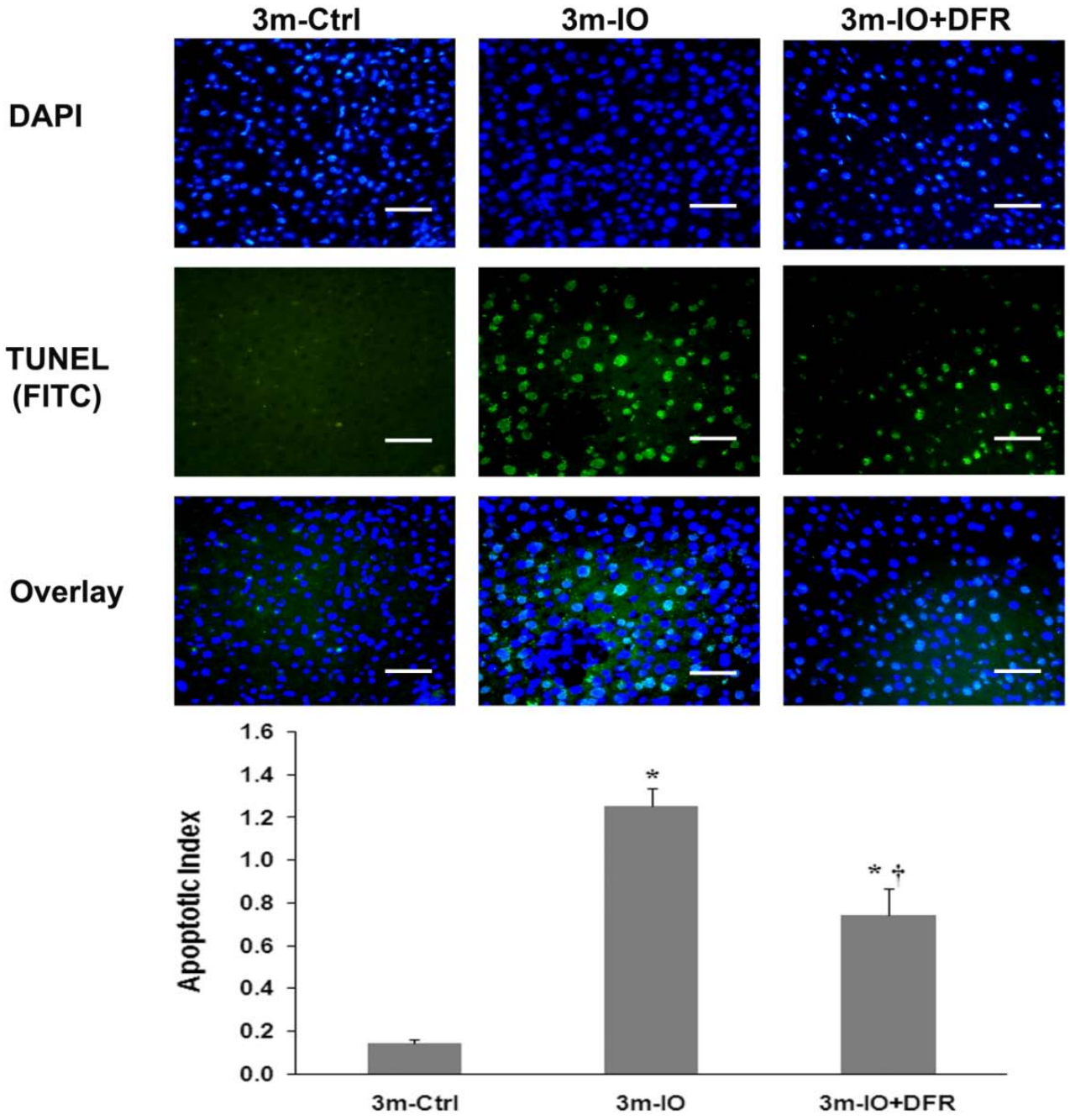

Figure 16. Representative cross sections showing the changes in nuclei exhibiting DNA strand breakage as determined by TUNEL staining in Ctrl, IO, and IO +DFR. Bar = 50 µm (upper panel). Quantification of hepatic apoptotic cells as determined by the number of TUNEL positive cells by the number of DAPI positive cells per $mm^{2,}$ apoptotic index, (Lower panel). 3m: 3 months interval. An asterisk (*) indicates significant difference from control animals, (†) indicates significant difference from iron overload ($P < 0.05$).

Bcl-2 apoptotic signaling

The expression of the anti-apoptotic (Bcl-2) and the pro-apoptotic (Bax and Bad) proteins and the ratio of Bax to Bcl-2 were evaluated by western blotting. When Bax is in excess, Bcl-2 cannot bind and sequester all the Bax protein, thus allowing Bax to oligomerize and act on the mitochondrial membrane to cause release of cytochrome c from the inter-membrane space to the cytosolic space. Thus a higher Bax to Bcl-2 ratio would potentially increase the susceptibility to mitochondrial permeability. We investigated if there were any changes in the anti-apoptotic (Bcl-2) and pro-apoptotic (Bax and Bad) proteins in the experimental groups. The expression of Bax/Bcl-2 was 62.1% higher than control after 10 weeks of iron loading ($P < 0.05$) (Figure 17). Bax/Bcl-2 levels remained consistently elevated and were 52% and 121% higher after 1- and 3-months follow up compared to respective age matched controls ($P < 0.05$) (Figure 17). We demonstrated decreased levels of Bax/Bcl-2 expression with deferasirox treatment and it was 21.7% and 47% lower after 1- and 3-months of treatment, respectively ($P < 0.05$) (Figure 17).

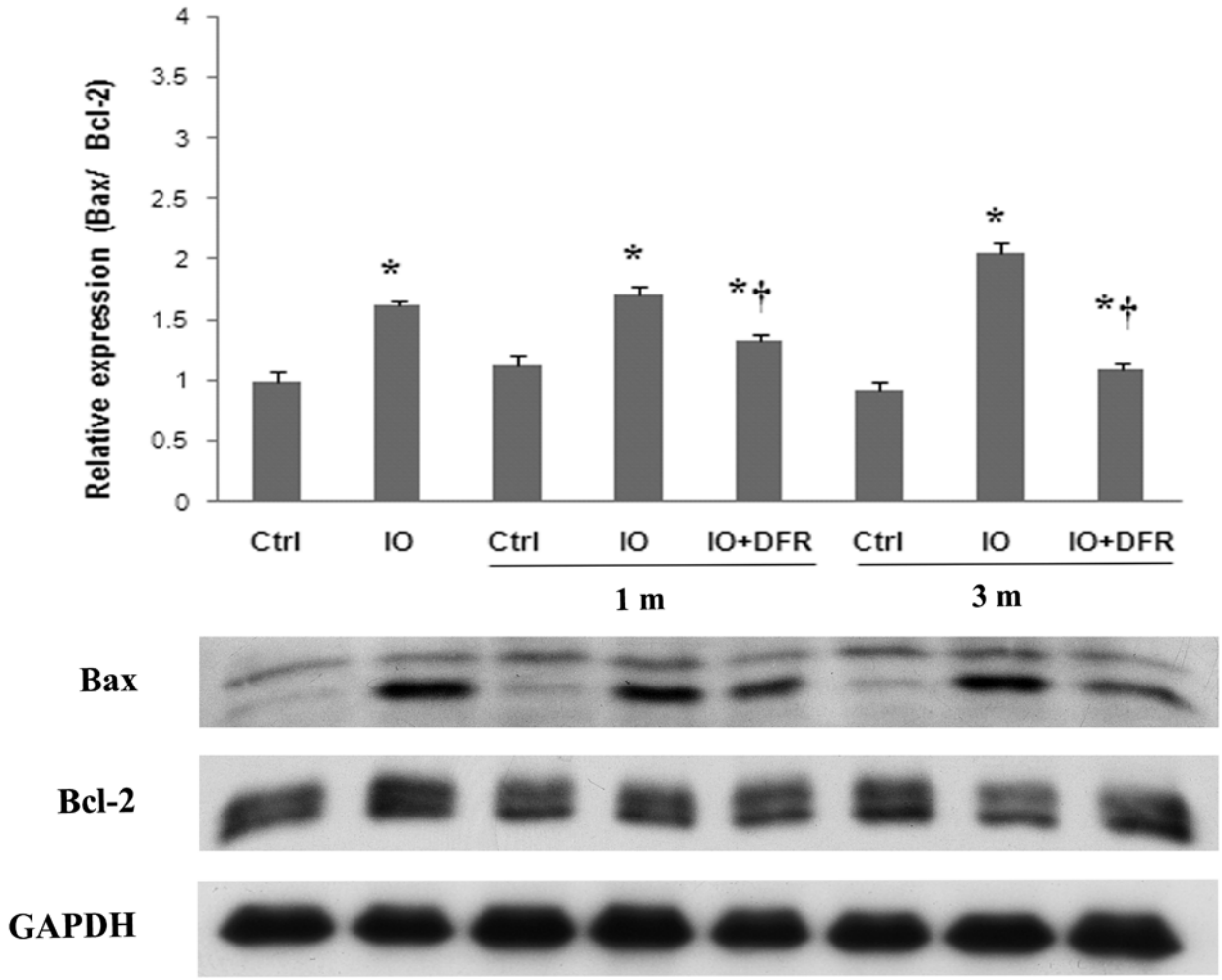

Figure 17. Effects of iron overload and deferasirox treatment on Bax/Bcl-2 protein level in hepatic tissue of gerbils in the experimental groups. Results were obtained from six experiments and expressed as a percentage of the corresponding age matched control value (upper panel). Representative Western blot (lower panel). 1 m = 1 month interval, 3 m = 3 months interval. (*) indicates significant difference from control, (†) indicates significant difference from iron overload group ($P < 0.05$).

In addition, Bad expression was 73%, 52%, and 77% higher in the IO, 1 month-IO and 3 months-IO, respectively ($P < 0.05$). With three months of deferasirox treatment Bad expression was reduced by 33% compared to age matched iron overload group ($P < 0.05$) (Figure 18).

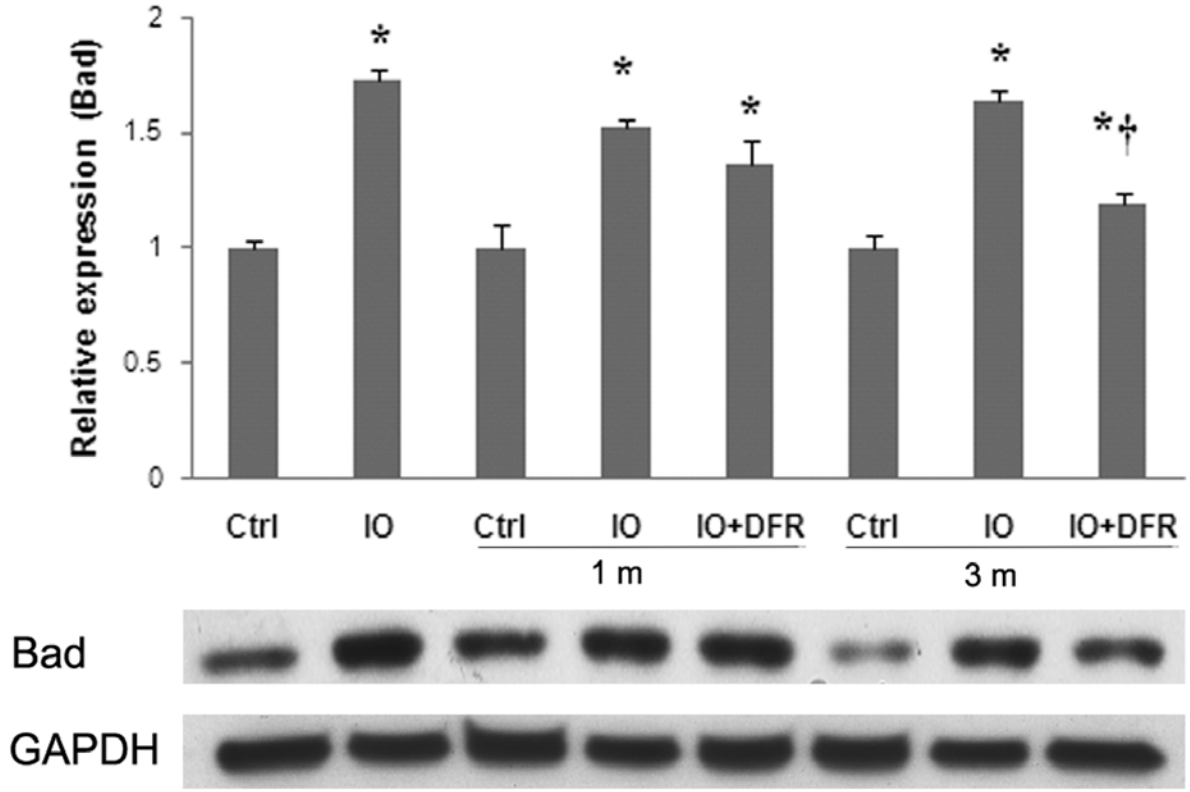

Figure 18. Effects of iron overload and deferasirox treatment on Bad protein level in hepatic tissue of gerbils in the experimental groups. Results are obtained from six experiments in each group and expressed as a percentage of the corresponding age matched control value (upper panel). Representative Western blot (lower panel). 1 m = 1 month interval, 3 m = 3 months interval. (*) indicates significant difference from control, (†) indicates significant difference from iron overload group ($P < 0.05$).

Caspase-3 activation

One critical step in the execution of the apoptotic program that elicits DNA fragmentation is cleavage of caspase-3 into 19- and 17-kDa fragments. Caspases are cysteine dependent aspartate specific proteases which activate endonucleases integral in the final execution of nuclei and cell death. Cleaved caspase-3 is downstream of the Bcl-2 family apoptotic cascade and integrates apoptotic signaling from the cytokine/Fas and $Ca^{2+/}$ER pathways as well. Caspase-3 activation, as measured by cleaved

caspase-3 fragment level, was markedly higher in the iron overload liver (86%, and 102% after 1 and 3 month of follow up, respectively) as compared to age matched control liver ($P < 0.05$) (Figure 19). We demonstrated a significant reduction of cleaved caspase-3 by 21% in the 3 months deferasirox treatment group ($P < 0.05$) (Figure 9). No significant difference in the expression of the full length caspase-3 was observed between groups.

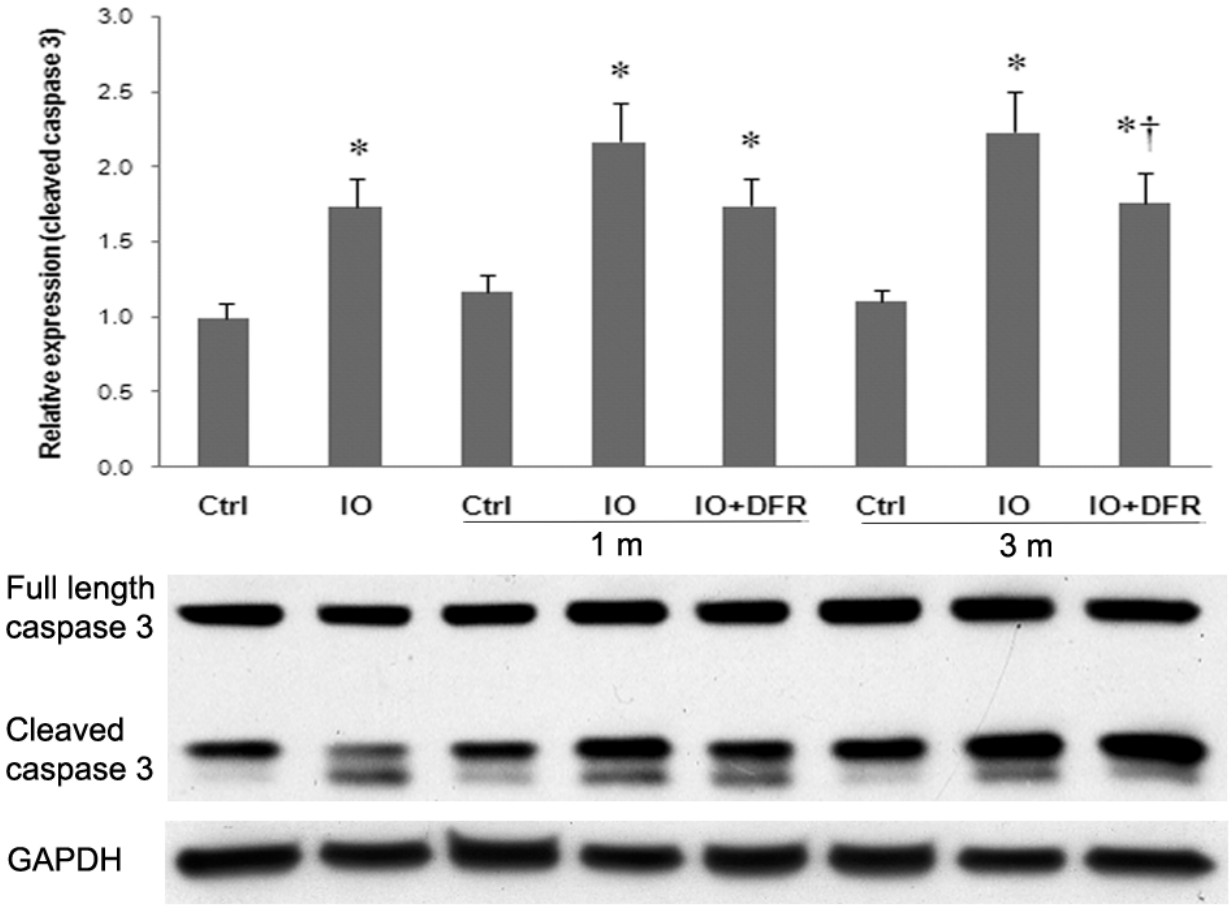

Figure 19. Effects of iron overload and deferasirox treatment on full length and cleaved caspase-3 in hepatic tissue of gerbils in the experimental groups. Results were obtained from six experiments and expressed as a percentage of the corresponding age matched control value (upper panel). Representative Western blot (lower panel). 1 m = 1 month interval, 3 m = 3 months interval. (*) indicates significant difference from control, (†) indicates significant difference from iron overload group ($P < 0.05$).

Table 6. Regression analysis of the relationship between expression levels of specific proteins and TUNEL, HE staining intensity, liver weight, and hepatic iron levels obtained from experimental groups

	Liver wt	Iron	Ferritin	Oxyblot	HE	TUNEL
Independent variables						
Liver wt	N.T.	0.693†	0.703††	0.513†	0.511†	0.562†
Iron	0.693†	N.T.	0.957†††	0.911†††	0.919†††	0.949†††
Ferritin	0.703††	0.957†††	N.T.	0.922†††	0.935†††	0.927†††
Oxyblot	0.513†	0.911†††	0.922†††	N.T.	0.922†††	0.852††
HE	0.511†	0.919†††	0.935†††	0.922†††	N.T.	0.869††
TUNEL	0.562†	0.949†††	0.927†††	0.852††	0.869††	N.T.
Apoptotic regulators						
Bax	0.427*	0.661†	0.696†	0.550†	0.535†	0.341*
Bcl-2	0.135	0.299	0.321*	0.329*	0.272	0.111
Bad	0.127	0.127	0.138	0.583†	0.575†	0.362*
Caspase-3 (cleaved)	0.424*	0.637†	0.659†	0.846††	0.824††	0.689†

(†††) indicates very high correlation, (††) indicates high correlation, (†) indicates moderate correlation, (*)indicates low correlation, N.T. = not tested.

Discussion

The iron overloaded gerbil, a well accepted animal model of iron overload, is thought to closely resemble many of the effects of iron overload seen in humans (Carthew, Dorman et al. 1993; Yang, Brittenham et al. 2003). Using the gerbil model of

iron overload, we have previously demonstrated that deferasirox treatment removes cardiac iron and reduces the iron associated increase in oxidative stress and ferritin expression (Al-Rousan, Paturi et al. 2009). Similar to our finding in the heart, here we demonstrate that iron overload caused hepatic iron deposition and lipid accumulation and resulted in a dramatic increase in hepatic iron content. This elevated level of iron deposition was also associated with increased ferritin protein expression, elevated levels of ROS, and cell death signals. Iron chelation by deferasirox reduced iron deposition and the induction of ferritin and Bax proteins, whose gene expression is thought to be linked to oxidative stress, suppressed iron overload-induced superoxide formation and protein oxidation, and reduced the incidence of hepatocyte death. These data collectively suggest that deferasirox may afford hepatic protection against iron-induced pathogenesis.

Deferasirox decreases hepatic iron and ferritin levels in the iron-overloaded gerbil

We found that hepatic iron levels after three months of follow up were significantly lower than observed in the 10-week iron overload animals ($P < 0.05$). These observations are consistent with the findings by Wood et al. (Wood, Otto-Duessel et al. 2006) that body iron levels exhibit spontaneous (non chelator-mediated) redistribution and elimination. These levels, however, remained elevated and potentially harmful to hepatic tissue. Three months of deferasirox treatment significantly reduced hepatic iron content by 43.5% compared to that of the age-matched iron overloaded group ($P < 0.05$) (Figure 11). As expected from its predominantly biliary elimination clearance (Hershko, Konijn et al. 2001), these iron removal data suggest that deferasirox appears to be particularly efficient for hepatocyte clearance. Similar to our

biochemical assessment, the findings from our histological data suggest that deferasirox is efficacious in removing liver iron. In addition, we also observed evidence of lipid accumulation in the iron-overloaded liver (Figure 12, B arrows). Elevated free iron has been shown to be hepatotoxic, possibly exerting its effects by interfering with mitochondrial or microsomal function which disrupts lipoprotein transport and fatty acids homeostasis (Baptista-Gonzalez, Chavez-Tapia et al. 2008; Duncan 2008; Raszeja-Wyszomirska, Lawniczak et al. 2008). Interestingly, with deferasirox treatment we failed to find any evidence of fatty acid accumulation suggesting perhaps that this agent is efficacious in preventing iron-induced liver damage. More research to specifically address hepatic mitochondrial function in these groups will no doubt be useful in furthering our understanding the effect of deferasirox on liver physiology.

It is well accepted that ferritin is the principal storage protein for iron (Arosio and Levi 2002). The increase in ferritin expression in response to iron overload is thought to provide a cytoprotective mechanism against iron induced toxicity (Balla, Jacob et al. 1992; de Valk and Marx 1999). Nonetheless, it should be noted that although ferritin and hemosiderin have traditionally been regarded as ‘safe’ storage forms of iron, this does not mean that the iron contained in these molecules cannot potentiate the development of oxidative stress under certain conditions. Indeed, it has been recently demonstrated that the superoxide radical is capable of mobilizing iron from ferritin and that this can result in the production of iron-catalyzed hydroxyl radicals (Bartfay, Dawood et al. 1999).

The synthesis of ferritin is tightly regulated and is dependent on intracellular iron levels. When iron is low, binding of the iron-regulatory proteins (IRP-1) to iron-responsive elements (IRE) inhibits translation of ferritin. Conversely, when cellular iron

is high, the opposite regulation takes place (Ferrara and Taylor 2005). In the present study, we demonstrated a significant increase in ferritin levels with iron loading and more importantly, that these elevations were significantly suppressed with deferasirox treatment (Figure 13). These results are in agreement with previous findings that chelation therapy with deferoxamine reduced iron-induced ferritin upregulation in rat aorta (Ishizaka, Saito et al. 2005). To our knowledge, the present study is the first description of the effect of iron overload and deferasirox treatment on hepatic ferritin expression.

It is thought that deferasirox does not chelate tightly bound iron stores (eg, hemoglobin or the cytochromes), but instead extracts iron from storage proteins such as ferritin with relatively weak bonds (Evens, Mehta et al. 2004). On the other hand, in vitro studies have shown that deferasirox is able to access the intracellular labile iron pool (LIP) (Glickstein, El et al. 2005; Glickstein, El et al. 2006). It is important to note here that ferritin-bound iron is in an equilibrium state with the free iron in the LIP (Crichton and Ward 2003). Thus, it is plausible to postulate that deferasirox may indirectly reduce ferritin bound iron by shifting the equilibrium in favor of the more accessible iron in the LIP.

Reduced hepatic iron levels are associated with decreases in tissue ROS

Because humans have no physiologic means of eliminating excess iron, any persistent increase in intake may eventually result in iron overload. When the extent of iron accumulation exceeds the body's ability to safely sequester the surplus iron, free iron builds up in the LIP (Breuer, Epsztejn et al. 1996). Normally, the LIP represents only 3–5% of the total cellular iron (Arosio and Levi 2002). Iron overload can induce

about a three-fold increase in the iron level in hepatic LIP, which triggers oxidative stress and cell injury (Arosio and Levi 2002)**.**

The formation of highly toxic hydroxyl radical via Fenton and Haber-Weiss reactions, followed by the subsequent formation of lipid peroxidation products, is postulated to be an underlying mechanism of iron mediated liver injury (Britton and Bacon 1994; Staubli and Boelsterli 1998). In the liver, iron overload is thought to damage the hepatocytes and dysregulate a variety of metabolic pathways, which if allowed to proceed unchecked could eventually result in liver fibrosis, cirrhosis, or other liver diseases (Ramm and Ruddell 2005; Tsukada, Parsons et al. 2006). Iron chelators decrease the redox activity of iron through their ability to form complexes with Fe (III), preventing the reduction of Fe(III) by superoxide to the reactive Fe(II) state.

In the present study, we showed that ROS levels as superoxide anion ($O_2\bullet^-$) were increased in the iron-overloaded hepatic tissue as determined by hydroethidium staining (Figure 14). These findings are consistent with earlier data which have suggested that increased iron levels are associated with increases in liver ROS (Glickstein, El et al. 2006; Pardo Andreu, Inada et al. 2008). Possible sources of increased ROS with iron loading are not fully elucidated but could include the iron catalyzed Fenton-Haber Weiss reaction, redox cycling, and possibly iron associated changes in NADPH oxidoreductases and mitochondrial function (MacCarthy, Grieve et al. 2001; Galaris and Pantopoulos 2008; Kim, Kim et al. 2008; Pardo Andreu, Inada et al. 2008). Whether these changes in ROS are directly related to the improvements in histological appearance we observe with deferasirox treatment are not fully elucidated.

Our data suggested that iron overload was associated with increased levels of protein oxidation in the liver (Figure 15) and importantly, that deferasirox treatment is

capable of decreasing the amount of oxidized proteins in the iron overloaded liver. Although the physiological effects of protein oxidation in the liver are not entirely elucidated, recent work has suggested that protein oxidation can alter hepatic enzyme activity. For example, the increased oxidative levels have been shown to alter the activity of 3-hydroxy-3-methylglutaryl coenzyme A reductase (HMGCoAR), the rate limiting enzyme in the production of cholesterol (Pallottini, Martini et al. 2005). Whether the proteins identified in our analysis are related to hepatic metabolism is unknown and will necessitate further experimentation. Nonetheless, the decreases we see in the quantity of modified proteins and liver ROS levels are highly correlated with deferasirox-associated improvements in liver iron levels and liver histology (Table 6). Taken together, these data suggest that deferasirox may be efficacious in preventing iron accumulation, ROS accumulation and iron-overload induced liver pathology.

Reduced hepatic iron levels are associated with decreases in iron-associated cell death

A link between oxidative stress and cell death has been reported in several conditions including hemochromatosis (Cooksey, Jouihan et al. 2004), alcoholic liver disease (Zima and Kalousova 2005), hepatitis, and liver cirrhosis (Kaplowitz 2000). However, the mechanism by which free radicals can induce cell death is not well understood. Here, we demonstrated that iron overload was associated with increased hepatic cell death as determined by increased incidence of TUNEL reactive nuclei (Figure 16). Interestingly, the number of TUNEL positive nuclei was significantly reduced with deferasirox treatment.

To investigate the mechanism of iron overload-related DNA strand breakage that we observed in our TUNEL studies, we examined the expression of Bcl-2 family

proteins. It is thought that the ratio of Bax to Bcl-2 plays an important role in regulating the release of cytochrome-c from the mitochondria into the cytosol. This latter effect is favored as the balance shifts toward Bax leading to cell death (Oltvai, Milliman et al. 1993). In iron overloaded animals, we found that Bax expression was elevated and that these levels were reduced with deferasirox treatment (Figure 17). To expand upon this finding we also examined the regulation of Bad, a pro-apoptotic member of the Bcl-2 family that can displace Bax binding from Bcl-2 and Bcl-XL, resulting in cell death (Hengartner 2000). Similar to our findings with Bax, deferasirox treatment significantly decreased the expression of Bad (Figure 18).

Caspase-3 is a key effector of mitochondrial-mediated apoptosis (Cai, Yang et al. 1998; Porter and Janicke 1999; Goldspink 2003) that is normally activated by proteolytic cleavage (Cohen 1997). To investigate whether alterations in the regulation of caspase-3 may be involved, here we examined the expression of caspase-3 with iron overload and deferasirox treatment. With iron overload, we observed increases in the amount of cleaved caspase-3 (Figure 19). Further, we demonstrated that deferasirox administration decreased caspase-3 cleavage. These data, in conjunction with our findings that deferasirox alters the regulation of Bcl-2, Bax and Bad, suggest that deferasirox may decrease iron-induced apoptosis by affecting the regulation of the mitochondrial apoptotic cascade. This is in agreement with the results of other recent investigations that have implicated increased iron levels as causing mitochondrial dysfunction and apoptosis (Eaton and Qian 2002; Walter, Knutson et al. 2002). Whether the activation of the mitochondrial apoptotic pathway is dependent upon iron-associated increases in ROS *per se*, or ROS acting in concert with other factors, is worthy of detailed studies.

Conclusions

In conclusion, our data suggest that iron overload is associated with increases in hepatic iron levels, indices of ROS, and increased hepatic apoptosis and that deferasirox is efficacious in attenuating these parameters. Given that iron overload is associated with an increased risk of developing liver fibrosis, decreased hepatic function, and hepatic cancer (Bonkovsky and Lambrecht 2000; Fattovich, Stroffolini et al. 2004) it is likely that deferasirox treatment may find a use for the treatment and / or prevention of several hepatic disorders.

Article #3: Corresponds to Specific Aim #3

To determine the long term cardiovascular complications associated with iron overload and to determine if chronic deferasirox administration is able to prevent/reduce these complications, including those related to cardiac remodeling and functional abnormalities.

LONG TERM EFFICACY OF DEFERASIROX IN PREVENTING CARDIOVASCULAR COMPLICATIONS IN THE IRON OVERLOADED GERBIL

Rabaa M. AL-Rousan[1,6] , Kamran Manzoor[2], Satyanarayana Paturi[3], Ravi Arvapalli[3], Joseph P. Laurino[4], Lucy Dornon[5], Ernest M. Walker[6], and Eric R. Blough[1,3,7,8]

[1]Department of Pharmacology, Physiology and Toxicology, Joan C. Edwards School of Medicine, Marshall University, Huntington WV; [2]Charleston Area Medical Center, Charleston, WV; [3]Department of Biological Sciences, Marshall University, Huntington WV; [4]Department of Chemistry, University of Tampa, Tampa FL; [5]Department of cardiology, Cabell Huntington Hospital, Huntington, WV; [6]Department of Pathology, Marshall University, Huntington WV; [7]Department of Exercise Science, Sport and Recreation, College of Education and Human Services, Marshall University, Huntington WV; [8]Cell Differentiation and Development Center, Marshall University, Huntington WV;

Abstract

Iron-induced cardiovascular disease is the leading cause of death in iron-overload patients. Deferasirox is a novel tridentate oral chelator that exhibits a half-life suitable for once-daily dosing; however, little is known regarding the effectiveness of this agent in preventing iron-induced cardiovascular dysfunction. Adult male Mongolian Gerbils were randomly divided into three groups: control, iron overload, and iron overload followed by deferasirox treatment. Iron overload animals received iron-dextran 100 mg/kg i.p /5 d for 10 wks while deferasirox was given 100 mg/kg/d p.o for 9 months post iron loading. Cardiac and aortic iron levels were determined by inductively coupled plasma atomic emission spectrometry. Gerbil EKG (standard leads I, II, & III) and echocardiograms (Philips Sonos 5500) were obtained in anesthetized animals at regular intervals. Compared to control animals, iron concentration was 3.3 and 2.4 fold higher in iron overloaded heart and aorta respectively ($P < 0.05$). Deferasirox treatment reduced cardiac and aortic iron levels by 31.6%, and 34.6%, respectively ($P < 0.05$). These results were consistent with the decrease in cellular iron deposition observed with Prussian blue iron staining. Cardiac mass/body wt ratio was increased by 34% in the iron overloaded group and was 24% lower with deferasirox treatment. Iron overloaded gerbils were found to exhibit frequent arrhythmias including premature ventricular tachycardia (6/10), supraventricular tachycardia (3/10), recurrent ventricular tachycardia (4/10), and increased mortality (3/10) with the latter occurring most likely due to fatal arrhythmias. Echocardiographic assessment demonstrated iron-induced increases in LVPWd, LVIDd, and LVSd by 48.6%, 26.2%, and 42.4%, respectively ($P < 0.05$). Similarly, ejection fraction and fractional shortening were reduced by 29.6% and 22.9% compared to controls ($P < 0.05$). Deferasirox reduced the incidence of iron-induced

arrhythmia and either prevented or significantly decreased iron-induced changes in cardiac structure (LVIDd: 23.6%; $P < 0.05$), LVPWd (21.5%; $P < 0.05$), LVSd (27.2%; $P < 0.05$) and function (EF: 29.8%; $P < 0.05$), (FS: 27.8%; $P < 0.05$). Taken together, these data suggest that once daily oral deferasirox treatment appears to be effective in preventing or reducing iron-induced cardiovascular abnormalities.

Introduction

Despite dramatic improvements in care, iron induced cardiac disease remains the most frequent cause of death in thalassemia major and a major life-limiting complication of other transfusion-dependent patients, hereditary hemochromatosis, and other forms of iron overload (Neufeld 2006). The most common form of cardiac hemosiderotic injury is dilated cardiomyopathy, generally manifesting as systolic or diastolic dysfunction (Liu and Olivieri 1994). Signs of myocardial damage due to iron overload include arrhythmia, angina, cardiomegaly, heart failure, and pericarditis. Iron overload can also produce conduction defects secondary to iron deposition in the Bundle of His and the Purkinje system (Schwartz, Li et al. 2002). Sudden death due to arrhythmia can therefore occur among patients with advanced iron overload (Klintschar and Stiller 2004). Although prophylactic therapy with angiotensin converting enzyme inhibitors and β-blockers can help reduce cardiac morbidity and mortality (Trad, Hamdan et al. 2009), the mainstay of therapy for cardiac iron overload remains iron chelating agents. The goal of chelation therapy is primarily the prevention of iron overload in order to preserve organ function and improve patient survivability. To date, only deferoxamine is globally available for the first-line treatment of transfusion-related iron overload. Effective chelation with deferoxamine has been shown to increase

survival rate and prolong length and quality of life for transfusion patients (Obejero-Paz, Yang et al. 2003). However, deferoxamine chelation therapy is associated with a cumbersome treatment regimen and toxic side effects resulting in low patient adherence. In addition, treatment with deferoxamine has limited clinical outcomes and some patients still die of iron-induced cardiac disease despite apparently adequate liver iron chelation.

Unlike deferoxamine, deferasirox is an orally effective once daily iron chelating agent with favorable patient satisfaction (Neufeld 2006; Cappellini and Pattoneri 2009). Deferasirox was recently approved by the Food and Drug Administration (FDA) and is the first oral medication approved in the United States for this purpose (Lindsey and Olin 2007; Stumpf 2007). As deferasirox is well tolerated, it is expected to greatly enhance the acceptance of iron chelation therapy and offer a new alternative to burdensome continuous infusion therapy (Stumpf 2007). Whether deferasirox is efficacious in preventing the cardiovascular complications associated with iron overload is not yet clear. To address this gap in our understanding, we examined if the chronic administration of deferasirox is capable of removing excess iron from heart and other tissues, and whether it is capable of preventing or reducing the severity of iron-induced cardiac complications in the iron overloaded gerbil, a well accepted animal model of iron overload that is thought to closely resemble the effects of iron overload seen in humans (Carthew, Dorman et al. 1993). Our data suggest that once daily oral deferasirox treatment appears to be effective in preventing or reducing iron-induced cardiovascular abnormalities.

Results

Characterization of animals

Total body and heart weights were obtained and compared. All animals tolerated the iron loading and chelation without any apparent ill effects. The body weights of iron overloaded gerbils were similar to controls, indicating that the injection of iron dextran did not result in debilitation or weight loss. Cardiac, hepatic and kidney weights were increased 34%, 41.4% and 30.9% ($P < 0.05$), respectively, in the iron overloaded group, and deferasirox treatment was effective in reducing iron-associated increases in whole tissue weight by 23.9%, 16.3%, 23.7% (Table 7).

Table 7. Average heart, liver, and Kidney weights of gerbils in the experimental groups followed for 9 months

Group n = 10/ group	Heart/body wt (%)	Liver/body wt (%)	Kidney/body wt (%)
Ctrl	**0.39 ± 0.01**	**4.1 ± 0.31**	**0.81 ± 0.02**
IO	**0.52 ± 0.02***	**5.8 ± 0.30***	**1.05 ± 0.03***
IO + DFR	**0.40 ± 0.01†**	**4.9 ± 0.34†**	**0.8 ± 0.02†**

An asterisk (*) or cross (+) indicates significant difference from age matched control and iron overloaded groups, respectively.

Cardiac, aortic, and hepatic iron levels

Compared to hearts obtained from control animals, iron concentration was 3.3 fold higher in iron overloaded hearts ($P < 0.05$). Deferasirox treatment for 9 months resulted in a 31.6% decrease in cardiac iron level ($P < 0.05$) (Figure 20, A). Aortic iron concentration was 2.4 fold higher in the iron overloaded group compared to controls ($P < 0.05$). Nine months of deferasirox treatment decreased aortic iron level by 34.6% ($P < 0.05$) (Figure 20, B). Similarly, hepatic iron concentration was 49.5 fold higher than that

of control after nine months of follow up after iron overload. Hepatic iron concentration was 47.4% lower after 9 months of deferasirox treatment compared to that observed in the untreated iron overloaded animals. Prussian Blue iron staining of the left ventricle from the iron overloaded group indicates an increase in iron deposition and tissue damage compared to that of control. In sections of the left ventricular sections obtained from deferasirox treated animals, a lower iron deposition and preservation of tissue morphology was observed (Figure 21).

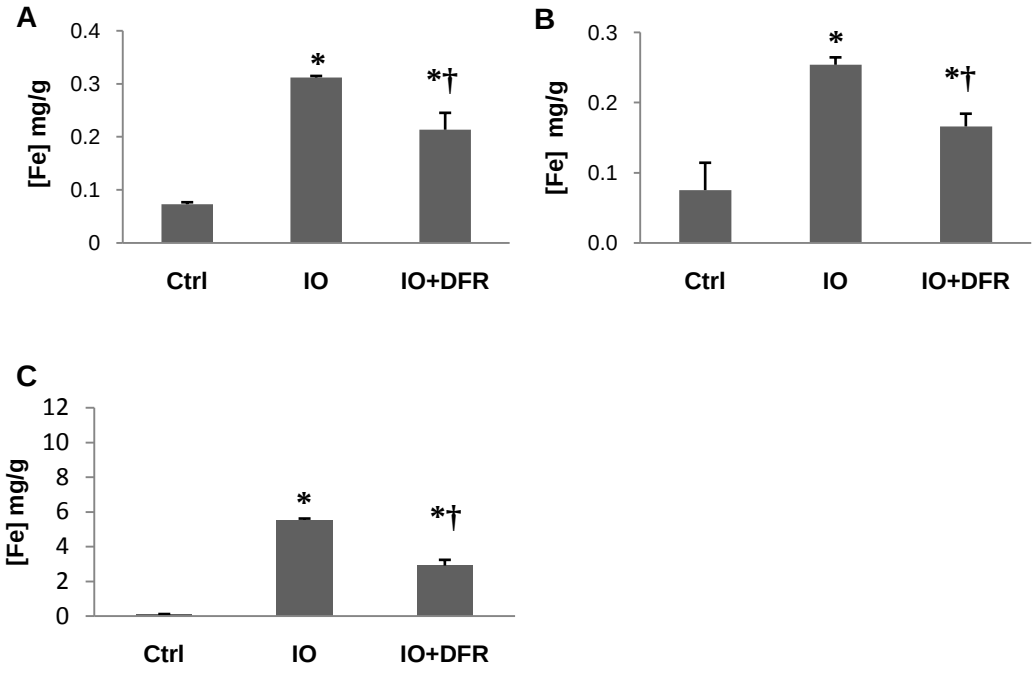

Figure 20. Average iron levels in mg/g tissue weight in cardiac (A), aortic (B), and hepatic (C) tissue of gerbils in the experimental groups followed for 9 months. Ctrl: control, IO: Iron overload, IO+ DFR: Iron overload followed by deferasirox treatment. (*) indicates significant difference from control, (†) indicates significant difference from iron overload group.

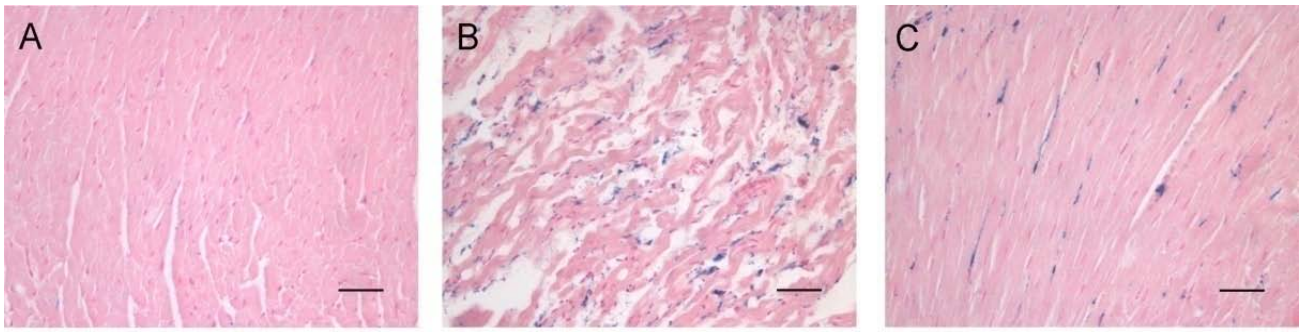

Figure 21. **Histological analysis of cardiac tissue of Ctrl (A), IO (B), and IO+DFR (C) gerbils followed for 9 months**. Ferric iron was detected by Prussian blue staining. No apparent iron deposition was observed in control gerbils. Iron overload resulted in morphological alteration and iron accumulation in the interstitium and in cardiac myocytes. Deferasirox treatment preserved tissue morphology and diminished iron deposition. Bar represents 100 µm; images were taken at 400X original magnification.

Electrocardiographic evaluation

Electrocardiographic measurements suggested an increased incidence of arrhythmias with iron overload (Figure 22). Iron overloaded gerbils were found to exhibit frequent premature ventricular tachycardia, (PVC) (6/10), supraventricular tachycardia, (SVT) (3/10), recurrent sustained and non sustained ventricular tachycardia, (VT) (4/10), and increased incidence of death (3/10) with the latter occurring most likely due to fatal arrhythmias (Figure 23). In addition, we observed an increased incidence of bundle branch block, (BBB) (6/10), negative P wave (8/10), and T wave flattening (5/10) (Figure 23).

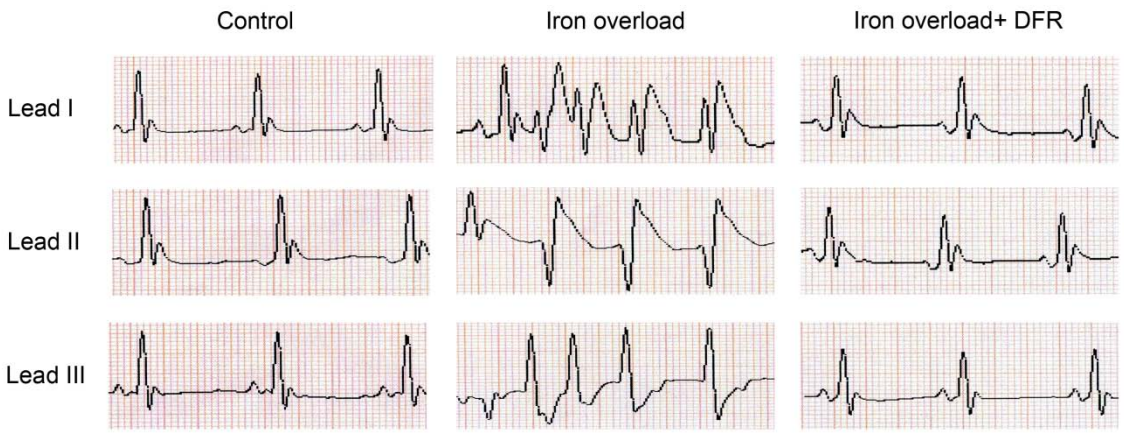

Figure 22. Representative ECGs (standard leads I, II, III) from control, iron overload, and deferasirox (DFR) treated groups followed for 9 months. EKG trace from iron overloaded animal (middle) exhibits ventricular tachycardia, EKG trace from control (left) and deferasirox treated animal (right) exhibit normal rhythm.

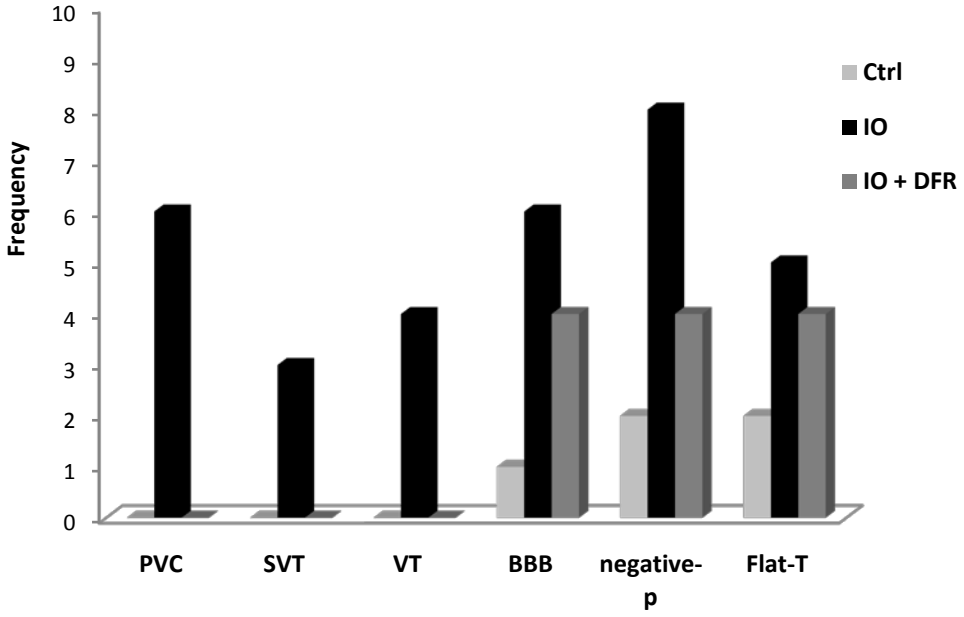

Figure 23. Frequency of electrocardiographic abnormalities observed in Ctrl, IO, and IO+ DFR followed for 9 months. PVC = premature ventricular tachycardia, SVT = supraventricular tachycardia, VT = ventricular tachycardia, BBB = bundle branch block, p = p wave, T = T wave.

Echocardiographic evaluation (cardiac structure)

Alterations in cardiac structure were evaluated by echocardiographic measurements. Our data demonstrated that LVPWd increased by 39.1% and 48.6% in the iron overloaded group after 6 and 9 months of follow up, respectively ($P < 0.05$) (Figure 24). LVPWd was 21.4% and 21.5% lower after 6, and 9 months of follow up, respectively, with deferasirox treatment ($P < 0.05$) (Figures 24, 25). Similarly, LVIDd increased by 18.5%, and 26.2% in the iron overloaded animals after 6, and 9 months of follow up, respectively ($P < 0.05$) (Figure 24). In the deferasirox treatment group, LVIDd was 16.5% and 23.6% lower after 6 and 9 months of follow up, respectively than that observed with iron overload ($P < 0.05$). In addition, LVSd was 31.5% and 42.4% higher

in the iron overloaded group after 6 and 9 months of follow up, respectively compared to control ($P < 0.05$). These levels were lower by 23.4% and 27.2% with 6 and 9 months of deferasirox treatment, respectively ($P < 0.05$) (Figure 24).

Alterations in cardiac structure were evaluated by echocardiographic measurements. Our data demonstrated that LVPWd was increased by 39.1% and 48.6% in the iron overloaded group after 6 and 9 months of follow up, respectively ($P< 0.05$) (Figure 24). LVPWd was 21.4% and 21.5% lower after 6, and 9 months of follow up, respectively, with deferasirox treatment ($P < 0.05$) (Figures 24, 25). Similarly, LVSd was 31.5% and 42.4% higher in the iron overloaded group after 6 and 9 months of follow up, respectively compared to control ($P < 0.05$). These levels were lower by 23.4% and 27.2% with 6 and 9 months of deferasirox treatment, respectively ($P < 0.05$) (Figure 24).

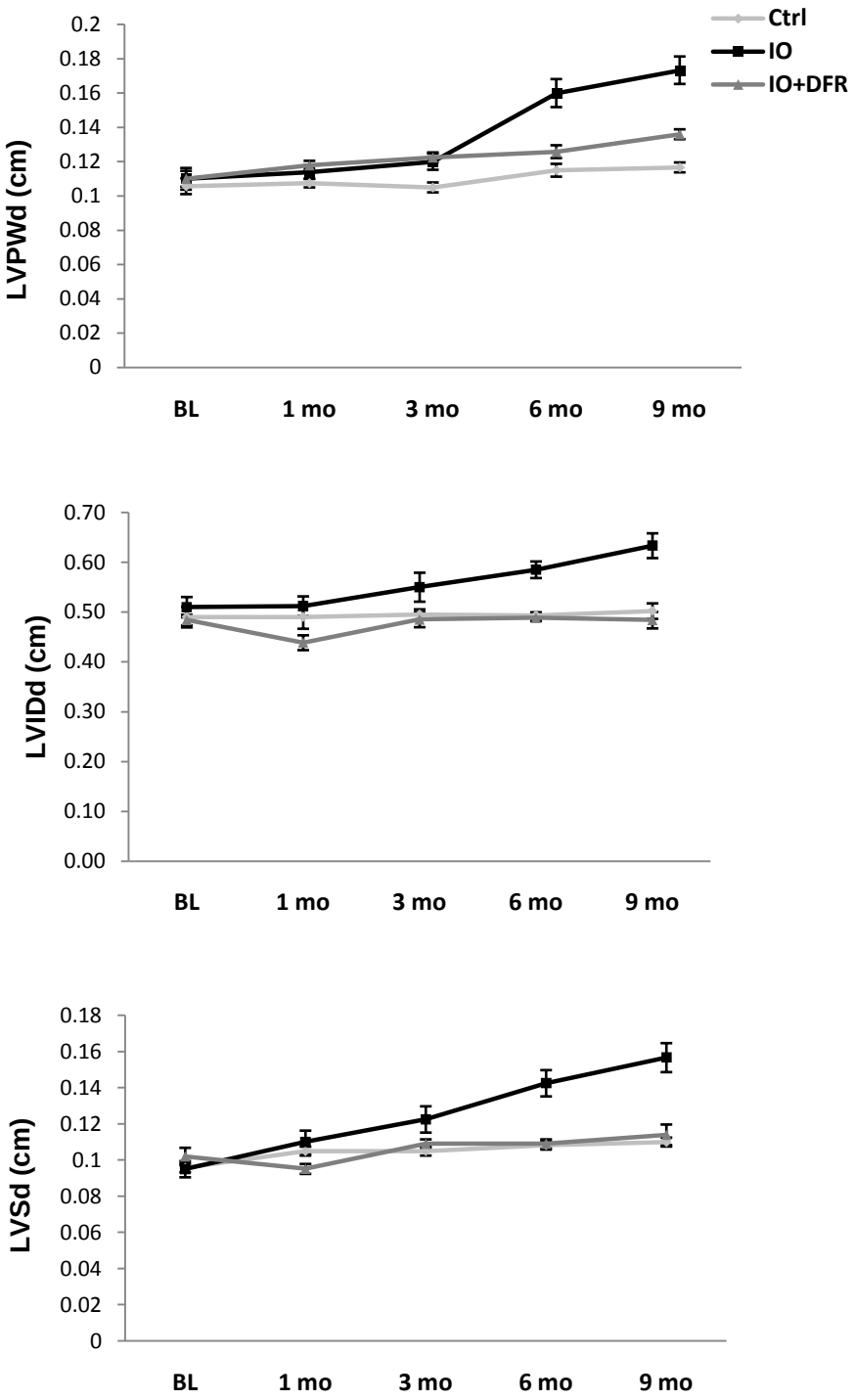

Figure 24. Effect of iron overload and deferasirox treatment on left ventricular dimension. Ctrl: control, IO: Iron overload, IO+ DFR: Iron overload followed by deferasirox treatment. BL = baseline (before iron loading), mo = months of follow up. LVPWd = left ventricular posterior wall dimension during diastole, LVIDd = left ventricular internal wall dimension during diastole, LVSd = left ventricular septal dimension during diastole

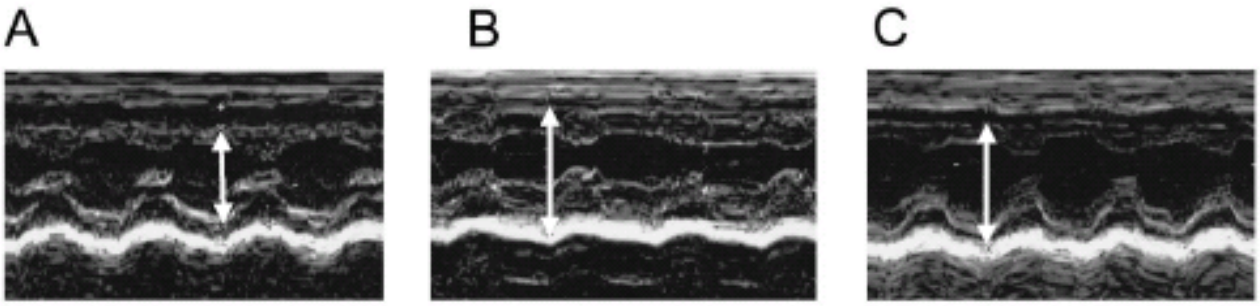

Figure 25. Representative M-mode echocardiograms from Ctrl (A), IO (B), and IO+ DFR (C) groups followed for 9 months. Arrows indicate left ventricular posterior wall dimension (LVPW) and is 0.127 cm, 0.153 cm, and 0.136 cm in A, B, and C respectively.

Echocardiographic evaluation (cardiac function)

Cardiac systolic and diastolic function was evaluated by echocardiographic measurements. Compared to control, ejection fraction was reduced by 22%, and 29.6% in the iron overloaded group after 6, and 9 months of follow up, respectively ($P < 0.05$) (Figure 26). Similarly, fractional shortening was 12.9% and 29.9% lower than control after 6, and 9 months of follow up, respectively ($P < 0.05$) (Figure 26).

Iron-induced decreases in ejection fraction were 17.7% and 29.8% higher than iron overload group after 6 and 9 months of deferasirox treatment, respectively ($P < 0.05$) (Figure 26). Likewise, iron induced alteration in fractional shortening were 10% and 27.8% higher than iron overload group after 6 and 9 months of deferasirox treatment ($P < 0.05$) (Figure 26). In addition, gerbils in the iron overloaded group exhibited a higher frequency of regurgitation of all three cardiac valves (mitral 6/10, tricuspid 6/10, and aortic 3/10) (Figure 27).

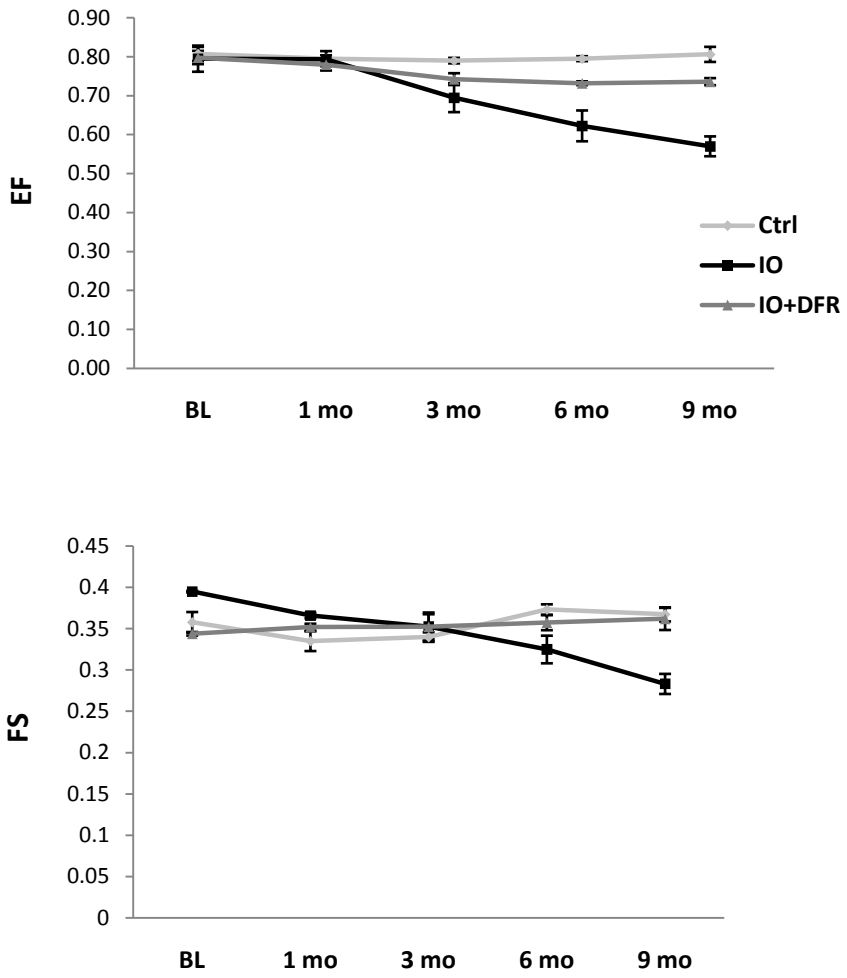

Figure 26. Effect of iron overload and deferasirox treatment on left ventricular ejection fraction (EF), and fractional shortening (FS) in gerbils from experimental groups. Ctrl: control, IO: Iron overload, IO+ DFR: Iron overload followed by deferasirox treatment. BL = baseline (before iron loading), mo = months of follow up.

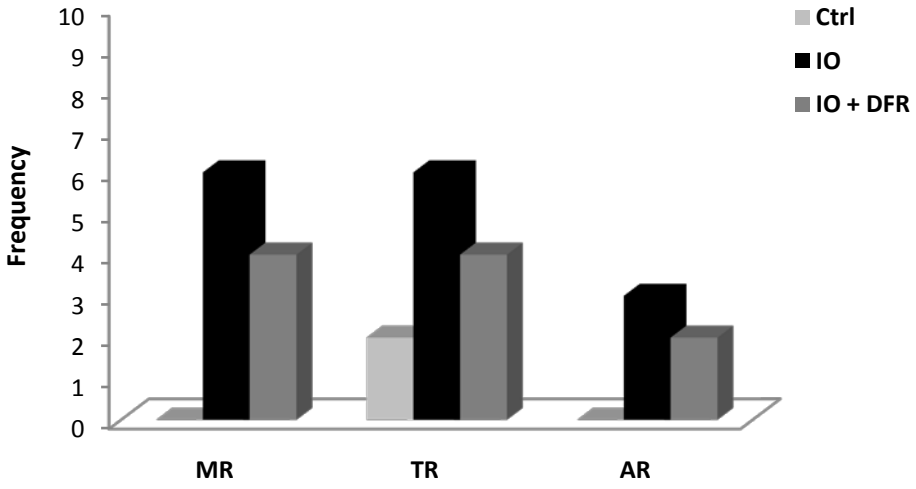

Figure 27. Frequency of cardiac valvular regurgitations observed in Ctrl, IO, IO+ DFR followed for 9 months. MR = mitral valve regurgitation, TR = tricuspid valve regurgitation, AR = Aortic valve regurgitation.

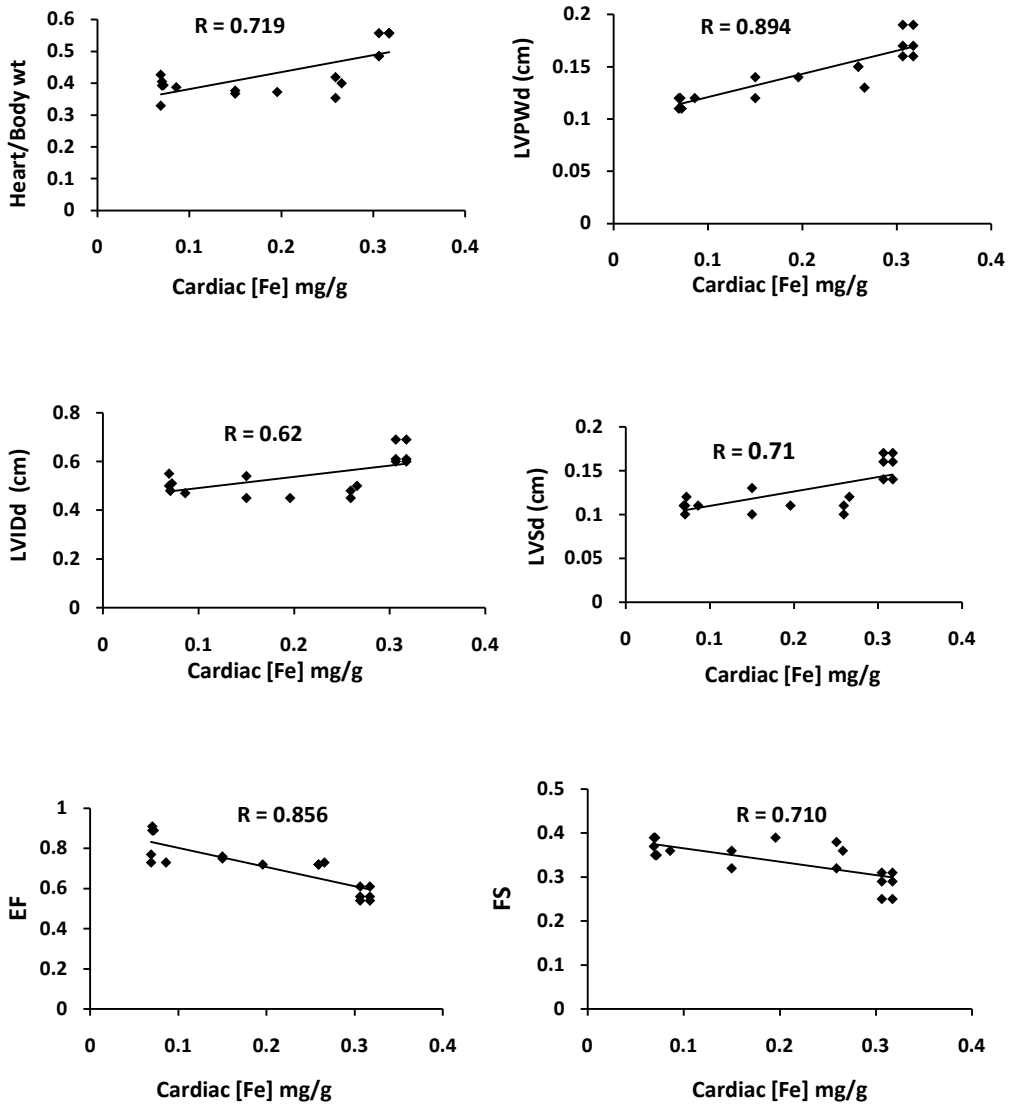

Figure 28. Correlation between cardiac iron concentration and heart/body wt, or echocardiographic parameters. LVPWd = left ventricular posterior wall dimension during diastole, LVIDd = left ventricular internal wall dimension during diastole, LVSd = left ventricular septal dimension during diastole, EF = ejection fraction, FS = fractional shortening. R = correlation coefficient.

Discussion

Here, we examine the efficacy of chronic deferasirox administration in preventing iron induced cardiac complications in the gerbil model of iron overload. Our data are consistent with the notion that deferasirox treatment removes cardiac iron and reduces cardiac damage, remodeling, arrhythmias, and declines in indices of cardiac function that are typically associated with iron overload.

Deferasirox removes cardiac, aortic, and hepatic iron

Iron distribution in the hearts of iron overloaded gerbils is thought to be similar to that reported in iron overloaded human hearts (Carthew, Dorman et al. 1993). Our findings demonstrated that cardiac and aortic iron concentrations nine months post iron loading were 3.3- and 2.4- fold higher than that of control. Hepatic iron levels were strikingly higher than that of heart and aorta and were 49.5 fold higher than that of corresponding control. Chronic deferasirox administration significantly reduced iron concentrations from these tissues and were 31.6%, 34.6%, and 47.4% lower than iron overload group in heart, aorta, and liver, respectively (Figures 20, 21). These results are consistent with previous studies suggesting that deferasirox is effective in cardiac and hepatic iron removal (Wood, Otto-Duessel et al. 2006; Otto-Duessel, Brewer et al. 2008). Whether the disparity in iron levels that we see among tissues is related to relative differences in the rate or the mechanism of iron uptake or clearance is not clear. It has been previously suggested that the liver has especially high efficiency of iron clearance that is related to membrane potential (de Silva, Askwith et al. 1996). In addition, it is thought that the rate of iron clearance from the myocardium is six times slower than that of liver (Oudit, Sun et al. 2004). Nonetheless, as similar findings have

been observed with deferoxamine treatment (Anderson, Westwood et al. 2004), it is less likely that these differences are chelator-dependent. Specific mechanisms remain to be established.

Deferasirox treatment preserves cardiac structure and prevents ventricular remodeling

Iron induced cardiac hypertrophy and ventricular remodeling is a serious long term complication associated with iron overload (Hahalis, Alexopoulos et al. 2005). Previous findings have suggested that chelation therapy with deferoxamine helps prevent iron induced cardiac hypertrophy and failure in the clinic (Pennell, Sutcharitchan et al. 2008) and in animal studies (Yang, Brittenham et al. 2003). Whether deferasirox produces a similar effect is not clear. Our findings suggest that iron overload was associated with increased cardiac mass, and a progressive increase in left ventricular wall dimensions, which reached significance at six- and nine- months following iron loading. With chronic deferasirox treatment, both cardiac mass and left ventricular dimensions tended to be preserved with values similar to that found in the control animals (Table 7, Figure 24). This is in agreement with recent case reports that have demonstrated that deferasirox treatment restored cardiac left ventricular diameter, left ventricular septum thickness, and left ventricular posterior wall dimension (Kiguchi, Ito et al. 2009) and reversed dilated cardiomyopathy (Kiguchi, Ito et al. 2009; Trad, Hamdan et al. 2009) in patients with iron overload. The mechanism by which chelation therapy with deferasirox confers such cardioprotection is not known. We have previously demonstrated that deferasirox treatment reduced iron induced oxidative stress and MAPK phosphorylation (Al-Rousan, Paturi et al. 2009), both of which are thought to be implicated in cardiac hypertrophy. Nevertheless, a causal link between

oxidative stress, MAPK phosphorylation, and cardiac remodeling, along with the effect that we see with deferasirox treatment, cannot be established from the current evidence and will necessitate further experimentation.

Deferasirox treatment preserves cardiac function and reduces incidence of arrhythmia

Without adequate control of iron overload, ongoing cardiac iron accumulation results in iron deposition in cardiac myocytes and the conduction system, which is thought to predispose the heart to recurrent arrhythmias and heart failure (Klintschar and Stiller 2004; Demant, Schmiedel et al. 2007). The mechanism of iron induced cardiac arrhythmias is not entirely elucidated, but it has been suggested that labile “free” iron can directly interact and interfere with a variety of ion channels within cardiomyocytes including L-type calcium channel, the ryonidine sensitive calcium channel, voltage gated sodium channel, and delayed rectifier potassium channel (Oudit, Sun et al. 2003; Wood, Enriquez et al. 2005; Oudit, Trivieri et al. 2006). Similar to findings from previous studies, we demonstrate that iron overload was associated with increased incidence of arrhythmias including premature ventricular contractions, supraventricular- and ventricular tachycardia, and frequent bundle branch blocks (Yang, Dong et al. 2002; Laurita, Chuck et al. 2003). As predicted, chronic deferasirox treatment was associated with lower incidence of EKG changes, and no evidence of ventricular tachycardia was observed in treated animals (Figure 23). This is consistent with previous findings that suggested that deferoxamine treatment prevents EKG abnormalities in the iron overloaded gerbil (Obejero-Paz, Yang et al. 2003). How chelation therapy may produce these effects is not clear. It is thought that iron accumulation in the bundle of His and Purkinje fibers results in delay or blockage of

myocardial electrical conduction (Schwartz, Li et al. 2002). Thus, it is likely that chelating agents, by removing iron accumulated in the conduction system, may improve electrical conduction and thus reduce the incidence of EKG abnormalities associated with iron overload. Future experiments designed to directly test this possibility will no doubt be useful in increasing our understanding of how deferasirox exerts its effects.

Iron overload was also associated with progressive decline in left ventricular ejection fraction and fractional shortening accompanied with an increase in the frequency of cardiac valve regurgitation. Deferasirox treatment tended to preserve cardiac function and only a slight decline in ejection fraction was observed (Figure 26). Similar findings have been demonstrated by Kiguchi and collegues (Kiguchi, Ito et al. 2009) where deferasirox treatment restored ejection fraction and cardiac functions in a patient with cardiac iron overload. Whether the abnormalities in cardiac structure and function we observed are directly related to iron induced toxicity is unknown and will necessitate further experimentation. Nonetheless, the changes that we see in heart mass, left ventricular dimension, ejection fraction, and fractional shortening are highly correlated with cardiac iron concentration (Figures 27, 28). Taken together, these data suggest that deferasirox may be efficacious in the treatment and / or prevention of iron-overload induced cardiac complications.

IRON LEVELS IN OTHER TISSUES

Pancreatic iron level

We examined the effect of deferasirox treatment at one and three months on pancreatic iron concentration in the Mongolian gerbil. Compared to control, iron concentration was significantly higher in the overloaded animals. Our results demonstrated 37.9% reduction in pancreatic iron after three months of deferasirox treatment compared to age matched-untreated group ($P < 0.05$) (Figure 29). Similar results have been observed with Prussian Blue iron staining were iron deposition was increased in the pancreatic tissue of the iron overloaded animals especially in the parenchyma. Tissue sections from animals treated with deferasirox for three months exhibited an observable clearance of iron deposits and no apparent iron deposition was observed in control tissues (Figure 30).

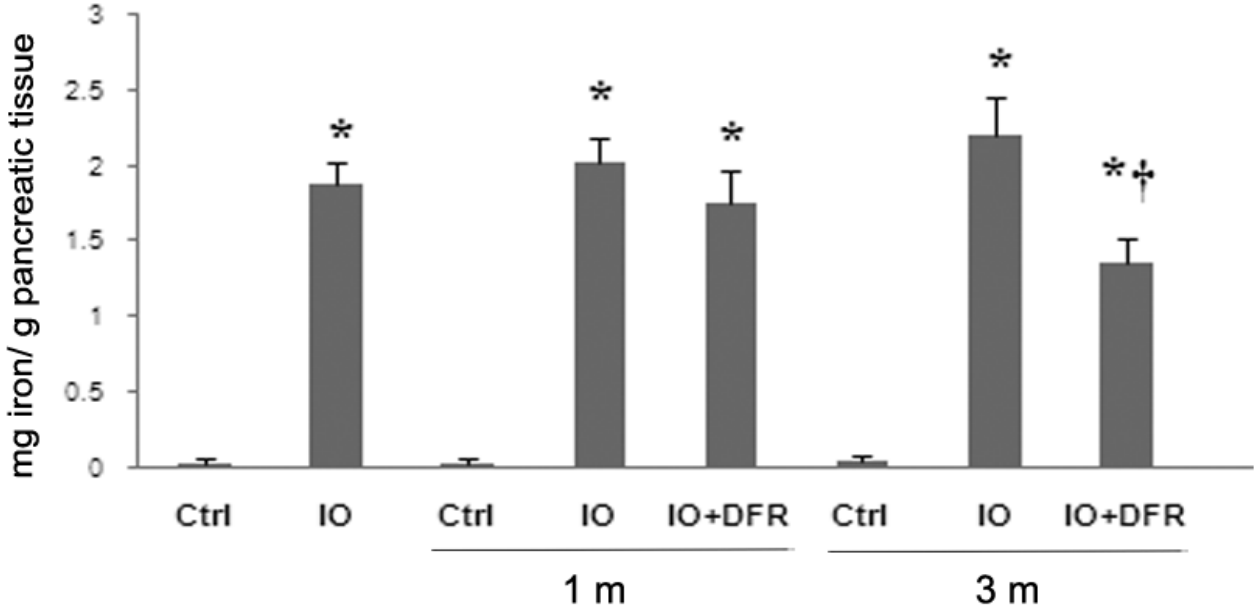

Figure 29. Average iron levels in mg/g tissue weight in pancreatic tissue of gerbils in the experimental groups. Ctrl: control, IO: Iron overload, IO+ DFR: Iron overload followed by deferasirox treatment, 1 m: 1 month interval, 3 m: 3 months interval. (*) indicates significant difference from control, (†) indicates significant difference from iron overload group ($P < 0.05$).

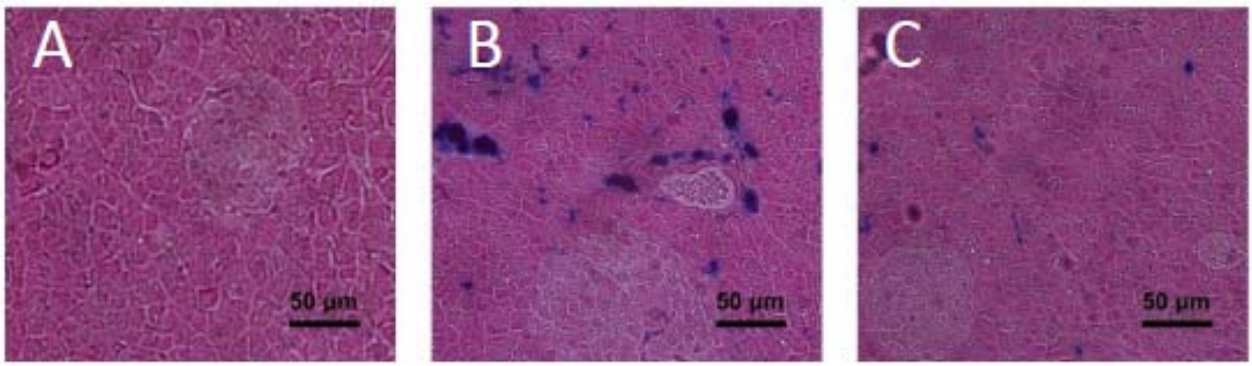

Figure 30. Histological analysis of pancreatic tissue of control, iron overload, and deferasirox treated groups followed for 3 months. Ferric iron was detected by Prussian blue staining. No apparent iron deposition was observed in control gerbils. Iron overload resulted in iron accumulation in parenchymal cells and to a lesser extent in pancreatic β-cells. Deferasirox treatment diminished iron deposition from all regions of pancreatic tissue. Images were taken at 400X original magnification.

Kidney iron level

Kidney samples from animals in the experimental groups have been examined for iron level using ICP-AES technique. Compared to that of the corresponding age matched control group iron concentration in the iron overloaded groups were 97-, 51-, and 57- fold higher in IO, 1 month-IO, and 3 months-IO, respectively, ($P < 0.05$) (Figure 31). No significant reduction in kidney iron levels were observed after 1, or 3 months of deferasirox treatment.

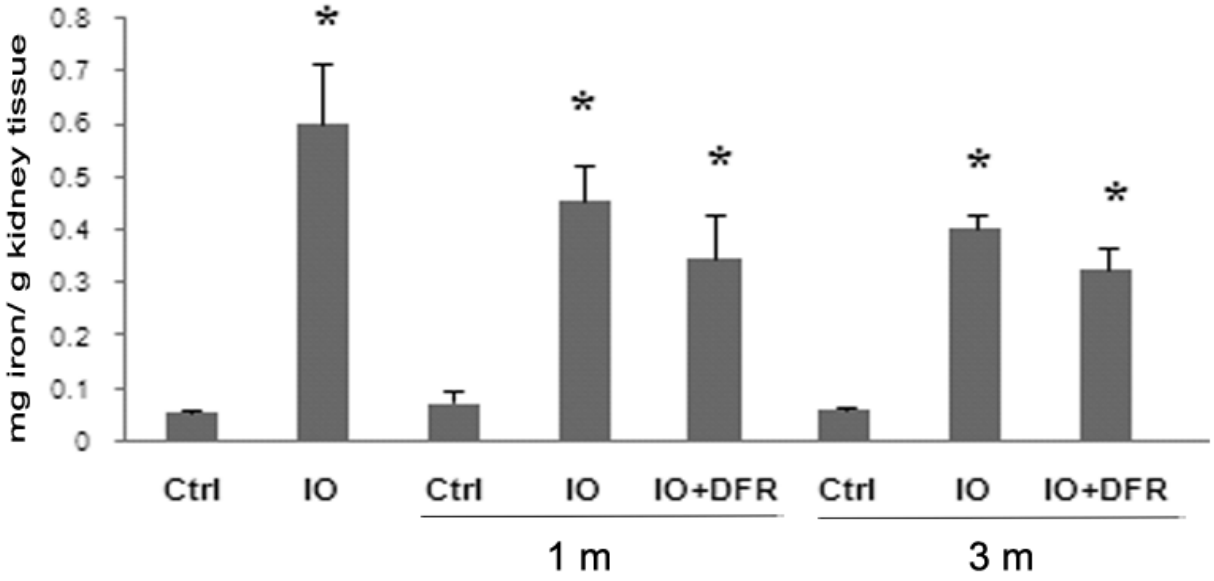

Figure 31. Average iron levels in mg/g tissue weight in kidney tissue of gerbils in the experimental groups. Ctrl: control, IO: Iron overload, IO+ DFR: Iron overload followed by deferasirox treatment, 1 m: 1 month interval, 3 m: 3 months interval. (*) indicates significant difference from control. ($P < 0.05$)

CHAPTER V

GENERAL DISCUSSION

The primary purpose of the present study was to investigate the effect of deferasirox treatment on iron overload-related complications with special emphasis on the heart. To address this purpose, iron overload associated alterations in cardiac and hepatic mass, iron content, histology, oxidative stress, protein expression, and cardiac structure and function were assessed in iron overloaded or deferasirox treated gerbils in comparison to control.

More than a decade ago, Carthew and his colleagues (Carthew, Dorman et al. 1993) introduced the Mongolian gerbil model of iron overload. It duplicated, for the first time, the structural cardiomyopathy and hepatic dysfunction found clinically in patients with chronic iron excess. In a series of studies by others (Schwartz, Li et al. 2002; Yang, Dong et al. 2002) and in our own laboratory (Walker, Epling et al. 2007), the gerbil has been found to provide an animal model that reproduces many of the essential functional and structural features of iron-induced liver and heart disease in patients. Tissue iron levels, however, vary among studies based on the dosing regimen of iron-dextran administration (Kaiser, Davis et al. 2004). Cardiac and hepatic iron levels measured in the present study fall within the range of iron levels detailed in other studies that have used a similar dosing regimen (Wood, Otto-Duessel et al. 2006; Otto-Duessel, Aguilar et al. 2007). Iron chelation with deferasirox was given at 100mg/kg/day. This dose was chosen based on an earlier study evaluating the dose-response of deferasirox in the gerbil model (Wood at al. 2004). The highest dose, 100 mg/kg daily, was shown to significantly reduce hepatic iron content, while lower doses were not effective. Gerbils

have a 7.8-fold higher surface area to mass ratio, and corresponding metabolic rate, than humans. The gerbil deferasirox dose of 100 mg/kg translates to only two-thirds of the standard human dose (20 mg/kg) when normalized according to body surface area (Otto-Duessel, Aguilar et al. 2007); this is appropriate given that there is not ongoing transfusional iron accumulation.

Effect of iron overload and deferasirox treatment on tissue iron concentration

Results from previous studies and from the present investigation indicate that iron accumulates primarily in the liver and to lower extent in the heart and other tissues. For example, hepatic iron concentration measured in the present study was approximately 58 fold higher whereas cardiac iron concentration was only 7.4 fold higher than age matched control animals after 3 months of follow up. On the other hand, deferasirox treatment for three months resulted in 43.5% reduction in hepatic iron whereas cardiac iron was reduced by only 23.5%. It is thought that the mechanisms of iron uptake and clearance differ in heart and liver tissue, resulting in differing iron transport kinetics (Schwartz, Li et al. 2002). Previous studies have suggested that cardiac iron is cleared six-times more slowly than liver iron (Oudit, Sun et al. 2004). Although not directly examined, this phenomenon may explain why many iron overload patients develop cardiac dysfunction even though their liver iron levels appear to be only slightly elevated. As such, there is a need for more research to determine how elevated liver iron concentrations may correspond to elevations in cardiac iron levels and an increased risk of possibility of cardiac damage.

Effect of iron overload and deferasirox treatment on tissue iron distribution

It has been suggested that tissue iron deposition occurs in a non-homogenous fashion. Similar to previous studies, histological examination of cardiac sections from iron overloaded gerbils demonstrated that excess iron accumulates primarily in the cardiomyocytes, cardiac macrophages, and in interstitial spaces of the heart. In patients with iron overload, it has been reported that iron deposition tends to be more extensive in the epicardial third of the ventricle, followed by the subendocardium and papillary muscle, and least in the middle third of the ventricular wall (Walker, Black et al. 2004). Iron accumulations in the cardiac conduction system, coronary arteries, and valves are usually limited, but involvement of the conduction system is associated with cardiac arrhythmias. In the liver, iron deposition tends to be more localized to the periportal region as opposed to the centrilobular region. Given the high oxygen concentration and mitochondrial volume in the periportal zone, it has been suggested that iron can be especially toxic to this particular region of the hepatic plate. Indeed, periportal necrosis has been described in both humans (Deugnier, Loreal et al. 1992; Hubscher 2003) and experimental animals (Whittaker, Hines et al. 1996) suffering from hepatic toxicity due to iron overload. Histological examination of cardiac and hepatic tissue sections from deferasirox treated gerbils suggest that deferasirox removes iron from cardiomyocytes and hepatocytes, and perhaps from macrophages, albeit at a much lower rate.

Effect of iron overload and deferasirox treatment on ferritin protein expression

Changes in tissue iron concentration were paralleled by changes in ferritin protein expression. We demonstrated that ferritin heavy chain levels were 1.6 fold and 2.1 fold higher than control in the iron overloaded heart and liver, respectively, after

three months of follow up. Similar to our observation with tissue iron clearance, deferasirox treatment reduced cardiac and hepatic ferritin by 38% and 47.5%, respectively. The effect of iron chelation therapy on serum ferritin expression is well documented in the literature as serum ferritin is a common diagnostic tool of body iron (Perifanis, Christoforidis et al. 2007; Walter, Macklin et al. 2008). However, there is a limited body of evidence on the effect of iron overload or chelation therapy on ferritin expression in intact tissue. Only one study has addressed the effect of iron overload on cellular ferritin expression *in vitro* (Tran, Eubanks et al. 1997) while one other study demonstrated that chelation therapy with deferoxamine is associated with reduced iron-induced ferritin upregulation in rat aorta (Ishizaka, Saito et al. 2005). To our knowledge, the present study is the first description of the effect of iron overload and deferasirox treatment on cardiac and hepatic ferritin expression.

It is thought that the increase in ferritin expression in response to iron overload provides a cytoprotective mechanism against iron induced toxicity (de Valk and Marx 1999). Nonetheless, it should be noted that although ferritin and hemosiderin have traditionally been regarded as ‘safe’ storage forms of iron, this does not mean that the iron contained in these molecules cannot potentiate the development of oxidative stress under certain conditions. Indeed, it has been recently demonstrated that the superoxide radical is capable of mobilizing iron from ferritin and that this can result in the production of iron-catalyzed hydroxyl radicals (Bartfay, Dawood et al. 1999).

Effect of iron overload and deferasirox treatment on oxidative stress indices and apoptosis

While no single mechanism is likely to account for the complex pathophysiology of iron-induced organ damage, it is believed that iron mediated formation of harmful free radicals plays a major role (Kell 2009). Indeed, several different investigations have reported an increase in ROS generation in response to iron overload. For example, previous studies have demonstrated an increase in aldehyde-derived peroxidation products in both murine (Bartfay, Dawood et al. 1999), and gerbil models (Otto-Duessel, Aguilar et al. 2007) of iron overload. In addition, using an oxidative fluorescent dye, Day and collegues (Day, Duquaine et al. 2003) have suggested an increase in aortic oxidative stress in the iron overloaded mouse. Here, we demonstrated that iron overload was associated with an increase in superoxide generation and protein oxidation in heart and liver. It is thought that metal catalyzed oxidation of proteins introduces carbonyl groups (aldehydes and ketones) at lysine, arginine, proline or threonine residues in a site-specific manner (Stadtman 1993). This oxidative modification can modulate essential biochemical characteristics of proteins such as enzymatic activity (Oliver, 1987), the DNA binding activity of transcription factors (Pognonec, Kato et al. 1992), or the susceptibility of proteins to proteolytic degradation (Wolff and Dean 1986). Although similar findings of reduced ROS with deferasirox have been found *in vitro* using cardiac myocytes (Glickstein, El et al. 2006), to our knowledge this is the first report to demonstrate that deferasirox is capable of reducing ROS in the intact tissue.

In the present study, the origin of iron-induced increases in superoxide anion was not investigated. Previous studies have shown that the mitochondria play a primary role

within the cell both in the handling of iron and in energy production by oxidative phosphorylation process. Indeed, it is well accepted that mitochondria represent a primary target of oxidative injury, and thus are the main source for ROS. It has been shown that ROS are produced through the respiratory chain at a rate which is dependent on the metabolic state of the mitochondria (Pietrangelo, Montosi et al. 2002). In the presence of iron ions, ROS give rise to highly-reactive oxidizing species like the hydroxyl radical (HO•) (Burkitt and Mason 1991; Nunoshiba, Obata et al. 1999). This increase in oxidizing species in turn may destabilize one or more components of the electron transport chain that could lead to further ROS accumulation (Bacon, O'Neill et al. 1993). Experiments designed to assess mitochondrial function with iron overload and the effects of deferasirox on mitochondrial function will no doubt be useful in examining this possibility.

How increased iron (or ROS) levels may negatively influence the structure and function of target tissue is not well understood but recent data suggests that excessive iron and iron mediated ROS elicit a wide spectrum of responses. These responses depend upon the severity of the damage, which is further influenced by the cell type, the magnitude of the dose, and the duration of the exposure. Nonetheless, there are controversial reports regarding the ultimate physiological outcome of these triggered responses, ranging from cell survival and adaptation (hypertrophy) to cell death (apoptosis) (Martindale and Holbrook 2002). In the present investigation, we demonstrated that iron overload was associated with increased phosphorylation of the three subfamilies of MAPK: ERK1/2, p38, and JNK. Interestingly, the maximum phosphorylation signal for p38 and JNK was higher than that observed for ERK1/2. This result could be justified in the context of p38-MAPK and JNKs being the two principal

MAPK subfamilies mediating cellular stress signals, whereas the ERKs are primarily associated with cell growth and proliferation. These results are in agreement with previous work that suggested increased MAPK phosphorylation associated with ROS alone (Bhat and Zhang 1999; Park, Yoo et al. 2005) or ROS together with iron overload (Dai, Huang et al. 2004). In the present report we show that deferasirox treatment diminishes the extent of iron overload-dependent MAPK phosphorylation. Whether the induction of MAPK phosphorylation is dependent upon iron excess, ROS, or these acting in concert with other factors is worthy of detailed studies.

It is thought that the magnitude of ROS plays a role in influencing the particular course taken by a cell. For example, it has been suggested that intermediate levels of ROS result in growth arrest whereas severe oxidative stress causes cell death via either apoptotic or necrotic mechanisms (Martindale and Holbrook 2002). Here we demonstrated that the increase in hepatic iron concentration together with ROS accumulation was associated with increased cell death. These results are consistent with previous findings that suggested that iron overload induced apoptotic cell death in isolated rat hepatocytes which is thought to be mediated by reactive oxygen species (Allameh et al. 2008). The increase in cell death as determined by TUNEL was also associated with an increase in the ratio of Bax/Bcl-2 and Bad expression as well as caspase-3 cleavage, suggesting the involvement of apoptosis. Although similar findings have been demonstrated *in vitro* (Yajun, Hongshan et al. 2005), this is the first report that describes the effect of iron overload on the apoptotic cascade in intact liver. As expected, deferasirox treatment was associated with lower cell death signal, Bax/Bcl-2 ratio, Bad expression, and caspase-3 cleavage. These results suggest that apoptosis may be involved in iron overload induced hepatic toxicity and most importantly, that

deferasirox may confer protection against these effects. Nonetheless, given the important role of iron overload in cardiovascular and hepatic disorders, further studies are required to fully investigate the diversity and multiplicity of interactions between the signaling cascades involved in their pathogenesis.

Effect of iron overload and deferasirox treatment on cardiac structure and function

Iron overload is toxic to the heart, and in the syndromes of chronic iron overload the majority of deaths are due to cardiac failure and sudden death, with the latter probably due to arrhythmia. In animal studies, a dose relationship between iron load and the development of cardiac impairment is seen (Carthew, Dorman et al. 1993; Bartfay, Dawood et al. 1999; Yang, Dong et al. 2002). This wealth of evidence supports the hypothesis that cardiac complications in iron overload have a direct relationship with the amount of iron in the heart. Therefore, effective removal of cardiac iron is likely to reduce the incidence of cardiac complications associated with iron overload. In the present investigation, cardiac iron levels in the iron overloaded animals were 3.3 fold that of the control animals and were associated with structural and functional abnormalities including increased cardiac mass, ventricular remodeling, arrhythmia, valvular regurgitation, systolic dysfunction, and reduced survival. Chronic deferasirox administration reduced cardiac iron by 31.6% and this was associated with preserved cardiac structure and function along with improved survival. These results are in agreement with previous reports suggesting beneficial effects of chelation therapy with deferoxamine (Obejero-Paz, Yang et al. 2003; Yang, Brittenham et al. 2003) or

deferasirox (Kiguchi, Ito et al. 2009; Trad, Hamdan et al. 2009) in preventing/ reversing iron induced cardiac alterations.

Although cardiac iron deposition, ROS accumulation, and biochemical changes were evident within a few weeks after iron loading, no significant changes in cardiac structure or function were observed until 6 and 9 months of follow up. These observations resemble the time course of the disorder as described in humans. It has been reported that cardiac iron toxicity begins to occur after a total of 10 blood transfusions or approximately 5 g of iron; however, patients may remain asymptomatic for years. The symptoms of cardiac iron overload normally occur long after the probable initiation of cardiac iron accumulation with the mean survival falling to a few months once these complications have arisen (Wood, Enriquez et al. 2005). Intensive iron chelation therapy may help restore cardiac rhythm and function, which could increase survival.

It is important to note here that iron deposition is not necessarily the sole cause of cardiac disease in iron overload conditions. It is well accepted that chronic anemia itself plays a role in the development of cardiovascular abnormalities regardless of cardiac iron status (Hahalis, Alexopoulos et al. 2005). For example, thalassemia is oftentimes associated with elevated cardiac output and stroke volume with the possibility of systolic dysfunction or severe pulmonary hypertension in advanced stages of the disease (Bosi, Crepaz et al. 2003). In the present investigation, the effect of the underlying condition on cardiac health was not examined and cannot be addressed from the present study design. The development of animal models that better resemble iron overload in these conditions will no doubt be useful in furthering our understanding of cardiac pathology in these diseases.

In conclusion, the work presented here strongly suggests a protective role of deferasirox against iron induced complications. Evidence from the clinical setting is needed to confirm these interesting findings and will no doubt be useful in developing better therapeutic regimens to control iron overload.

CONCLUSIONS

1. Deferasirox treatment was found to remove iron from target tissues including heart, liver, and pancreas. Deferasirox treatment to a similar extent did not reduce iron accumulated in the kidney or aorta to a significant level.

2. Iron overload was found to increase the relative expression of ferritin in both cardiac and hepatic tissue. Deferasirox treatment reduced iron-related increase in ferritin expression from both tissues.

3. Deferasirox treatment was found to attenuate oxidative stress indices observed with iron overload from both cardiac and hepatic tissue. This includes the ability to reduce cumulative protein oxidation, superoxide overproduction, and MAPK phosphorylation.

4. Deferasirox treatment was found to reduce iron overload-related cell death as well as the relative expression of members of the apoptotic cascade including Bax/Bcl-2, Bad, and caspase-3.

5. Long term deferasirox treatment was found to further reduce accumulated tissue iron from heart, liver, and aorta.

6. Iron overload was found to profoundly impact cardiac structure and function. Iron overload was associated with increase heart/body wt, left ventricular

interior and posterior dimensions, left ventricular septal thickness, frequency of arrhythmia and valvular regurgitation whereas ejection fraction and fractional shortening were decreased. Long term deferasirox treatment was found to preserve both cardiac structure and function.

FUTURE DIRECTIONS

The present study focused on examining the efficacy of deferasirox treatment in preventing cardiac complications associated with iron overload. Future investigations should focus on examining whether deferasirox treatment is protective against other complications associated with iron overload including, among others, hepatic fibrosis, hepatocellular carcinoma, and diabetes mellitus.

A critical target of future investigation would also be the assessment of the efficacy of combination therapy with other chelating agents or antioxidants. Previous research by Hershko and collegues (2001) have illustrated that the administration of DFO in combination with deferiprone provides a “shuttling effect” where the smaller and hydrophilic chelator deferiprone mobilized intracellular iron stores, subsequently transferring it to intra- or extracellular DFO. Such a strategy was found to enhance iron excretion and reduce the side effects associated with monotherapy. Whether a combination therapy of DFO with deferasirox can induce a similar effect is worth investigating.

Given the fact that oxidative stress is the major contributor to iron-induced toxicity, it is logical to propose that antioxidants might provide a protective effect. Recently, Duessel and collegues (Otto-Duessel, Aguilar et al. 2007) have demonstrated that the administration of the antioxidant taurine improved cardiac indices of oxidative stress in the iron overloaded gerbil. However, the effect of a combination therapy of antioxidants with iron chelation therapy is not known. Based on our understanding of the mechanisms involved in iron-induced toxicity and on previous research suggesting that

chelating agents improve the efficacy of antioxidants, we propose that the administration of deferasirox with antioxidants would provide a synergistic effect.

Mitochondria and lysosomes are the major cellular targets of iron mediated damage. *In vitro* studies have suggested that deferasirox is able to cross the plasma membrane and access the cytoplasm. Whether deferasirox possesses accessibility to subcellular compartments is not known and is worth investigation.

REFERENCES

Afanas'ev, I. B. (2005). "Superoxide and nitric oxide in pathological conditions associated with iron overload: the effects of antioxidants and chelators." Curr Med Chem **12**(23): 2731-9.

Agarwal, M. B. (2009). "Advances in management of thalassemia." Indian J Pediatr **76**(2): 177-84.

Al-Rousan, R. M., S. Paturi, et al. (2009). "Deferasirox removes cardiac iron and attenuates oxidative stress in the iron-overloaded gerbil." Am J Hematol **84**(9): 565-70.

Alustiza, J. M., A. Castiella, et al. (2007). "Iron overload in the liver diagnostic and quantification." Eur J Radiol **61**(3): 499-506.

Anderson, L. J., M. A. Westwood, et al. (2004). "Myocardial iron clearance during reversal of siderotic cardiomyopathy with intravenous desferrioxamine: a prospective study using T2* cardiovascular magnetic resonance." Br J Haematol **127**(3): 348-55.

Andrews, N. C. (2005). "Molecular control of iron metabolism." Best Pract Res Clin Haematol **18**(2): 159-69.

Andrews, N. C. (2008). "Forging a field: the golden age of iron biology." Blood **112**(2): 219-30.

Andrews, N. C. and P. J. Schmidt (2007). "Iron homeostasis." Annu Rev Physiol **69**: 69-85.

Antosiewicz, J., W. Ziolkowski, et al. (2007). "Tumor necrosis factor-alpha-induced reactive oxygen species formation is mediated by JNK1-dependent ferritin degradation and elevation of labile iron pool." Free Radic Biol Med **43**(2): 265-70.

Arosio, P. and S. Levi (2002). "Ferritin, iron homeostasis, and oxidative damage." Free Radic Biol Med **33**(4): 457-63.

Bacon, B. R. (2001). "Hemochromatosis: diagnosis and management." Gastroenterology **120**(3): 718-25.

Bacon, B. R., R. O'Neill, et al. (1993). "Hepatic mitochondrial energy production in rats with chronic iron overload." Gastroenterology **105**(4): 1134-40.

Balla, G., H. S. Jacob, et al. (1992). "Ferritin: a cytoprotective antioxidant strategem of endothelium." J Biol Chem **267**(25): 18148-53.

Ballas, S. K. (2001). "Iron overload is a determinant of morbidity and mortality in adult patients with sickle cell disease." Semin Hematol **38**(1 Suppl 1): 30-6.

Baptista-Gonzalez, H., N. C. Chavez-Tapia, et al. (2008). "Importance of iron and iron metabolism in nonalcoholic fatty liver disease." Mini Rev Med Chem **8**(2): 171-4.

Barouki, R. and Y. Morel (2001). "Repression of cytochrome P450 1A1 gene expression by oxidative stress: mechanisms and biological implications." Biochem Pharmacol **61**(5): 511-6.

Bartfay, W. J., F. Dawood, et al. (1999). "Cardiac function and cytotoxic aldehyde production in a murine model of chronic iron-overload." Cardiovasc Res **43**(4): 892-900.

Bhat, N. R. and P. Zhang (1999). "Hydrogen peroxide activation of multiple mitogen-activated protein kinases in an oligodendrocyte cell line: role of extracellular signal-regulated kinase in hydrogen peroxide-induced cell death." J Neurochem **72**(1): 112-9.

Boddaert, N., K. H. Le Quan Sang, et al. (2007). "Selective iron chelation in Friedreich ataxia: biologic and clinical implications." Blood **110**(1): 401-8.

Bonkovsky, H. L. and R. W. Lambrecht (2000). "Iron-induced liver injury." Clin Liver Dis **4**(2): 409-29, vi-vii.

Borgna-Pignatti, C., S. Rugolotto, et al. (2004). "Survival and complications in patients with thalassemia major treated with transfusion and deferoxamine." Haematologica **89**(10): 1187-93.

Bosi, G., R. Crepaz, et al. (2003). "Left ventricular remodelling, and systolic and diastolic function in young adults with beta thalassaemia major: a Doppler echocardiographic assessment and correlation with haematological data." Heart **89**(7): 762-6.

Breuer, W., S. Epsztejn, et al. (1996). "Dynamics of the cytosolic chelatable iron pool of K562 cells." FEBS Lett **382**(3): 304-8.

Brissot, P. (2009). "[Haemochromatoses. New understanding, new treatments]." Gastroenterol Clin Biol **33**(8-9): 859-67.

Brittenham, G. M. (2003). "Iron chelators and iron toxicity." Alcohol **30**(2): 151-8.

Brittenham, G. M., P. M. Griffith, et al. (1994). "Efficacy of deferoxamine in preventing complications of iron overload in patients with thalassemia major." N Engl J Med **331**(9): 567-73.

Britton, R. S. and B. R. Bacon (1994). "Role of free radicals in liver diseases and hepatic fibrosis." Hepatogastroenterology **41**(4): 343-8.

Britton, R. S., R. O'Neill, et al. (1990). "Hepatic mitochondrial malondialdehyde metabolism in rats with chronic iron overload." Hepatology **11**(1): 93-7.

Brown, K. E., M. T. Kinter, et al. (1998). "Enhanced gamma-glutamyl transpeptidase expression and selective loss of CuZn superoxide dismutase in hepatic iron overload." Free Radic Biol Med **24**(4): 545-55.

Burkitt, M. J. and R. P. Mason (1991). "Direct evidence for in vivo hydroxyl-radical generation in experimental iron overload: an ESR spin-trapping investigation." Proc Natl Acad Sci U S A **88**(19): 8440-4.

Cabantchik, Z. I., W. Breuer, et al. (2005). "LPI-labile plasma iron in iron overload." Best Pract Res Clin Haematol **18**(2): 277-87.

Cai, J., J. Yang, et al. (1998). "Mitochondrial control of apoptosis: the role of cytochrome c." Biochim Biophys Acta **1366**(1-2): 139-49.

Cappellini, M. D. (2005). "Iron-chelating therapy with the new oral agent ICL670 (Exjade)." Best Pract Res Clin Haematol **18**(2): 289-98.

Cappellini, M. D. (2008). "Long-term efficacy and safety of deferasirox." Blood Rev **22 Suppl 2**: S35-41.

Cappellini, M. D. and P. Pattoneri (2009). "Oral iron chelators." Annu Rev Med **60**: 25-38.

Cappellini, M. D. and A. Piga (2008). "Current status in iron chelation in hemoglobinopathies." Curr Mol Med **8**(7): 663-74.

Cappellini, M. D. and A. Taher (2008). "Long-term experience with deferasirox (ICL670), a once-daily oral iron chelator, in the treatment of transfusional iron overload." Expert Opin Pharmacother **9**(13): 2391-402.

Cario, H., G. Janka-Schaub, et al. (2007). "Recent developments in iron chelation therapy." Klin Padiatr **219**(3): 158-65.

Carthew, P., B. M. Dorman, et al. (1993). "A unique rodent model for both the cardiotoxic and hepatotoxic effects of prolonged iron overload." Lab Invest **69**(2): 217-22.

Chaston, T. B. and D. R. Richardson (2003). "Iron chelators for the treatment of iron overload disease: relationship between structure, redox activity, and toxicity." Am J Hematol **73**(3): 200-10.

Chen, H. L., H. I. Tseng, et al. (2009). "Effect of blood transfusions on the outcome of very low body weight preterm infants under two different transfusion criteria." Pediatr Neonatol **50**(3): 110-6.

Choudhry, V. P. and R. Naithani (2007). "Current status of iron overload and chelation with deferasirox." Indian J Pediatr **74**(8): 759-64.

Cianciulli, P. (2008). "Treatment of iron overload in thalassemia." Pediatr Endocrinol Rev **6 Suppl 1**: 208-13.

Cohen, A. (1990). "Treatment of transfusional iron overload." Am J Pediatr Hematol Oncol **12**(1): 4-8.

Cohen, A. R. (2006). "New advances in iron chelation therapy." Hematology Am Soc Hematol Educ Program: 42-7.

Cohen, G. M. (1997). "Caspases: the executioners of apoptosis." Biochem J **326 (Pt 1)**: 1-16.

Cooksey, R. C., H. A. Jouihan, et al. (2004). "Oxidative stress, beta-cell apoptosis, and decreased insulin secretory capacity in mouse models of hemochromatosis." Endocrinology **145**(11): 5305-12.

Crichton, R. R. and R. J. Ward (2003). "An overview of iron metabolism: molecular and cellular criteria for the selection of iron chelators." Curr Med Chem **10**(12): 997-1004.

Crowder, M. S. and R. Cooke (1984). "The effect of myosin sulphydryl modification on the mechanics of fibre contraction." J Muscle Res Cell Motil **5**(2): 131-46.

Dai, J., C. Huang, et al. (2004). "Iron-induced interleukin-6 gene expression: possible mediation through the extracellular signal-regulated kinase and p38 mitogen-activated protein kinase pathways." Toxicology **203**(1-3): 199-209.

Day, S. M., D. Duquaine, et al. (2003). "Chronic iron administration increases vascular oxidative stress and accelerates arterial thrombosis." Circulation **107**(20): 2601-6.

De Domenico, I., D. M. Ward, et al. (2007). "Hepcidin regulation: ironing out the details." J Clin Invest **117**(7): 1755-8.

de Silva, D. M., C. C. Askwith, et al. (1996). "Molecular mechanisms of iron uptake in eukaryotes." Physiol Rev **76**(1): 31-47.

de Valk, B. and J. J. Marx (1999). "Iron, atherosclerosis, and ischemic heart disease." Arch Intern Med **159**(14): 1542-8.

Deb, S., E. E. Johnson, et al. (2009). "Modulation of intracellular iron levels by oxidative stress implicates a novel role for iron in signal transduction." Biometals.

Demant, A. W., A. Schmiedel, et al. (2007). "Heart failure and malignant ventricular tachyarrhythmias due to hereditary hemochromatosis with iron overload cardiomyopathy." Clin Res Cardiol **96**(12): 900-3.

Denecker, G., D. Vercammen, et al. (2001). "Apoptotic and necrotic cell death induced by death domain receptors." Cell Mol Life Sci **58**(3): 356-70.

Deugnier, Y. M., O. Loreal, et al. (1992). "Liver pathology in genetic hemochromatosis: a review of 135 homozygous cases and their bioclinical correlations." Gastroenterology **102**(6): 2050-9.

Donovan, A. and N. C. Andrews (2004). "The molecular regulation of iron metabolism." Hematol J **5**(5): 373-80.

Donovan, A., C. N. Roy, et al. (2006). "The ins and outs of iron homeostasis." Physiology (Bethesda) **21**: 115-23.

Duane, P., K. B. Raja, et al. (1992). "Intestinal iron absorption in chronic alcoholics." Alcohol Alcohol **27**(5): 539-44.

Duncan, J. G. (2008). "Lipotoxicity: what is the fate of fatty acids?" J Lipid Res **49**(7): 1375-6.

Eaton, J. W. and M. Qian (2002). "Molecular bases of cellular iron toxicity." Free Radic Biol Med **32**(9): 833-40.

Evens, A. M., J. Mehta, et al. (2004). "Rust and corrosion in hematopoietic stem cell transplantation: the problem of iron and oxidative stress." Bone Marrow Transplant **34**(7): 561-71.

Fattovich, G., T. Stroffolini, et al. (2004). "Hepatocellular carcinoma in cirrhosis: incidence and risk factors." Gastroenterology **127**(5 Suppl 1): S35-50.

Fernandes, A., G. C. Preza, et al. (2009). "The molecular basis of hepcidin-resistant hereditary hemochromatosis." Blood **114**(2): 437-43.

Ferrara, D. E. and W. R. Taylor (2005). "Iron chelation and vascular function: in search of the mechanisms." Arterioscler Thromb Vasc Biol **25**(11): 2235-7.

Franchini, M. (2005). "Recent acquisitions in the management of iron overload." Ann Hematol **84**(10): 640-5.

Galaris, D. and K. Pantopoulos (2008). "Oxidative stress and iron homeostasis: mechanistic and health aspects." Crit Rev Clin Lab Sci **45**(1): 1-23.

Gamberini, M. R., V. De Sanctis, et al. (2008). "Hypogonadism, diabetes mellitus, hypothyroidism, hypoparathyroidism: incidence and prevalence related to iron overload and chelation therapy in patients with thalassaemia major followed from 1980 to 2007 in the Ferrara Centre." Pediatr Endocrinol Rev **6 Suppl 1**: 158-69.

Ganz, T. (2003). "Hepcidin, a key regulator of iron metabolism and mediator of anemia of inflammation." Blood **102**(3): 783-8.

Gao, X., J. L. Campian, et al. (2009). "Mitochondrial DNA damage in iron overload." J Biol Chem **284**(8): 4767-75.

Gardenghi, S., M. F. Marongiu, et al. (2007). "Ineffective erythropoiesis in beta-thalassemia is characterized by increased iron absorption mediated by down-regulation of hepcidin and up-regulation of ferroportin." Blood **109**(11): 5027-35.

Gentry-Nielsen, M. J., L. C. Preheim, et al. (2001). "Use of rat models to mimic alterations in iron homeostasis during human alcohol abuse and cirrhosis." Alcohol **23**(2): 71-81.

Glickstein, H., R. B. El, et al. (2006). "Action of chelators in iron-loaded cardiac cells: Accessibility to intracellular labile iron and functional consequences." Blood **108**(9): 3195-203.

Glickstein, H., R. B. El, et al. (2005). "Intracellular labile iron pools as direct targets of iron chelators: a fluorescence study of chelator action in living cells." Blood **106**(9): 3242-50.

Goldspink, G. (2003). "Gene expression in muscle in response to exercise." J Muscle Res Cell Motil **24**(2-3): 121-6.

Gordeuk, V. R., B. R. Bacon, et al. (1987). "Iron overload: causes and consequences." Annu Rev Nutr **7**: 485-508.

Griendling, K. K., D. Sorescu, et al. (2000). "Modulation of protein kinase activity and gene expression by reactive oxygen species and their role in vascular physiology and pathophysiology." Arterioscler Thromb Vasc Biol **20**(10): 2175-83.

Gucev, Z., V. Tasic, et al. (2009). "Friedreich ataxia (FA) associated with diabetes mellitus type 1 and hyperthrophic cardiomyopathy." Bosn J Basic Med Sci **9**(2): 107-10.

Hahalis, G., D. Alexopoulos, et al. (2005). "Heart failure in beta-thalassemia syndromes: a decade of progress." Am J Med **118**(9): 957-67.

Han, D., E. Williams, et al. (2001). "Mitochondrial respiratory chain-dependent generation of superoxide anion and its release into the intermembrane space." Biochem J **353**(Pt 2): 411-6.

Harrison-Findik, D. D. (2007). "Role of alcohol in the regulation of iron metabolism." World J Gastroenterol **13**(37): 4925-30.

Heeney, M. M. and N. C. Andrews (2004). "Iron homeostasis and inherited iron overload disorders: an overview." Hematol Oncol Clin North Am **18**(6): 1379-403, ix.

Hengartner, M. O. (2000). "The biochemistry of apoptosis." Nature **407**(6805): 770-6.

Hershko, C. (2007). "Iron loading and its clinical implications." Am J Hematol **82**(12 Suppl): 1147-8.

Hershko, C. (2007). "Mechanism of iron toxicity." Food Nutr Bull **28**(4 Suppl): S500-9.

Hershko, C., A. M. Konijn, et al. (2001). "ICL670A: a new synthetic oral chelator: evaluation in hypertransfused rats with selective radioiron probes of hepatocellular and reticuloendothelial iron stores and in iron-loaded rat heart cells in culture." Blood **97**(4): 1115-22.

Hershko, C., G. Link, et al. (1998). "Pathophysiology of iron overload." Ann N Y Acad Sci **850**: 191-201.

Hershko, C., G. Link, et al. (2005). "Objectives and mechanism of iron chelation therapy." Ann N Y Acad Sci **1054**: 124-35.

Hertelendi, Z., A. Toth, et al. (2008). "Oxidation of myofilament protein sulfhydryl groups reduces the contractile force and its Ca2+ sensitivity in human cardiomyocytes." Antioxid Redox Signal **10**(7): 1175-84.

Hider, R. C. and T. Zhou (2005). "The design of orally active iron chelators." Ann N Y Acad Sci **1054**: 141-54.

Hubscher, S. G. (2003). "Iron overload, inflammation and fibrosis in genetic haemochromatosis." J Hepatol **38**(4): 521-5.

Ishizaka, N., K. Saito, et al. (2005). "Iron chelation suppresses ferritin upregulation and attenuates vascular dysfunction in the aorta of angiotensin II-infused rats." Arterioscler Thromb Vasc Biol **25**(11): 2282-8.

Janssen, M. C. and D. W. Swinkels (2009). "Hereditary haemochromatosis." Best Pract Res Clin Gastroenterol **23**(2): 171-83.

Kaiser, L., J. M. Davis, et al. (2003). "Does the gerbil model mimic human iron overload?" J Lab Clin Med **141**(6): 419-20; author reply 420-2.

Kaiser, L., J. M. Davis, et al. (2004). "Are there problems with the "time compressed model" of iron overload?" J Lab Clin Med **143**(2): 130-2; author reply 133-4.

Kakhlon, O. and Z. I. Cabantchik (2002). "The labile iron pool: characterization, measurement, and participation in cellular processes(1)." Free Radic Biol Med **33**(8): 1037-46.

Kalinowski, D. S. and D. R. Richardson (2005). "The evolution of iron chelators for the treatment of iron overload disease and cancer." Pharmacol Rev **57**(4): 547-83.

Kaplowitz, N. (2000). "Cell death at the millennium. Implications for liver diseases." Clin Liver Dis **4**(1): 1-23, v.

Kell, D. B. (2009). "Iron behaving badly: inappropriate iron chelation as a major contributor to the aetiology of vascular and other progressive inflammatory and degenerative diseases." BMC Med Genomics **2**: 2.

Keyer, K. and J. A. Imlay (1996). "Superoxide accelerates DNA damage by elevating free-iron levels." Proc Natl Acad Sci U S A **93**(24): 13635-40.

Kiguchi, T., Y. Ito, et al. (2009). "Restoration of cardiac function by an iron chelator, deferasirox, in a patient with aplastic anemia and cardiac iron overload." Int J Hematol **89**(4): 546-8.

Kim, E., S. N. Giri, et al. (1995). "Iron(II) is a modulator of ryanodine-sensitive calcium channels of cardiac muscle sarcoplasmic reticulum." Toxicol Appl Pharmacol **130**(1): 57-66.

Kim, M., J. Kim, et al. (2008). "Increased expression of the F(1)F(o) ATP synthase in response to iron in heart mitochondria." BMB Rep **41**(2): 153-7.

Klintschar, M. and D. Stiller (2004). "Sudden cardiac death in hereditary hemochromatosis: an underestimated cause of death?" Int J Legal Med **118**(3): 174-7.

Kohgo, Y., K. Ikuta, et al. (2008). "Body iron metabolism and pathophysiology of iron overload." Int J Hematol **88**(1): 7-15.

Konijn, A. M., H. Glickstein, et al. (1999). "The cellular labile iron pool and intracellular ferritin in K562 cells." Blood **94**(6): 2128-34.

Kontoghiorghes, G. J. (2006). "Future chelation monotherapy and combination therapy strategies in thalassemia and other conditions. comparison of deferiprone, deferoxamine, ICL670, GT56-252, L1NAll and starch deferoxamine polymers." Hemoglobin **30**(2): 329-47.

Kontoghiorghes, G. J., K. Neocleous, et al. (2003). "Benefits and risks of deferiprone in iron overload in Thalassaemia and other conditions: comparison of epidemiological and therapeutic aspects with deferoxamine." Drug Saf **26**(8): 553-84.

Kontoghiorghes, G. J., K. Pattichi, et al. (2000). "Transfusional iron overload and chelation therapy with deferoxamine and deferiprone (L1)." Transfus Sci **23**(3): 211-23.

Kruszewski, M. (2003). "Labile iron pool: the main determinant of cellular response to oxidative stress." Mutat Res **531**(1-2): 81-92.

Kuryshev, Y. A., G. M. Brittenham, et al. (1999). "Decreased sodium and increased transient outward potassium currents in iron-loaded cardiac myocytes. Implications for the arrhythmogenesis of human siderotic heart disease." Circulation **100**(6): 675-83.

Kurz, T., A. Terman, et al. (2008). "Lysosomes and oxidative stress in aging and apoptosis." Biochim Biophys Acta **1780**(11): 1291-303.

Kurz, T., A. Terman, et al. (2008). "Lysosomes in iron metabolism, ageing and apoptosis." Histochem Cell Biol **129**(4): 389-406.

Kushner, J. P., J. P. Porter, et al. (2001). "Secondary iron overload." Hematology Am Soc Hematol Educ Program: 47-61.

Lash, A. and A. Saleem (1995). "Iron metabolism and its regulation. A review." Ann Clin Lab Sci **25**(1): 20-30.

Laurita, K. R., E. T. Chuck, et al. (2003). "Optical mapping reveals conduction slowing and impulse block in iron-overload cardiomyopathy." J Lab Clin Med **142**(2): 83-9.

Lee, P. L. and E. Beutler (2009). "Regulation of hepcidin and iron-overload disease." Annu Rev Pathol **4**: 489-515.

Lekawanvijit, S. and N. Chattipakorn (2009). "Iron overload thalassemic cardiomyopathy: iron status assessment and mechanisms of mechanical and electrical disturbance due to iron toxicity." Can J Cardiol **25**(4): 213-8.

Li, D., E. Ueta, et al. (2004). "Reactive oxygen species (ROS) control the expression of Bcl-2 family proteins by regulating their phosphorylation and ubiquitination." Cancer Sci **95**(8): 644-50.

Li, T. Q., A. M. Aisen, et al. (2004). "Assessment of hepatic iron content using magnetic resonance imaging." Acta Radiol **45**(2): 119-29.

Lindsey, W. T. and B. R. Olin (2007). "Deferasirox for transfusion-related iron overload: a clinical review." Clin Ther **29**(10): 2154-66.

Link, G., A. Saada, et al. (1998). "Mitochondrial respiratory enzymes are a major target of iron toxicity in rat heart cells." J Lab Clin Med **131**(5): 466-74.

Liu, P. and N. Olivieri (1994). "Iron overload cardiomyopathies: new insights into an old disease." Cardiovasc Drugs Ther **8**(1): 101-10.

Liu, Z. D. and R. C. Hider (2002). "Design of clinically useful iron(III)-selective chelators." Med Res Rev **22**(1): 26-64.

Livrea, M. A., L. Tesoriere, et al. (1996). "Oxidative stress and antioxidant status in beta-thalassemia major: iron overload and depletion of lipid-soluble antioxidants." Blood **88**(9): 3608-14.

Lucesoli, F. and C. G. Fraga (1995). "Oxidative damage to lipids and DNA concurrent with decrease of antioxidants in rat testes after acute iron intoxication." Arch Biochem Biophys **316**(1): 567-71.

Lund, D. D., F. M. Faraci, et al. (2000). "Gene transfer of endothelial nitric oxide synthase improves relaxation of carotid arteries from diabetic rabbits." Circulation **101**(9): 1027-33.

MacCarthy, P. A., D. J. Grieve, et al. (2001). "Impaired endothelial regulation of ventricular relaxation in cardiac hypertrophy: role of reactive oxygen species and NADPH oxidase." Circulation **104**(24): 2967-74.

MacKenzie, E. L., K. Iwasaki, et al. (2008). "Intracellular iron transport and storage: from molecular mechanisms to health implications." Antioxid Redox Signal **10**(6): 997-1030.

Maiese, K., Z. Z. Chong, et al. (2007). "Mechanistic insights into diabetes mellitus and oxidative stress." Curr Med Chem **14**(16): 1729-38.

Malcovati, L. (2009). "Red bood cell transfusion therapy and iron chelation in patients with myelodysplastic syndromes." Clin Lymphoma Myeloma **9 Suppl 3**: S305-11.

Martindale, J. L. and N. J. Holbrook (2002). "Cellular response to oxidative stress: signaling for suicide and survival." J Cell Physiol **192**(1): 1-15.

Meneghini, R. (1997). "Iron homeostasis, oxidative stress, and DNA damage." Free Radic Biol Med **23**(5): 783-92.

Miller, F. J., Jr., D. D. Gutterman, et al. (1998). "Superoxide production in vascular smooth muscle contributes to oxidative stress and impaired relaxation in atherosclerosis." Circ Res **82**(12): 1298-305.

Molkentin, J. D. (2004). "Calcineurin-NFAT signaling regulates the cardiac hypertrophic response in coordination with the MAPKs." Cardiovasc Res **63**(3): 467-75.

Munoz, M., I. Villar, et al. (2009). "An update on iron physiology." World J Gastroenterol **15**(37): 4617-26.

Nabavizadeh, S. H., A. Anushiravani, et al. (2007). "Evaluation of growth parameters in patients with thalassemia major." Hematology **12**(5): 445-7.

Neufeld, E. J. (2006). "Oral chelators deferasirox and deferiprone for transfusional iron overload in thalassemia major: new data, new questions." Blood **107**(9): 3436-41.

Nunoshiba, T., F. Obata, et al. (1999). "Role of iron and superoxide for generation of hydroxyl radical, oxidative DNA lesions, and mutagenesis in Escherichia coli." J Biol Chem **274**(49): 34832-7.

Obejero-Paz, C. A., T. Yang, et al. (2003). "Deferoxamine promotes survival and prevents electrocardiographic abnormalities in the gerbil model of iron-overload cardiomyopathy." J Lab Clin Med **141**(2): 121-30.

Olivieri, N. F. and G. M. Brittenham (1997). "Iron-chelating therapy and the treatment of thalassemia." Blood **89**(3): 739-61.

Olivieri, N. F., S. De Silva, et al. (2000). "Iron overload and iron-chelating therapy in hemoglobin E-beta thalassemia." J Pediatr Hematol Oncol **22**(6): 593-7.

Oltvai, Z. N., C. L. Milliman, et al. (1993). "Bcl-2 heterodimerizes in vivo with a conserved homolog, Bax, that accelerates programmed cell death." Cell **74**(4): 609-19.

Orrenius, S. (2007). "Reactive oxygen species in mitochondria-mediated cell death." Drug Metab Rev **39**(2-3): 443-55.

Otto-Duessel, M., M. Aguilar, et al. (2007). "Antioxidant-mediated effects in a gerbil model of iron overload." Acta Haematol **118**(4): 193-9.

Otto-Duessel, M., M. Aguilar, et al. (2007). "Comparison of twice-daily vs once-daily deferasirox dosing in a gerbil model of iron cardiomyopathy." Exp Hematol **35**(7): 1069-73.

Otto-Duessel, M., C. Brewer, et al. (2008). "Safety and efficacy of combined chelation therapy with deferasirox and deferoxamine in a gerbil model of iron overload." Acta Haematol **120**(2): 123-8.

Oudit, G. Y., H. Sun, et al. (2004). "The role of phosphoinositide-3 kinase and PTEN in cardiovascular physiology and disease." J Mol Cell Cardiol **37**(2): 449-71.

Oudit, G. Y., H. Sun, et al. (2003). "L-type Ca2+ channels provide a major pathway for iron entry into cardiomyocytes in iron-overload cardiomyopathy." Nat Med **9**(9): 1187-94.

Oudit, G. Y., M. G. Trivieri, et al. (2004). "Taurine supplementation reduces oxidative stress and improves cardiovascular function in an iron-overload murine model." Circulation **109**(15): 1877-85.

Oudit, G. Y., M. G. Trivieri, et al. (2006). "Role of L-type Ca2+ channels in iron transport and iron-overload cardiomyopathy." J Mol Med **84**(5): 349-64.

Ozment, C. P. and J. L. Turi (2009). "Iron overload following red blood cell transfusion and its impact on disease severity." Biochim Biophys Acta **1790**(7): 694-701.

Pallottini, V., C. Martini, et al. (2005). "3-Hydroxy-3-methylglutaryl coenzyme A reductase deregulation and age-related hypercholesterolemia: a new role for ROS." Mech Ageing Dev **126**(8): 845-51.

Pantopoulos, K. (2004). "Iron metabolism and the IRE/IRP regulatory system: an update." Ann N Y Acad Sci **1012**: 1-13.

Papakonstantinou, O. G., T. G. Maris, et al. (1995). "Assessment of liver iron overload by T2-quantitative magnetic resonance imaging: correlation of T2-QMRI measurements with serum ferritin concentration and histologic grading of siderosis." Magn Reson Imaging **13**(7): 967-77.

Pardo Andreu, G. L., N. M. Inada, et al. (2008). "Uncoupling and oxidative stress in liver mitochondria isolated from rats with acute iron overload." Arch Toxicol.

Park, B. G., C. I. Yoo, et al. (2005). "Role of mitogen-activated protein kinases in hydrogen peroxide-induced cell death in osteoblastic cells." Toxicology **215**(1-2): 115-25.

Parkes, J. G. and D. M. Templeton (2003). "Modulation of stellate cell proliferation and gene expression by rat hepatocytes: effect of toxic iron overload." Toxicol Lett **144**(2): 225-33.

Pennell, D., J. B. Porter, et al. (2008). "Efficacy and Safety of Deferasirox (Exjade(R)) in Reducing Cardiac Iron in Patients with {beta}-Thalassemia Major: Results from the Cardiac Substudy of the EPIC Trial." ASH Annual Meeting Abstracts **112**(11): 3873.

Pennell, D., P. Sutcharitchan, et al. (2008). "Efficacy and Safety of Deferasirox (Exjade(R)) in Preventing Cardiac Iron Overload in {beta}-Thalassemia Patients with Normal Baseline Cardiac Iron: Results from the Cardiac Substudy of the EPIC Trial." ASH Annual Meeting Abstracts **112**(11): 3874.

Perifanis, V., A. Christoforidis, et al. (2007). "comparison of effects of different long-term iron-chelation regimens on myocardial and hepatic iron concentrations assessed with T2* magnetic resonance imaging in patients with beta-thalassemia major." Int J Hematol **86**(5): 385-9.

Pietrangelo, A., G. Montosi, et al. (2002). "Iron-induced oxidant stress in nonparenchymal liver cells: mitochondrial derangement and fibrosis in acutely iron-dosed gerbils and its prevention by silybin." J Bioenerg Biomembr **34**(1): 67-79.

Piperno, A. (1998). "Classification and diagnosis of iron overload." Haematologica **83**(5): 447-55.

Pognonec, P., H. Kato, et al. (1992). "The helix-loop-helix/leucine repeat transcription factor USF can be functionally regulated in a redox-dependent manner." J Biol Chem **267**(34): 24563-7.

Ponka, P. (1999). "Cellular iron metabolism." Kidney International **55**(69): S2-S11.

Porter, A. G. and R. U. Janicke (1999). "Emerging roles of caspase-3 in apoptosis." Cell Death Differ **6**(2): 99-104.

Porter, J. B. (2007). "Concepts and goals in the management of transfusional iron overload." Am J Hematol **82**(12 Suppl): 1136-9.

Porter, J. B., A. T. Taher, et al. (2008). "Ethical issues and risk/benefit assessment of iron chelation therapy: advances with deferiprone/deferoxamine combinations and concerns about the safety, efficacy and costs of deferasirox [Kontoghiorghes GJ, Hemoglobin 2008; 32(1-2):1-15.]." Hemoglobin **32**(6): 601-7.

Rachmilewitz, E. A., O. Weizer-Stern, et al. (2005). "Role of iron in inducing oxidative stress in thalassemia: can it be prevented by inhibition of absorption and by antioxidants?" Ann N Y Acad Sci **1054**: 118-23.

Ramey, G., J. C. Deschemin, et al. (2009). "Hepcidin targets ferroportin for degradation in hepatocytes." Haematologica.

Ramm, G. A. and R. G. Ruddell (2005). "Hepatotoxicity of iron overload: mechanisms of iron-induced hepatic fibrogenesis." Semin Liver Dis **25**(4): 433-49.

Raszeja-Wyszomirska, J., M. Lawniczak, et al. (2008). "[Non-alcoholic fatty liver disease--new view]." Pol Merkur Lekarski **24**(144): 568-71.

Rice, K. M., D. L. Preston, et al. (2006). "Aging influences multiple incidices of oxidative stress in the aortic media of the Fischer 344/NNiaxBrown Norway/BiNia rat." Free Radic Res **40**(2): 185-97.

Rivella, S. (2009). "Ineffective erythropoiesis and thalassemias." Curr Opin Hematol **16**(3): 187-94.

Rothe, G., A. Emmendorffer, et al. (1991). "Flow cytometric measurement of the respiratory burst activity of phagocytes using dihydrorhodamine 123." J Immunol Methods **138**(1): 133-5.

Safarinejad, M. R. (2008). "Evaluation of semen quality, endocrine profile and hypothalamus-pituitary-testis axis in male patients with homozygous beta-thalassemia major." J Urol **179**(6): 2327-32.

Sarnaik, S. A. (2005). "Thalassemia and related hemoglobinopathies." Indian J Pediatr **72**(4): 319-24.

Schulz, K. and H. J. Sanft (1984). "[Iron metabolism in chronic alcohol abuse]." Z Gesamte Inn Med **39**(8): 172-6.

Schwartz, K. A., Z. Li, et al. (2002). "Earliest cardiac toxicity induced by iron overload selectively inhibits electrical conduction." J Appl Physiol **93**(2): 746-51.

Sela, B. A. (2008). "[Hepcidin--the discovery of a small protein with a pivotal role in iron homeostasis]." Harefuah **147**(3): 261-6, 276.

Singhi, S. C., A. K. Baranwal, et al. (2003). "Acute iron poisoning: clinical picture, intensive care needs and outcome." Indian Pediatr **40**(12): 1177-82.

Stadtman, E. R. (1993). "Oxidation of free amino acids and amino acid residues in proteins by radiolysis and by metal-catalyzed reactions." Annu Rev Biochem **62**: 797-821.

Stal, P., H. Glaumann, et al. (1990). "Liver cell damage and lysosomal iron storage in patients with idiopathic hemochromatosis. A light and electron microscopic study." J Hepatol **11**(2): 172-80.

Staubli, A. and U. A. Boelsterli (1998). "The labile iron pool in hepatocytes: prooxidant-induced increase in free iron precedes oxidative cell injury." Am J Physiol **274**(6 Pt 1): G1031-7.

Storz, G. and J. A. Imlay (1999). "Oxidative stress." Curr Opin Microbiol **2**(2): 188-94.

Stumpf, J. L. (2007). "Deferasirox." Am J Health Syst Pharm **64**(6): 606-16.

Taher, A., C. Hershko, et al. (2009). "Iron overload in thalassaemia intermedia: reassessment of iron chelation strategies." Br J Haematol.

Tanno, T., N. V. Bhanu, et al. (2007). "High levels of GDF15 in thalassemia suppress expression of the iron regulatory protein hepcidin." Nat Med **13**(9): 1096-101.

Tavill, A. S. (2001). "Diagnosis and management of hemochromatosis." Hepatology **33**(5): 1321-8.

Trad, O., M. A. Hamdan, et al. (2009). "Reversal of iron-induced dilated cardiomyopathy during therapy with deferasirox in beta-thalassemia." Pediatr Blood Cancer **52**(3): 426-8.

Tran, T. N., S. K. Eubanks, et al. (1997). "Secretion of ferritin by rat hepatoma cells and its regulation by inflammatory cytokines and iron." Blood **90**(12): 4979-86.

Tsukada, S., C. J. Parsons, et al. (2006). "Mechanisms of liver fibrosis." Clin Chim Acta **364**(1-2): 33-60.

Turrens, J. F. (2003). "Mitochondrial formation of reactive oxygen species." J Physiol **552**(Pt 2): 335-44.

Valko, M., C. J. Rhodes, et al. (2006). "Free radicals, metals and antioxidants in oxidative stress-induced cancer." Chem Biol Interact **160**(1): 1-40.

Vermylen, C. (2008). "What is new in iron overload?" Eur J Pediatr **167**(4): 377-81.

Vichinsky, E. (2008). "Clinical application of deferasirox: practical patient management." Am J Hematol **83**(5): 398-402.

Vichinsky, E., Z. Pakbaz, et al. (2008). "Patient-reported outcomes of deferasirox (Exjade, ICL670) versus deferoxamine in sickle cell disease patients with transfusional hemosiderosis. Substudy of a randomized open-label phase II trial." Acta Haematol **119**(3): 133-41.

Victor Hoffbrand, A. (2005). "Deferiprone therapy for transfusional iron overload." Best Pract Res Clin Haematol **18**(2): 299-317.

Walker, E., J. Black, et al. (2004). "Effect of experimental hyperhomocysteinemia on cardiac structure and function in the rat." Ann Clin Lab Sci **34**(2): 175-80.

Walker, E. M., Jr., C. P. Epling, et al. (2007). "Acetaminophen protects against iron-induced cardiac damage in gerbils." Ann Clin Lab Sci **37**(1): 22-33.

Walter, P. B., M. D. Knutson, et al. (2002). "Iron deficiency and iron excess damage mitochondria and mitochondrial DNA in rats." Proc Natl Acad Sci U S A **99**(4): 2264-9.

Walter, P. B., E. A. Macklin, et al. (2008). "Inflammation and oxidant-stress in beta-thalassemia patients treated with iron chelators deferasirox (ICL670) or deferoxamine: an ancillary study of the Novartis CICL670A0107 trial." Haematologica **93**(6): 817-25.

Wenzel, S., C. Muller, et al. (2005). "p38 MAP-kinase in cultured adult rat ventricular cardiomyocytes: expression and involvement in hypertrophic signalling." Eur J Heart Fail **7**(4): 453-60.

Whittaker, P., F. A. Hines, et al. (1996). "Histopathological evaluation of liver, pancreas, spleen, and heart from iron-overloaded Sprague-Dawley rats." Toxicol Pathol **24**(5): 558-63.

Wolff, S. P. and R. T. Dean (1986). "Fragmentation of proteins by free radicals and its effect on their susceptibility to enzymic hydrolysis." Biochem J **234**(2): 399-403.

Wood, J. C., C. Enriquez, et al. (2005). "Physiology and pathophysiology of iron cardiomyopathy in thalassemia." Ann N Y Acad Sci **1054**: 386-95.

Wood, J. C., M. Otto-Duessel, et al. (2006). "Deferasirox and deferiprone remove cardiac iron in the iron-overloaded gerbil." Transl Res **148**(5): 272-80.

Wood, M. J., R. Skoien, et al. (2009). "The global burden of iron overload." Hepatol Int.

Yajun, Z., C. Hongshan, et al. (2005). "Translocation of Bax in rat hepatocytes cultured with ferric nitrilotriacetate." Life Sci **76**(24): 2763-72.

Yang, T., G. M. Brittenham, et al. (2003). "Deferoxamine prevents cardiac hypertrophy and failure in the gerbil model of iron-induced cardiomyopathy." J Lab Clin Med **142**(5): 332-40.

Yang, T., W. Q. Dong, et al. (2002). "Bimodal cardiac dysfunction in an animal model of iron overload." J Lab Clin Med **140**(4): 263-71.

Zima, T. and M. Kalousova (2005). "Oxidative stress and signal transduction pathways in alcoholic liver disease." Alcohol Clin Exp Res **29**(11 Suppl): 110S-115S.

CURRICULUM VITAE

RABAA M. AL-ROUSAN, R.Ph, M.S., Ph.D. candidate

OBJECTIVE To pursue academic position in Pharmacology/Toxicology in a college of pharmacy, where I can integrate my academic and professional backgrounds.

LICENSES: Pharmacist (Active), Illinois State # 051.293231

University Address and Phone

Department of Pharmacology & Toxicology

School of Medicine at Marshall University

Huntington, WV 25755

Fax: 304-696-6777

Home Address and Phone

6000 Gideon Rd apt 2

Huntington, WV 25705

Cell phone: 304-380-5813

Education

2007- 2010

Ph.D. in Biomedical Sciences (Pharmacology & Toxicology), GPA=4.0, Marshall University School of Medicine, Huntington, WV

2005- 2007

M.S. in (Molecular Physiology and Biophysics), GPA=3.7, University of Iowa School of Medicine, Iowa City, IA

1999-2004

Bachelor of Science, **Pharmacy** Jordan University of Science & Technology (JUST), Jordan (170 credit hours course work + 3-month hospital practical training). Student on honor list. Cumulative Grade = Excellent

Employment Experience

July 2007- Present

Graduate research assistant, Joan C. Edwards school of Medicine, Marshall University, Huntington, WV

July 2005 - May 2007

Graduate research assistant, Carver College of Medicine, the University of Iowa, Iowa city, IA

January 2004- August 2004

Hospital Pharmacist at King Abdullah University Hospital, Irbid, Jordan

Publications

1) Alkhateeb FM, Clauson KA, Latif DA, **Al-Rousan RM**. The Foreign Pharmacy Graduate Equivalency Examination (FPGEE): Global Education Implications. American Journal of Pharmaceutical Education (In press).

2) **Al-Rousan RM**, Satyanarayana P, Laurino JP, Kakarla SK, Gutta AK, Walker EM, Blough ER. Deferasirox Removes Cardiac Iron and Attenuates Oxidative Stress in the Iron-Overloaded Gerbil. *American Journal of Hematology* 2009, 84(9):565-70

3) Alkhateeb FM, Unni E, Latif DA, Shawaqfeh MS, **Al-Rousan RM**. Physicians Attitudes towards Collaborative Agreement with Pharmacists and their Expectations of Pharmacists Responsibilities in West Virginia*. JAPhA.* 2009, 49(6):48-51

Presentations

1. **Al-Rousan RM**, Katta A, Paturi S, Kidd B, Manzoor K, Walker EM, and Blough ER. Chronic Deferasirox Administration Decreases Hepatic Oxidative Stress and Apoptosis in the Iron Overloaded Gerbil. American Society of Hematology (ASH) Annual Meeting & Exposition, New Orleans, LA, December 5-8, 2009.
2. Alkhateeb FM**,** Latif DA, **Al-Rousan RM**. The Foreign Pharmacy Graduate Equivalency Examination (FPGEE): Global Educational Implications. American Association of Colleges of Pharmacy (AACP) Annual Meeting, Boston, MA, July 19-23, 2009.
3. **Al-Rousan RM**, Walker EM, Laurino JP, Paturi S, and Blough ER. Deferasirox and Iron Removal in the Iron Overloaded Gerbil. Clinical Science Trumpet, Tampa, FL, May 13-16, 2009.
4. Alkhateeb FM, Unni E, Latif DA, Shawaqfeh MS, **Al-Rousan RM**. Physicians Attitudes towards Collaborative Agreement with Pharmacists and their Expectations of Pharmacists Responsibilities in West Virginia. American Pharmacists Association (APhA) Annual Meeting & Exposition. San Antonio, Texas, April 3-6, 2009.

5. **Al-Rousan RM**, Satyanarayana P, Laurino JP, Gutta AK, Arvapalli RK, Kakarla SK, Devashish H. Desai, Walker EM, Blough ER. Deferasirox attenuates iron-induced oxidative stress and prevents cardiotoxicity in the iron-overloaded gerbil. The 2008 ACCP Annual Meeting. Louisville, KY, October 19–22, 2008.
6. Arvapalli RK, **Al-Rousan RM**, Laurino JP , Kakarla SK, Katta A, Paturi S, Gutta AK, Dornon L, Rice KM, Walker EM, and Blough ER. Deferasirox attenuates age-associated increases in cardiac and hepatic iron accumulation and improves blood glucose regulation. The 2008 ACCP Annual Meeting. Louisville, KY, October 19–22, 2008.

Other Experience and Professional Memberships

2009-present	American Pharmacists Association, USA
2007-present	Cell Differentiation and Development Center, Marshall University
2007-present	American Association for the Advancement of Science
2008-present	American College of Clinical Pharmacy

Honors

2008	Best Academic Performance Award
2008	CDDC Symposium Poster Award
2009	STAR Symposium Poster Finalist

Teaching experience

2008- 2009 Nursing Physiology (BSC228)